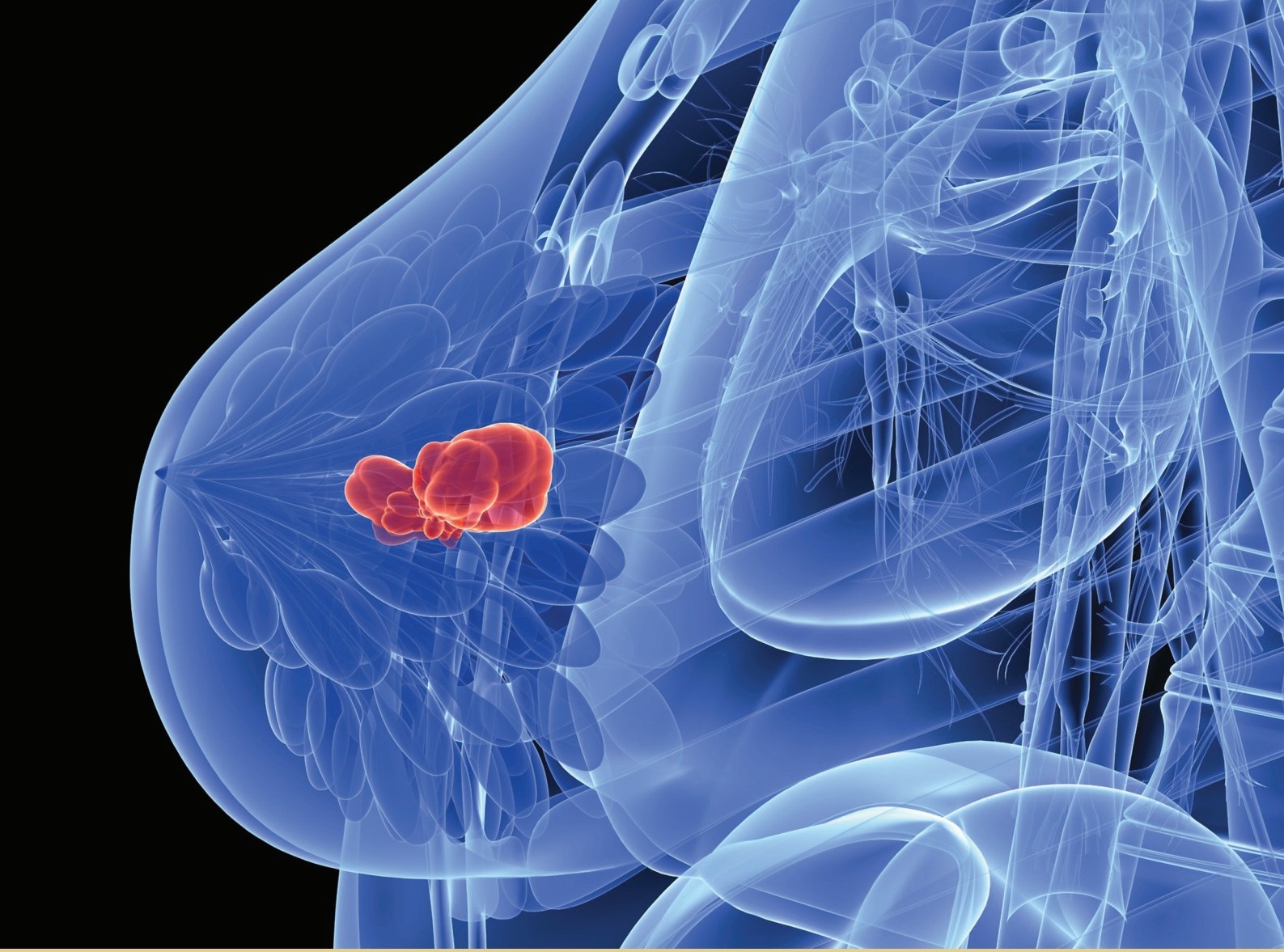

Ana Cristina Leal Gregório

MEETING THE NEEDS OF BREAST CANCER: *A NUCLEOLIN'S PERSPECTIVE*

Tese de Doutoramento em Biologia Experimental e Biomedicina, ramo de Oncobiologia, orientada pelo Professor Doutor João Nuno Moreira, Professor Doutor Sérgio Dias e Professor Doutor Sérgio Simões e apresentada ao Instituto de Investigação Interdisciplinar da Universidade de Coimbra.

Setembro de 2015

· U C ·

UNIVERSIDADE DE COIMBRA

Ana Cristina Leal Gregório

Meeting the needs of breast cancer: a *nucleolin's* perspective

2015

Thesis submitted to the Institute for Interdisciplinary Research of the University of Coimbra to apply for the degree of Doctor of Philosophy in the area of Biomedicine and Experimental Biology, specialization in Oncobiology.

The work described in this dissertation was conducted at the Center for Neuroscience and Cell Biology (CNC) from the University of Coimbra and in collaboration with the Portuguese Institute of Oncology (IPO) of Coimbra, under the scientific supervision of Professor João Nuno Moreira, Professor Sérgio Dias and Professor Sérgio Simões

Ana Gregório was a student of the PhD Program in Experimental Biology and Biomedicine (PDBEB) from the Institute for Interdisciplinary Research of the University of Coimbra (IIIUC), and recipient of the fellowship SFRH / BD / 51190 / 2010 from the Portuguese Foundation for Science and Technology (FCT). This work was supported by the grants PTDC/SAU-BMA/121028/2010 and PEst-C/SAU/LA0001/2013-2014.

UNIVERSIDADE DE COIMBRA

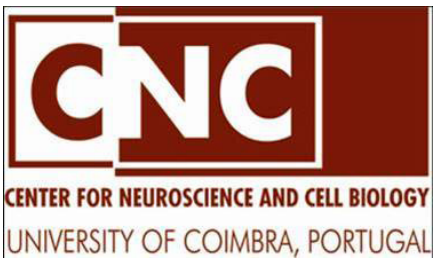

IIIUC INSTITUTO DE INVESTIGAÇÃO INTERDISCIPLINAR
UNIVERSIDADE DE COIMBRA

FCT
Fundação para a Ciência e a Tecnologia
MINISTÉRIO DA EDUCAÇÃO E CIÊNCIA

UNIÃO EUROPEIA
Fundo Europeu
de Desenvolvimento Regional

To my friends and family

Acknowledgements

To all of those that in some way contributed for the success of this work.

To Professor João Nuno Moreira, my supervisor and Principal Investigator in this project, I wish to express my gratitude for the opportunity to be part of his team and perform this work. My sincere thankfulness for the mentorship, scientific support, motivation and dedication demonstrated throughout the last years. To my co-supervisor Sérgio Dias, I am truly grateful for receiving me in his team, and for his kindness and insightful comments about the work. To my co-supervisor Professor Sérgio Simões I wish to thank for the critical observations and input.

To Dra. Manuela Lacerda and Dr. Paulo Figueiredo, from the Portuguese Institute of Oncology Francisco Gentil of Coimbra, I owe my deepest gratitude for the extensive collaboration, support and dedicated teaching throughout the developed research. I am deeply thankful to all the people working at the Laboratory of Anatomical Pathology for their contribution to this project, especially Manuela Henriques and Vasco Serra for their time and dedication to this work.

To the Vascular Biology & Cancer Microenvironment research team, I sincerely appreciate their kindness and warm reception! And I am truly thankful for all your help and the time taken with me. My special thankfulness to Germana Domingues for her help and friendship.

To all my colleagues in the Vectors and Gene Therapy Group I wish to express my deepest gratitude for the support, scientific brainstorming and, more importantly, your companionship. Thank you for the great lunchtimes and laughs. and your patience with me!

I also acknowledge all those working in the animal facility at CNC/ Faculty of Medicine for their support and guidance.

To my all my friends, specially Joana Real, Carla Jorge, Vitor Hugo, Carla Lopes, Nuno Fonseca, Ângela Fernandes, Joana Guedes, Mariangela Natale and Isabel Onofre … I couldn’t be more blissful for your friendship. Thank you!

À minha mana, obrigada pelo teu apoio, palavras de carinho e amizade e, por vezes o abrigo que me ofereceste. Eu não podia ter um melhor exemplo que o teu!

Por último, mas mais importante, quero expressar a minha mais sincera e profunda gratidão aos meus pais. Por estarem sempre presentes e me conduzirem na vida; por me terem proporcionado as oportunidades que tornaram possível a concretização desta “viagem”; e, acima de tudo, pelo carinho e amor.

Table of contents

Drawings

List of figures

List of tables

Abstract

Treatment and management of breast cancer imposes a heavy burden on the public health care, while the incidence rates continue to increase. Breast cancer is the most common female neoplasia and primary cause of death among women worldwide. The recognition of breast cancer as a complex and heterogeneous disease composed by different molecular entities was a landmark in our understanding of this malignancy. Valuing the impact of the molecular characteristics on tumor behavior allowed a better assessment of a patient's prognosis and increased the predictive power to therapeutic response and clinical outcome. However, in spite of the considerable advancements in the treatment of breast cancer in recent years, many of these patients continue to progress to metastatic disease and, for those with advanced breast cancer, palliative care is oftentimes the endpoint. From a therapeutic standpoint, developing new targeted approaches to address this malignancy has been a challenge due to significant molecular and genetic differences between primary cancers and their paired metastases, and potentially between metastases within the same patient. Molecular heterogeneity is also prominent in the triple-negative beast cancer subtype, and is reflected by the distinct prognostic and patient's sensitivity to treatment, to whom chemotherapy is the only systemic treatment currently available.

In face of these unmet needs of breast cancer, it is of utmost importance the design of novel targeted therapeutic strategies. In the last decade, nucleolin has emerged as an amenable target in cancer due to its involvement in various processes supporting tumorigenesis and angiogenesis. Its overexpression in cancer cells and endothelial cells of tumor-associated blood vessels, including expression at the cell surface, encouraged the development of various strategies targeting nucleolin, including the targeted pH-sensitive liposomes functionalized with the F3 peptide and containing doxorubicin, which have shown to cause a major impact on primary breast tumor invasiveness. The main goal of this project was to evaluate the therapeutic impact of the previously developed F3 peptide-targeted pH-sensitive liposomes on metastatic triple-negative breast cancer, and assess the translational value of nucleolin in this breast cancer subtype.

Mouse models are crucial to our comprehensive knowledge on the molecular basis and pathogenesis of cancer disease. However, the unavailability of suitable mouse models that accurately recapitulate the complexity of human tumor progression has been a handicap. In the present work we established the conditions enabling high metastatic take rate of the widespread triple-negative murine 4T1 syngeneic breast cancer model, towards a more reliable pre-clinical screening of anticancer drugs. It was demonstrated that

4T1 tumors grew in the mammary fat pad of mice when as few as 500 cancer cells were implanted, with 87% tumor incidence. The lungs were the main organs colonized with 100% efficiency, though distant lesions were also commonly identified in other tissues, such as the mesentery and pancreas. This significant reduction in the number of inoculated cells also resulted in increased tumor doubling times and decreased specific growth rates, following a Gompertzian tumor expansion. Extending the time frame of primary tumor development, without requiring its excision, was beneficial for metastatic progression, and set the ground to better assess the effect of antimetastatic therapies.

Using the 4T1 mouse model, the therapeutic potential of pH-sensitive liposomes containing doxorubicin and functionalized with the nucleolin-binding F3 peptide (PEGASEMP™) was further investigated, in the setting of metastatic triple-negative breast carcinoma. In vitro, F3 peptide-targeted liposomes led to 7 to 36-fold increase in cellular association with three metastatic (triple-negative or ER-positive) breast cancer cell lines, compared with non-targeted or targeted by a non-specific peptide counterpart. The increased cellular association enabled a 8.8 to 17-fold augment of cytotoxicity. In the 4T1 model, however, the therapeutic activity of PEGASEMP™ did not surmount the overall efficacy of Caelyx® (median survival of 46 days and two complete responses), and resulted in only a marginal tumor growth delay relative to non-treated mice. Nonetheless, PEGASEMP™ significantly extended the survival (16 *versus* 28 d, Log-rank $p = 0.0015$), and reduced the incidence of metastatic nodules in the mesentery (33% *versus* 77%, $p = 0.0409$) compared with non-treated mice.

In order to emphasize nucleolin's therapeutic relevance, its expression was further assessed in patient-derived breast tumor tissues, both in primary tumors and corresponding metastases, with emphasis on triple-negative breast carcinomas. A positive nucleolin staining was observed in the primary breast cancer samples and their matched lymph node metastases, although not all secondary lesions overexpressed the protein. Nucleolin expression was evident in 78% of the triple-negative breast cancer biopsies analyzed. Despite both triple-negative and luminal A tumor tissues presented a nuclear protein expression, differences were found on the staining pattern. The former revealed a diffuse nucleoplasm staining, with a clear nucleolar prominence, whereas the latter had a specked distribution of nucleolin throughout the nucleus. No significant associations between nucleolin expression in the triple-negative breast tumors and clinico-pathological factors were identified in this study. Notwithstanding, a significant association was found between nucleolin and CK5/6, with a frequency of nucleolin expression of 89.5% in CK5/6-negative tumors, compared to 60% in CK5/6-positive group ($p = 0.015$).

Overall, these results suggested that nucleolin is a valuable therapeutic target in

metastatic and/or triple-negative breast cancer, and sustained the rationale of nucleolin-targeting therapeutic approaches for the treatment of this disease. In respect to the use of F3 peptide-targeted pH-sensitive liposomes containing doxorubicin, different therapeutic schedules enabling a higher systemic exposure need to be further explored.

Resumo

O tratamento do cancro da mama e a sua gestão constituem uma enorme sobrecarga para a saúde pública, e para o qual tem contribuído o aumento da taxa de incidência desta doença. O cancro da mama é a neoplasia mais comum e principal causa de morte entre as mulheres a nível global. O reconhecimento da complexidade e heterogeneidade desta doença, constituída por diferentes entidades moleculares, e a valorização do impacto das características moleculares sobre o comportamento dos tumores, permitiu uma melhor avaliação prognóstica do doente e aumentou a capacidade preditiva da resposta à terapêutica e evolução clínica. No entanto, apesar dos avanços consideráveis no tratamento do cancro da mama nos últimos anos, muitos doentes continuam a evoluir para doença metastática, para os quais os cuidados paliativos constituem a única opção. Do ponto de vista terapêutico, o desenvolvimento de abordagens terapêuticas direcionadas tem sido um desafio face às diferenças moleculares e genéticas entre tumores primários e as respectivas metástases, e potencialmente entre diferentes metástases no mesmo doente. A heterogeneidade molecular é também proeminente no subtipo de cancro da mama triplo-negativo, reflectindo-se em prognóstico distinto e diferente sensibilidade do doente ao tratamento, e para os quais a quimioterapia é o único tratamento sistémico atualmente disponível.

Perante estas carências do cancro da mama, é de extrema importância a conceção de novas estratégias terapêuticas direcionadas. Na última década, e devido ao seu envolvimento nos processos de tumorigénese e angiogénese, a nucleolina emergiu como um potencial alvo no contexto do cancro. A sua sobre-expressão em células cancerígenas e células endoteliais de vasos sanguíneos associados aos tumores, incluindo a expressão na superfície da célula, estimulou o desenvolvimento de várias estratégias de direcionamento para a nucleolina. Entre estas destacam-se os lipossomas sensíveis ao pH, funcionalizados com o péptido F3, e contendo doxorrubicina, que anteriormente mostraram inibir a invasão de tumores da mama em ratinhos. O principal objetivo deste projecto foi avaliar o impacto terapêutico destes lipossomas em cancro da mama triplo-negativo metastático, e avaliar o valor translacional da nucleolina neste subtipo de cancro da mama.

Os modelos animais são fundamentais para a compreensão das bases moleculares e patogénese do cancro. No entanto, a ausência de modelos de murganho que reproduzam com precisão a complexidade da progressão dos tumores humanos tem sido uma desvantagem. No presente trabalho estabeleceram-se condições experimentais que permitiram obter uma elevada eficiência metastática no modelo 4T1 de cancro da mama triplo-negativo de murganho, perspetivando o desenvolvimento de estudos pré-clínicos mais confiáveis para o screening de medicamentos anticancerígenos. Demonstrou-se que a

inoculação ortotópica de apenas 500 células resultou no crescimento de tumores 4T1, com uma incidência de 87%. Os pulmões foram o principal órgão colonizado com uma eficiência de 100%, embora também se tenham identificado lesões secundárias noutros tecidos, tais como o mesentério e o pâncreas. A redução significativa do número de células inoculadas, resultou também num aumento do tempo necessário para os tumores duplicarem o seu volume, e na diminuição da taxa de crescimento específico, seguindo estes tumores um crescimento Gompertziano. A extensão do período de crescimento do tumor primário, sem a necessidade da sua excisão, beneficiou a progressão metastática, e gerou um modelo animal que permite uma melhor avaliação de terapias antimetastáticas.

O potencial terapêutico dos lipossomas sensíveis ao pH, funcionalizados com o péptido F3, e contendo doxorubicina (PEGASEMP™) foi investigado no contexto de carcinoma da mama metastático triplo-negativo, utilizando o modelo de murganho 4T1. In vitro, a associação celular dos lipossomas direcionados para a nucleolina, com três linhas celulares de cancro da mama metastático (triplo-negativos ou ER-positivo), foi 7 a 36 vezes superior comparativamente aos seus equivalentes não direcionados ou funcionalizados com um péptido não-específico. A superior associação celular conduziu a um incremento de citotoxicidade, na ordem das 8,8 a 17 vezes. No entanto, a actividade terapêutica do PEGASEMP™ *in vivo* não ultrapassou a eficácia geral do Caelyx® (sobrevivência média de 46 dias e duas respostas completas), e resultou apenas numa redução marginal do crescimento tumoral relativamente aos murganhos não tratados. Apesar disso, o PEGASEMP™ prolongou significativamente a sobrevivência (16 *versus* 28 dias, Log-rank p = 0,0015) e reduziu a incidência de nódulos metastáticos no mesentério (33% *versus* 77%, p = 0,0409), em comparação com murganhos não tratados.

Por forma a enfatizar a relevância terapêutica da nucleolina, a sua expressão foi avaliada em tecidos humanos de carcinoma mamário, em tumores primários e correspondentes metástases ganglionares, com destaque para o subtipo triplo-negativo. A nucleolina foi positivamente identificada nas amostras de cancro da mama primário e nas metástases dos nódulos linfáticos, apesar de nem todas as lesões secundárias sobre-expressarem a proteína. A expressão da nucleolina foi também evidente em 78% das biópsias de cancro da mama triplo-negativo analisadas. No entanto, foram observadas diferenças no padrão de expressão da proteína entre os subtipos de carcinoma triplo-negativo e luminal A. Apesar de ambos apresentaram um padrão de expressão nuclear, o primeiro revelou uma coloração com destaque do nucléolo, enquanto o último apresentou uma distribuição da nucleolina por todo o núcleo. Não foi identificada uma associação significativa entre a expressão da nucleolina nos tumores triplo-negativos com outros fatores clínico-patológicos. Não obstante, uma associação significativa foi identificada entre nucleolina e as citoqueratinas 5/6, com

uma frequência de expressão da nucleolina de 89,5% nos tumores CK5/6-negativos, em comparação com 60% no grupo CK5/6-positivos (p = 0.015).

No geral, estes resultados sugerem a nucleolina como um potencial alvo terapêutico no cancro da mama metastático e/ou triplo-negativo, e suporta a lógica do desenvolvimento de abordagens terapêuticas direccionadas para esta proteína com vista ao tratamento desta doença. No que diz respeito à utilização dos lipossomas sensíveis ao pH, funcionalizados com o péptido F3, e contendo doxorrubicina, será ainda necessário explorar diferentes regimes terapêuticos que permitam aumentar a exposição sistémica ao fármaco.

Abbreviations list

ADAMTS-2	ADAM metallopeptidase with thrombospondin type 1 motif 2
Aes	Amino-terminal enhancer of split
AIC	Akaike's information criteria
Akt	Protein kinase B
aPKC	Atypical protein kinase C
BRCA1	Breast cancer 1 gene
BCL2	B cell lymphoma 2
bFGF	Basic fibroblast growth factor
BL1	Basal-like 1
BL2	Basal-like 2
BMDC	Bone marrow-derived cell
CAF	Cancer-associated fibroblasts
CCL7	C-C motif chemokine ligand 7
CCR4	C-C motif chemokine receptor 4
Cdc42	Cell division cycle 42
c-FMS	Macrophage colony-stimulating factor receptor
CHEMS	3b-hydroxy-5-cholestene-3-hemisuccinate
CHOL	Cholesterol
CI	Confidence interval
CK2	Casein kinase 2
COX2	Cyclooxygenase 2
CRYAB	Alpha basic crystalline gene
CTC	Circulating tumor cells
CXCL12	Chemokine ligand 12
CXCR4	C-X-C motif chemokine receptor 4
DAB	3,3'-diaminobenzidine
DLG	Discs large
DNA	Desoxyribonucleic acid
DOPE	1,2-dioleoyl-sn-glycero-3-phosphoethanolamine
DSPC	1,2-distearoyl-sn-glycero-3-phosphocholine
DSPE-PEG_{2K}	1,2-distearoyl-sn-glycero-3-phosphoethanolamine-N [methoxy(polyethylene glycol)-2000]
DSPE-PEG_{2K}-maleimide	1,2-distearoyl-sn-glycero-3-phosphoethanolamine-N [maleimide(polyethylene glycol)-2000]
DT	Doubling time
DXR	Doxorubicin
E-cadherin	Epithelial-cadherin
ECM	Extracellular matrix

EDTA	Ethylenediaminetetraacetic acid disodium salt dihydrate
EGF	Epidermal growth factor
EGFR	Epidermal growth factor receptor
EMT	Epithelial-to-mesenchymal transition
ER	Estrogen receptor
ERK1/2	Extracellular signal-regulated protein kinases 1 and 2
FAK	Focal adhesion kinase
FDA	Food and Drug Administration
FGF2	Fibroblast growth factor 2
FGFR1	Fibroblast growth factor receptor 1
FGFR2	Fibroblast growth factor receptor 2
FISH	Fluorescence in situ hybridization
HBS	HEPES buffer saline
H&E	Hematoxylin and eosin
HEPES	4-(2-hydroxyethyl)piperazine-1-ethanesulfonic acid
HER2	Human epidermal receptor 2
HGF	Hepatocyte growth factor
HGFR	Hepatocyte growth factor receptor
HIF1a	Hypoxia inducible factor 1 a
HMEC-1	Human microvascular endothelial cell line
hnRNP K	Human heterogeneous nuclear ribonucleoprotein
HORMAD1	HORMA domain-containing protein 1 gene
HPC	Hematopoietic progenitor cells
HPV18	Human papillomavirus 18
HRP	Horse Radish Peroxidase
IC50	Inhibitory concentration at 50% effect
IGF1	Insulin-like growth factor 1
IHC	Immunohistochemistry
IM	Immunomodulatory subtype
JAK2	Janus kinase 2
KRAS	Kirsten ras oncogene homolog
LAR	Luminal androgen receptor subtype
LGL	Lethal giant larvae
LHRH	Luteinizing hormone–releasing hormone
LOX	Lysyl oxidase
LOXL2	Lysyl Oxidase-Like 2
M	Mesenchymal subtype
MAPK	Mitogen-activated protein kinase
M-CSF	Macrophage colony-stimulating factor

MDSC	Myeloid-derived suppressor cells
MEK1/2	Mitogen-activated protein kinase kinase 1/2
MES	2-(N-Morpholino) ethanesulfonic acid
MET	Mesenchymal-to-epithelial transition
miR	microRNA
MK	Midkine
MMP	Matrix metalloproteinase
MMP-2	Matrix metalloproteinase 2
MMP-7	Matrix metalloproteinase 7
MMP-9	Matrix metalloproteinase 9
mRNA	Messenger RNA
MSC	Mesenchymal stem cells
MSL	Mesenchymal stem-like subtype
mTOR	Mechanistic target of rapamycin
N-cadherin	Neuronal-cadherin
NFkB	Nuclear factor κB
NK	Natural killer
NPs	Nanoparticles
NTS	No special type
OPG	Osteoprotegerin
OR	Odds ratio
PALS1	Protein associated with Lin-7 1
PAR	Partitioning defective protein
PARP	Poly (adenosine diphosphate-ribose) polymerase
PATJ	PALS1-associated tight-junction protein
PBS	Phosphate-buffered saline
pCR	Pathological complete responses
PDGFR	Platelet-derived growth factor receptor
PDLLA	PEGylated poly (D, L-lactide)
PEG	Poly (ethylene glycol)
PEG–PLA	Poly (ethylene glycol)–polylactic acid
PI3K	Phosphoinositide-3-kinase
PIK3CA	Phosphatidylinositol-4,5-bisphosphate 3-kinase catalytic subunit alpha
PIK3R1	PIK3 regulatory subunit 1
PLGA	PEGylated poly (D, L-lactic-co-glycolic acid)
PR	Progesterone receptor
PRMT5	Protein arginine methyltransferase 5
PTEN	Phosphatase and tensin homolog
PTN	Pleiotrophin
RAKNL	Nuclear factor κB ligand

rDNA	Ribosomal DNA
RGG	Carboxyl (C)-terminal of arginine-glycine-glycine-rich
RhoD-PE	L-α-Phosphatidylethanolamine-N-(lissamine rhodamine B sulfonyl)
RNA	Ribonucleic acid
RPTPb/z	Receptor protein tyrosine phosphatase b/z
rRNA	Ribosomal RNA
S100A8	S100 calcium binding protein A8
S100A9	S100 calcium binding protein A9
SCRIB	Scribble complex
scuPA	Single-chain uPA
SGR	Specific growth rate
siRNA	Small interfering RNA
SIRPa	Signal regulatory protein a
STAT3	Signal transducer and activator of transcription 3
TAM	Tumor-associated macrophages
TGF-b	Transforming growth factor b
TIMP-3	Tissue inhibitor of metalloproteinase 3
TNBC	Triple-negative breast cancer
TNF-a	Tumor necrosis factor a
TNM	Tumor – Node – Metastasis
TRAIL	TNF-related apoptosis-inducing ligand
UICC	Classification of the International Union Against Cancer
UNS	Unstable subtype
uPAR	Urokinase receptor
VCAM1	Vascular cell adhesion molecule 1
VEGF	Vascular endothelial growth factor
VEGF-A	Vascular endothelial growth factor A
VEGF-C	Vascular endothelial growth factor C
VEGF-D	Vascular endothelial growth factor D
VEGFR1	Vascular endothelial growth factor receptor 1
VLA-4	a4b1 integrin
ZEB	Zinc-finger E-box-binding

Preface

The present dissertation intends to describe the main achievements of the project entitled “Meeting the needs of breast cancer: a *nucleolin’s* perspective”. The potential of nucleolin, expressed by cancer cells and endothelial cells of tumor blood vessels, as a therapeutic target in the settings of metastatic and/or triple-negative breast cancer is discussed. The dissertation is organized in five chapters reflecting the publication strategy followed in this project.

The ***first chapter*** addresses the problematic of breast cancer disease and the current therapeutic challenges faced in this field. In this respect, a special focus is given to metastatic breast cancer and the triple-negative subtype, which represent two major hurdles of the breast malignancy in the present days. Understanding the biology underlying metastases and the triple-negative subtype, and their clinical implications, are fundamental to adequately tailor therapeutic interventions capable of tackling these diseases.

The ***second chapter*** describes the optimization of a mouse model of metastatic breast cancer and the practical implications for the research work on the field of metastasis. The inoculation of different cell densities was performed in order to establish the requirements for an increased metastatic efficacy of the mouse model without the constraint of primary tumor surgical removal.

The ***third chapter*** focuses on the preclinical validation of nucleolin as a target in metastatic breast cancer, and evaluation of the therapeutic potential of F3 peptide-targeted pH-sensitive liposome containing doxorubicin. In vitro assays were performed in order to determine the specificity of the interaction between the F3 peptide-targeted liposomes and metastatic breast cancer cells. Using the conditions determined in the second chapter to establish the mouse model, the in vivo therapeutic study evaluated the impact of doxorubicin-encapsulating liposomes targeting nucleolin, on the progression of metastatic breast cancer.

The ***fourth chapter*** aimed at a preliminary evaluation of nucleolin expression in patient-derived breast tumor tissues, both in primary tumors and corresponding lymph node metastases, with emphasis on triple-negative breast carcinomas.

The ***fifth chapter*** summarizes the most relevant findings of the preceding chapters and contextualizes them in future work.

Chapter 1

General introduction

1.1. Breast cancer

In an aging and growing world population, cancer is a prevailing disease and a considerable societal pressure. Global estimates indicated that 14.1 million new cancer cases and 8.2 million deaths occurred in 2012. Amongst all cancers, lung and breast represent the most frequently diagnosed and the leading cause of cancer-related deaths in males and females, respectively. In respect to breast cancer, this affliction reached 1.7 million women in 2012, of which, approximately one third, died from the disease[1].

1.1.1. Molecular and clinico-pathological features of breast cancer

Human breast tumors differ in their natural history and responsiveness to therapy[2]. Currently, disease management relies on well-validated clinico-pathological prognostic variables and predictive biomarkers. Classical prognostic factors include tumor size, lymph node status, the proliferation index and tumor histological characteristics. Tumor size has been a good prognostic indicator for distant relapse in lymph node-negative breast carcinoma patients[3], while nodal status is predictive of both overall survival and disease-free survival[4]. Tumor histological grade is also an important factor with prognostic value. High grade tumors, poorly differentiated, are usually associated with a more aggressive behavior than well differentiated, low grade tumors[5]. Such parameters with individual prognostic significance have been integrated in multiparametric tools that assist clinical decisions. These include TNM (Tumor – Node – Metastases) staging[6] and the Nottingham prognostic index[7,8]. However, this classification of breast cancer fails to fully capture the biological diversity characterizing these tumors[9]. Prognostic signatures determined by the expression of estrogen (ER) and progesterone (PR) receptors, and the human epidermal growth factor receptor 2 (HER2), further aid in the stratification of patients, and are regarded as the main drivers for the selection of suitable therapeutic options[10-13].

The systematic analysis of gene expression patterns in human breast tumors contributed to the current knowledge of breast cancer molecular complexity and identified distinctive molecular portraits that unveiled similarities and differences among the tumors[14]. Through hierarchical clustering analysis of gene expression profiling (Figure 1.1), Perou *et al*. identified four biologically distinct disease entities – luminal, HER2-enriched, basal-like and normal breast-like[14]. The distinction between two luminal-like subtypes – luminal A and luminal B – was further uncovered by Sørlie *et al*., which were not evident with the traditional histopathological methods[15,16]. The expression of ER and ER-related genes, proliferation-related genes, and HER2 and other genes mapping to the region of HER2 amplicon on chromosome 17 were the major drivers determining the molecular subtypes (Figure 1.1)[14-17].

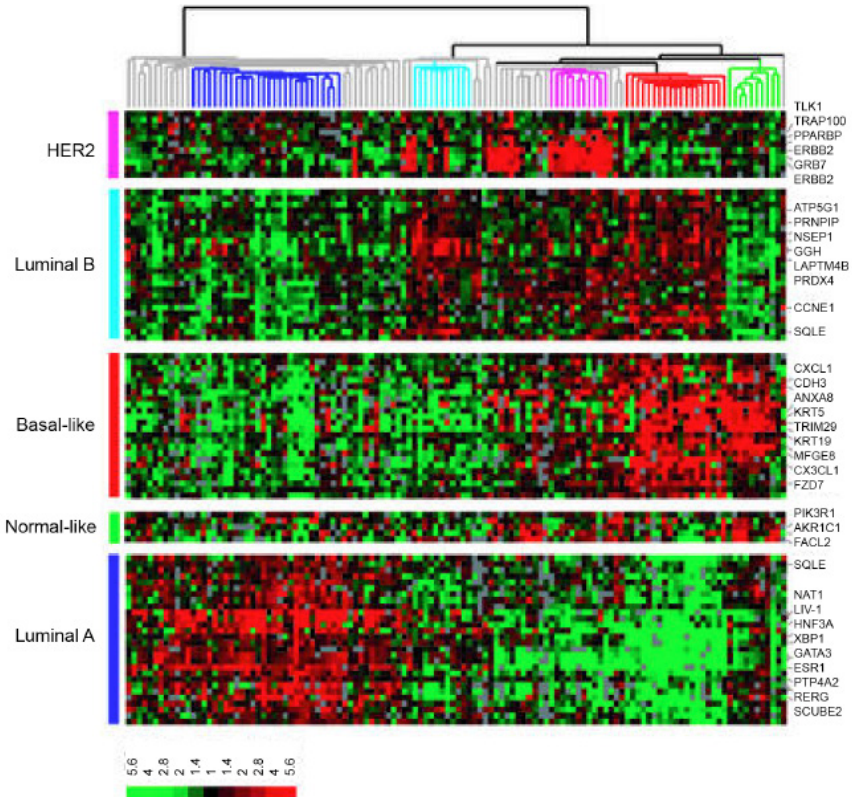

Figure 1.1: Hierarchical clustering of 115 tumor tissues and 7 nonmalignant tissues using the intrinsic gene set (adapted from Sørlie *et al.*, 2003[16]).

An intrinsic gene list comprising 534 genes was used for clustering 122 tissue samples based on similarities in gene expression. Tumor samples clustered into five major subgroups represented in the dendogram in a similar color-code, whereas branches corresponding to tumors with low correlation to any subtype are shown in gray. Gene clusters associated with each intrinsic breast cancer subtype are shown on the right. Scale bar represents fold change for any given gene relative to the median level of expression across all samples

The recognition of intrinsic biological subtypes within the breast cancer spectrum have now become part of the clinical practice through the use of a more familiar immunohistochemical approach[18]. As summarized in Table 1.1, the combined evaluation of ER and PR, HER2 protein overexpression and/or oncogene amplification, and Ki-67 labeling index was adopted for a simplified classification of breast tumor subtypes[18-20].

Table 1.1: Surrogate definitions of intrinsic subtypes of breast cancer (adapted from Coates *et al.*, 2015[21]).

Intrinsic subtype	Clinico-pathological definition	Notes
Luminal A	**Luminal A**	
	all of: ER and PR positive (≥20%) HER2 negative Ki-67 low (<20%)	An empiric cutoff of ≥20% PR-positive tumor cells was statistically chosen and proved significant for predicting survival differences within immunohistochemical-defined luminal A tumors[22].
Luminal B	**Luminal B (HER2 negative)**	
	ER positive HER2 negative *and at least one of:* Ki-67 high (≥20%) PR negative/low (<20%)	Standardized cutoffs for Ki-67 have not been established and might vary between laboratories. The 20% threshold was accepted as indicative of high Ki-67 status[23], although others have proposed a cutoff of 14%[19].
	Luminal B (HER2 positive)	
	ER positive HER2 overexpressed or amplified Any PR and Ki-67	
HER2-enriched	**HER2 positive (non-luminal)**	
	HER2 overexpressed or amplified ER and PR absent	
Basal-like	**Triple-negative (ductal)**	
	ER, PR and HER2 negative	Triple-negative tumors do not overlap completely with the basal-like subtype[24-26], and also includes some special histological types such as medullary and adenoid cystic carcinoma with low risks of distant recurrence[27].

Among the breast cancer intrinsic subtypes, the basal-like group has generated much interest due to its substantial overlap with a subset of tumors with a triple-negative immunohistochemical signature. Nevertheless, it is recognized that molecularly- and immunohistochemically-defined classes do not overlap completely[24-26]. Despite this topic still being subject for some controversy, other panels of immunohistochemical surrogate markers, which include the expression of cytokeratins 5/6 (CK5/6) and/or the epidermal growth factor receptor 1 (EGFR), have been proposed to define basal-like breast cancers[24,25,28]. According to this classification, approximately 74–84% of triple-negative tumors express basal cytokeratins and EGFR[24,25]. Therefore, it is reasonable to assume that the triple-negative identity comprises two subsets of breast tumors characterized by basal- and non-basal-like phenotypes[26].

1.1.2. Patterns of recurrence

Breast cancer subtypes have been related to distinct timing and patterns of recurrence. ER-negative tumors have a higher risk of relapse within the first four years of diagnosis, while ER-positive tumors are associated with late recurrence (> 5 years)[29-31]. Bone is the most common metastatic site in the luminal A subtype. Comparatively, luminal B (HER2-positive) and HER2-enriched tumors have been associated with a significantly higher rate of brain, liver, and lung metastases[32,33]. However, the incidence of visceral metastases in luminal B tumors is only attained in the long-term follow-up, compared to HER2-enriched subtype[31].

Patients with triple-negative breast cancer (TNBC) present an increased rate of brain, lung, and distant nodal metastases, and are associated with significantly lower incidence of liver and bone recurrence[32,33]. Underling this recurrence patterns, both HER2-enriched and the triple-negative subtypes present shorter overall survival. Yet, those patients with TNBC were shown to have an increased likelihood of mortality within 5 years of diagnosis, and did not follow the trend of other hormone-positive breast cancer subtypes, which showed annual improvements in 3-year survival rates between 1998 and 2004[34].

1.1.3. Current therapeutic approaches

The treatment of breast cancer relies on several factors, including disease stage, tumor burden (defined as the number and site of metastases), histological and molecular subtype, menopausal status, or previous therapies[35]. In the setting of early breast cancer, surgery (mastectomy or breast-conserving surgery) and radiotherapy play an important role in the management of the disease[21,36]. However, the value of surgery in patients with advanced breast cancer is still under debate[37-40], and systemic therapy is the predominant treatment in this setting[35]. Table 1.2 summarizes the therapeutic agents being currently used for the treatment of breast cancer.

Table 1.2: Therapeutic agents currently used in the treatment of breast cancer.

Type of therapy	Drug	Class	Target
Endocrine[35,41,42]	Tamoxifen	Estrogen receptor modulator	Estrogen receptor
	Anastrozole Letrozole Exemestane	Aromatase inhibitor	Aromatase enzyme
	Fulvestrant	Estrogen receptor downregulator	Estrogen receptor
	Goserelin	LHRH blocker	LHRH receptor
Anti-HER2[35,43,44]	Trastuzumab	Monoclonal antibody	HER2 receptor
	Lapatinib	Small molecule inhibitor	HER2/EGFR tyrosine kinase pathways
	Pertuzumab	Monoclonal antibody	HER2 receptor
	Trastuzumab-emtansine	Antibody-cytotoxic agent	HER2 receptor/tubuline
Chemotherapy[35,45]	Doxorubicin Epirubicin Liposomal doxorubicin	Anthracyclines	
	Paclitaxel Docetaxel Nanoparticle albumin-bound paclitaxel	Taxanes	
	Gemcitabine Capecitabine Fluorouracil	Antimetabolites	
	Vinorelbine	Vinca alkaloids	
	Ixabepilone	Epothilone B analog	
	Carboplatin Cisplatin	Platinum agents	
	Cyclophosphamide	Alkalyting agent	
Skeletal metastases[35,46]	Zelodronic acid Clodronate	Bisphosphonates	Osteoclast function
	Denosumab	Monoclonal antibody	RAKNL

Endocrine therapy is the preferred option for hormone receptor-positive disease, even in the presence of visceral metastases (Table 1.3)[35] . This therapy has shown significant activity in the treatment of patients with luminal A disease[47,48]. Tamoxifen is the standard of care for pre-menopausal women. The value of suppressing ovarian function has been a topic of controversy, particularly in patients previously treated with chemotherapy[36,49,50]. Factors arguing for the inclusion of ovarian suppression have been recently addressed in international consensus guidelines, and included age of 35 or less, the persistence of premenopausal estrogen level after adjuvant chemotherapy, or the involvement of four or more axillary nodes[21,35,51]. In patients contraindicated to Tamoxifen, a luteinizing hormone-releasing hormone (LHRH) agonist in combination with an aromatase inhibitor should be used (Table 1.2) [21,35,36]. The luminal B subtype has relatively lower benefit from endocrine treatment, partially due to a lower expression of estrogen receptors[12,52]. In addition, the expression of Ki-67 has also shown to predict benefit from endocrine therapy. A high Ki-67 score, determined after two weeks on endocrine therapy, predicted a poor long-term outcome for patients having neoadjuvant treatment with either Tamoxifen or an aromatase inhibitor[53,54]. Hence, the luminal B breast cancer subtype, being inherently more aggressive

than the luminal A, benefits from the addition of more aggressive therapy and is generally treated with both endocrine therapy and cytotoxic agents (Table 1.3)[21,35,36,55,56]. Although luminal A disease being usually less responsive to chemotherapy[55,56], a few selected patients at higher risk of relapse (extensive nodal involvement) might also benefit from the addition of cytotoxic agents[21].

The overexpression of HER2 in luminal tumors have also been associated with increased relapse rate in patients treated with endocrine therapy, compared with HER2 negative tumours[57]. Moreover, in those patients with HER2-overexpressing tumors, the combination of endocrine and anti-HER2 therapy revealed a significant therapeutic benefit (Table 1.3)[21,35,36,58,59], and recent evidence further suggested that complete resistance to both Anastrozole and Trastuzumab sequential monotherapies can be overcome in a proportion of patients, through the combined treatment with these compounds[60].

Table 1.3: Systemic treatment recommendations for breast cancer (adapted from Coates *et al.*, 2015[21]).

Breast cancer subtype	Treatment	Notes
Luminal A	Endocrine therapy	Chemotherapy could be used in selected patients under some indications (large tumor, grade 3 disease, involvement of four or more lymph nodes).
Luminal B (HER2-negative)	Endocrine therapy ± Chemotherapy	Inclusion of chemotherapy is supported by a high histological grade, high proliferation (Ki-67), and low hormone receptor status and HER2 positivity.
Luminal B (HER2-positive)	Chemotherapy + anti-HER2 + Endocrine therapy	
HER2-positive (non-luminal)	Chemotherapy + anti-HER2	
Triple negative	Chemotherapy	

Trastuzumab is a keystone systemic therapy for (non-luminal) HER2-overexpressing tumors[61]. The combination of this monoclonal antibody with chemotherapy has shown to improve overall survival and reduce the risk of disease recurrence in the adjuvant setting (Table 1.3)[62-64]. However, increased cardiac dysfunction has been observed when Trastuzumab is added to anthracycline-based chemotherapy[64,65]. Notwithstanding, Slamon *et al*. demonstrated that similar disease-free or overall survival could be attained with a taxane-based regimen, together with a lower risk of cardiotoxicity[64].

Among breast cancer subtypes, the triple-negative constitutes one of the most challenging groups. The interest in TNBC arises from the current absence of targeted therapies for this group of patients, associated with a poor prognosis. At the present time the only systemic therapy available for patients with triple-negative breast disease is

chemotherapy (Table 1.3). Current treatment strategies include anthracyclines, taxanes, Ixabepilone and platinum agents. Interestingly, triple-negative breast tumors are more sensitive to chemotherapy than the other subtypes, an observation supported by a number of studies on neoadjuvant chemotherapy[66-68]. The strong association of triple-negative breast tumors with germline mutations in the *BRCA1* gene[69] has also attracted attention to the potential use of platinum-based compounds in TNBC therapy (Table 1.2)[70-73]. However, platinum agents failed to demonstrate improved benefit in the context of advanced breast cancer[74], and warrant further elucidation on their efficacy. Platinum-based chemotherapy is currently recommended only for patients with known *BRCA* mutation[21,35]. In patients with breast cancer bone metastases, the routine use of bone-modifying agents, such as bisphosphonates or denosumab (Table 1.2), are advised in combination with other systemic therapy[35].

1.2. Meeting the needs of breast cancer

Triple-negative breast cancer and metastases represent two of the major hurdles in breast disease. On one hand, the benefits of targeted therapies have eluded patients with TNBC due to the absence of well-defined molecular targets. On the other hand, development of tumor metastases is the major cause of death of these patients. Therefore, uncovering novel therapeutic targets represent an area of great need.

1.2.1. Metastatic disease in breast cancer

Standard therapeutic strategies have shown limited success in the treatment of metastatic disease[75]. Currently, the main treatment goal is palliation of symptoms and maintenance of the patient's quality of life, thus reinforcing the need to establish effective therapies capable of preventing and/or targeting metastases. Hence, it is imperative to understand the biology underlying the metastatic process.

1.2.1.1. Molecular drivers of metastases

Progression towards overt metastatic disease comprises a complex process rationalized in a series of sequential and interrelated events portrayed by cancer cells: local invasion of the surrounding tissue, transendothelial migration into blood/lymphatic vessels (intravasation), survival and translocation through the hematogenous/lymphatic circulation, exit from the vessels into the parenchyma of distant tissues (extravasation), and survival and adaptation to the new microenvironment enabling proliferation into macroscopic lesions

(colonization)[76].

Migration and plasticity of cancer cells, as well as plasticity of the surrounding microenvironment, are important transformations taking place at the earliest stage of metastatic dissemination. By engaging into different cellular programs, cancer cells adopt distinct mobility patterns, either collective or as single-cell, which coexist within the tumor and can switch in response to changes in epithelial plasticity[77,78]. The epithelial to mesenchymal transition (EMT) has been increasingly recognized as a crucial event in cancer progression and metastases[79], and is a modulator of plasticity in single-cell invasion[77]. EMT is induced in response to microenvironmental cues involving transforming growth factor β (TGF-β) secreted by stromal cells, such as macrophages, mesenchymal stem cells and platelets[80-82]. The transcriptional control by EMT-inducing transcription factors induces the loss of epithelial phenotype and cell polarity and the concomitant gain of mesenchymal traits that favor motility and invasion (Figure 1.2)[83]. In addition, cancer cells undergoing EMT also acquire the CD44^{high}/CD24^{low} expression pattern and stem cell-like properties[84,85], which have been implicated in therapeutic resistance and tumor relapse[86-88]. Noteworthy, increased expression of EMT-related molecular markers was associated to the highly aggressive basal-like breast cancer subtype[14,15,89,90].

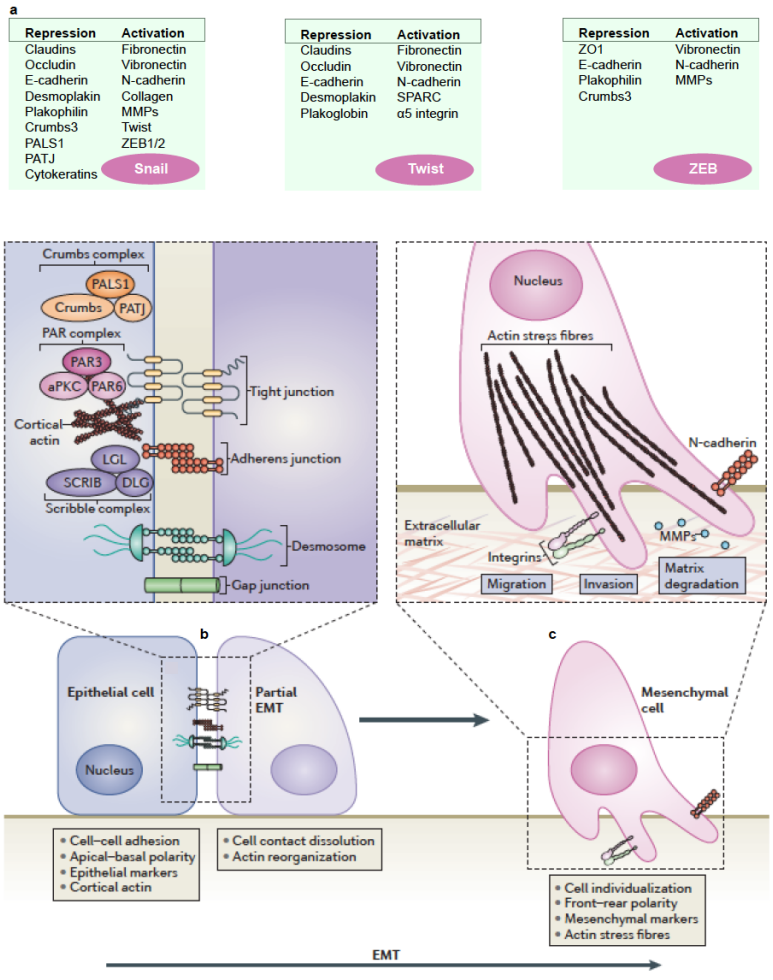

Figure 1.2: Cellular events during epithelial to mesenchymal transition (adapted and modified from Lamouille *et al*., 2014[83]).

Epithelial to mesenchymal transition (EMT) is driven by SailL, Twist and zinc-finger E-box-binding (ZEB) transcription factors that repress epithelial marker genes and activate genes associated with the mesenchymal phenotype (a). The first steps of EMT are the disassembly of epithelial cell–cell contacts (tight junctions, adherens junctions, desmosomes and gap junctions) and the loss of cell polarity through the disruption of the Crumbs, partitioning defective (PAR) and Scribble (SCRIB) polarity complexes. Following disassembly of adherence junctions, membrane-bound β-catenin is translocated to the cell nucleus where it modulates the expression of genes implicated in cell proliferation, transformation and tumor progression[91,92] (b). The expression of N-cadherin results in the rearrangement of the actin cytoskeleton by mediating Rho-induced stress fibers, and cells acquire motility and invasive capacities by forming lamellipodia, filopodia and invadopodia, and by expressing matrix metalloproteinases (MMPs) that degrade extracellular matrix (ECM) proteins[83,93] (c). Following dissemination, cancer cells can revert to an epithelial state by mesenchymal to epithelial transition (MET), leading to the formation of secondary carcinomas. aPKC, atypical protein kinase C; DLG, discs large; LGL, lethal giant larvae; PALS1, protein associated with Lin-7 1; PATJ, PALS1 associated tight-junction protein; E-cadherin, epithelial-cadherin; N-cadherin, neuronal-cadherin.

Invasion and intravasation events require the degradation of basement membrane and extracellular matrix. In this context, the proteolytic activity of matrix metalloproteinases (MMP) family has a prominent role in the modulation of tumor microenvironment[94]. Through the process of extracellular matrix (ECM) turnover, MMPs also regulate signaling pathways that control cell growth, inflammation and angiogenesis by releasing cell-surface and matrix-bound growth factors and cytokines, such as epidermal growth factor (EGF), tumor necrosis factor α (TNF-α), vascular endothelial growth factor (VEGF), TGF-β, or the receptor activator of nuclear factor κB ligand (RANKL)[94].

Abnormal remodeling of the extracellular milieu also characterizes cancer disease. In breast tumors, increased mammographic breast density has been correlated with poor prognosis[95]. Provenzano *et al*. additionally demonstrated that collagen-dense microenvironments promote mammary tumor formation, invasion, and metastases in a transgenic mouse model[96]. Crosslinking of collagen fibers by overexpressed lysyl oxidase (LOX) increases ECM stiffness and also promotes cancer cell invasion and progression through the activation of integrin signaling[97,98]. Additionally, macrophages localized to perivascular areas within tumors, help tumor cells traverse vessel barriers[99] (Figure 1.3). Although the leaky endothelium, *per se*, facilitates transendothelial migration of cancer cells[100], additional molecular changes also modulate their ability to cross pericyte and endothelial cell barriers. Cell division cycle 42 (Cdc42)-mediated expression of β1 integrin[101] and amino-terminal enhancer of split (Aes)-mediated inhibition of the Notch signaling[102] have been identified as regulatory mechanisms, promoting and blocking intravasation, respectively. Nevertheless, it is estimated that only 0.02% of cancer cells that enter into the systemic circulation will

ultimately develop into macroscopic metastases[103]. Resistance to anoikis is an important survival skill of cancer cells during systemic circulation. Neurotrophic tyrosine kinase receptor was shown to induce the formation of cellular aggregates that survive and proliferate in suspension by activating phosphoinositide-3-kinase/protein kinase B (PI3K/Akt) pathways[104]. Circulating tumor cells (CTC) are also exposed to clearance by the immune system and mechanical destruction by the hemodynamic shear forces. CD47, a molecule expressed on multiple human tumor types[105-110], has been implicated in CD47-signal regulatory protein α (SIRPα) pathway-mediated evasion of CTC from immune surveillance through the inhibition of phagocytosis[105]. Platelets also support cancer cell survival by escorting them in circulation and facilitating extravasation (Figure 1.3).

The activation of Akt signaling through context-dependent mechanisms plays a critical role for the survival of disseminated cancer cells in non-orthotopic tissue microenviroments. Survival and outgrowth of carcinoma cells in the bone marrow is regulated by c-Src-mediated Akt signaling in response to chemokine ligand 12 (CXCL12) and TNF-related apoptosis-inducing ligand (TRAIL)[111]. In the lung microenviroment, binding of macrophages to cancer cells through the vascular cell adhesion molecule 1 (VCAM1) and α4 integrins triggers Akt activation and protects cancer cells from pro-apoptotic cytokines such as TRAIL[112]. Additionally, the establishment of a supportive pre-metastatic niche facilitates the adaptation of these cells to the foreign tissues. Nevertheless, cancer cells might persist as microcolonies in a state of dormancy before they are able to proliferate and form large macroscopic metastases[113]. These occult micrometastases may persist in a state of cellular quiescency or macrometastatic dormancy achieved by a balance between proliferation and apoptosis due to the inability to trigger neoangiogenesis or overcome immunosurveillance[113].

1.2.1.2. Contribution of cancer-stromal cell interactions for tumor progression and the pre-metastatic niche

Cancer cells are supported by a rich microenvironment composed of various resident and recruited cell types, together with the extracellular matrix[114]. Among the most prominent components of the tumor stroma are endothelial cells. Under pathologic conditions, quiescent endothelial cells are activated (angiogenic switch) to form new blood vessels that sustain neoplastic expansion[115]. The most prominent inducer of angiogenesis is vascular endothelial growth factor A (VEGF-A), but the sprouting of new vessels can also be orchestrated by other molecules, such as fibroblast growth factor 2 (FGF2) or angiopoietins[116,117]. Additionally, the role of tumor pericytes in stabilizing vascular integrity and function is compromised in cancer disease, therefore promoting intravasation of carcinoma cells across the disrupted endothelium[118,119].

The chronic activation of angiogenesis is promoted by a repertoire of bone marrow-derived cell (BMDC) types, including macrophages, neutrophils, mast cells and myeloid progenitors that release a plethora of pro-angiogenic growth factors[120-122]. Activated macrophages produce vascular endothelial growth factors C and D (VEGF-C and VEGF-D), which correlates with peritumoral increase of lymphatic microvessels in human cervical cancer[123]. Additionally, BMDCs also produce matrix-degrading enzymes (MMPs, cysteine cathepsine proteases, heparanases), which release ECM-sequestered pro-angiogenic signals with otherwise limited bioavailability and, concomitantly, facilitate local invasion by cancer cells[121,122,124-127].

The pro-tumorigenic activity of cancer-associated fibroblasts (CAF) have been demonstrated in mouse models of prostate[128] and breast[129] cancer upon the transplantation of admixed neoplastic cells with CAFs. CAFs within the tumor microenvironment are activated by various stimuli, including TGFβ, FGF2 and secreted proteases[130,131], and have been implicated in aspects of tumor progression involving ECM remodeling[132] and vascular permeability and angiogenesis[133,134]. These cells also mediate tumor-enhancing inflammation through the activation of nuclear factor κB (NFκB) signaling by pro-inflammatory factors[135]. Interestingly, CAFs might also be involved in metastatic tropism. The cytokines CXCL12 and insulin-like growth factor 1 (IGF1), produced by these cells in the primary tumor microenvironment, induced a skew of a carcinoma population of triple-negative breast cancer cells toward a prevalence of clones with increased c-Src activation and a predisposition to the bone marrow[136].

The distribution pattern of metastases for individual solid tumors is not random. The “seed and soil” hypothesis, proposed over a century ago by Steven Paget[137], still forms the basis of our understanding of the metastatic process, and accumulating evidence suggests the formation of a permissive niche at the metastatic sites preceding the arrival of disseminated cancer cells[138]. In defining the pre-metastatic niche, Kaplan *et al*. demonstrated that vascular endothelial growth factor receptor 1 (VEGFR1)-positive bone marrow hematopoietic progenitor cells, and expressing α4β1 integrin (VLA-4), tethers to fibronectin expressed by fibroblasts at secondary sites, upon induction by primary tumor specific factors (Figure 1.3)[139]. The production of matrix metalloproteinase 9 (MMP-9) and increased expression of CXCL12 in these clusters, modify the microenvironment and create a chemokine gradient, enabling the attraction of C-X-C motif chemokine receptor 4 (CXCR4)-positive neoplastic cells and their incorporation into the lung niche[139].

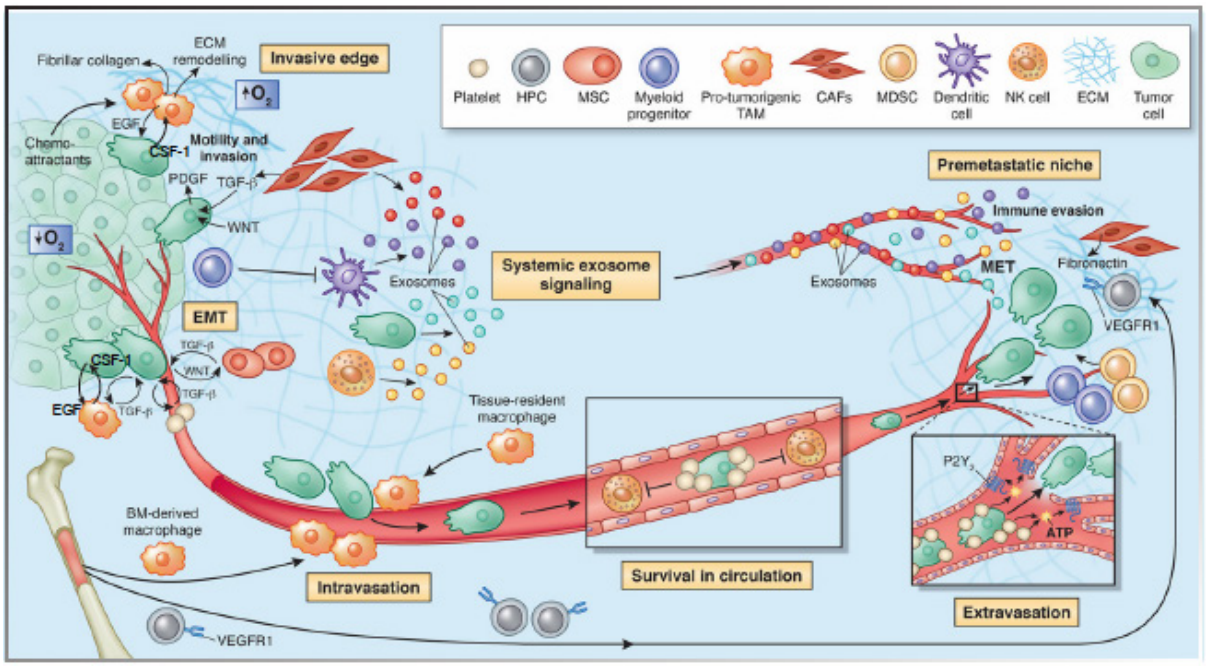

Figure 1.3: Cancer and stromal cells converge to support metastatic dissemination and colonization of secondary sites (adapted and modified from Quail & Joyce, 2013[140]).

Tumor-associated macrophages (TAM), platelets, and mesenchymal stem cells (MSC) contribute to epithelial-to-mesenchymal transition (EMT) at primary sites, enabling cancer cells to acquire a mobile/invasive phenotype. One major mediator of this event is TGF-β, which participates in a paracrine signaling loop with cancer cells. TAM, cancer-associated fibroblasts (CAF) and myeloid progenitor cells also tend to cluster at the invasive/leading edge of the primary tumor, where they play an immunosuppressive role by interfering with dendritic cell differentiation. Additionally, the synergistic interaction between neoplastic cells and macrophages via EGF/CSF-1 paracrine loop leads to chemotaxis-mediated comigration and invasion of both cell types[141]. Interestingly, this mechanism is also involved during the intravasation of carcinoma cells at perivascular areas with macrophage clusters[99]. A potential mechanism by which circulating tumor cells survive in the bloodstream is through the formation of platelet-fibrinogen microthrombi, which act as a physical barrier partially protecting the malignant cells from natural killer (NK) cell–mediated elimination[142,143]. An additional platelet-mediated mechanism, involving the activation of endothelial P2Y2 receptor, was further shown to promote neoplastic extravasation[144]. At secondary sites such as the lung, fibroblasts upregulate fibronectin, which serves as a docking site for hematopoietic progenitor cells (HPC) and the subsequent arrival of tumor cells. Immunosuppressive cell types, such as MDSC, also populate pre-metastatic niches where they help to direct metastatic dissemination by creating a niche permissive to tumor colonization. Recent studies have demonstrated that primary and secondary sites can communicate through exosomes, shed by primary cancer cells, immune and stromal cells. Factors contained in exosomes have organ tropism, modulate immune evasion, support mesenchymal-to-epithelial transition (MET), and are predictive of metastases and patient outcome.

Similarly, binding of VCAM1-expressing breast cancer cells to macrophages through α4β1 integrin, triggers the activation of Ezrin-PI3K/Akt survival pathway and shields cancer cells from pro-apoptotic cytokines such as TRAIL, and enables their survival in the pulmonary leukocyte-rich microenvironment[112]. Bone marrow-derived cells also play an important part in creating an immunosuppressed microenvironment, both at primary and secondary tumor sites. Myeloid-derived suppressor cells (MDSC) have been implicated in evading immune destruction by disabling the activity of $CD8^+$ cytotoxic T lymphocytes and natural killer (NK) cells (Figure 1.3)[145]. Secretion of VEGF-A, TNFα and TGFβ by primary tumors likely serves as the main mechanism for MDSCs recruitment to the pre-metastatic milieu through the expression of inflammatory chemoattractants S100 calcium binding protein A8 and A9 (S100A8 and S100A9)[146,147]. S100A9 was further implicated in the accumulation of MDSCs by inhibiting denditric cell differentiation[148]. The generation of a MDSC phenotype through impaired differentiation and maturation of immature myeloid precursor cells can also be mediated by tumor-derived exosomes (Figure 1.3)[149]. Moreover, horizontal transfer between carcinoma-derived exosomes and bone marrow progenitor cells was shown to "educate" these progenitors towards a pro-vasculogenic phenotype at pre-metastatic sites[150]. Nevertheless, exosomes secreted by some stromal cells, such as denditric and natural killer cells, are able to promote immune responses and tumor rejection[151,152].

1.2.1.3. Challenges in the treatment of metastatic disease

The development of therapeutic strategies for metastatic disease has been challenged by the complex nature of secondary lesions. Treatments are usually determined based on the characteristics of the primary tumors, but genetic and phenotypical discrepancies between primary lesions and their correspondent metastases have been reported[153,154]. One such example is the discordance in expression profile of ER, PR and HER2 observed in metastases from breast cancer patients. Shifting from positive to negative expression of these receptors was the prevailing alteration observed[154], which might partially explain the limited success of the conventional therapies in this setting[75]. The early dissemination of cancer cells also exposes them to selection and expansion of clones with the genetic changes most fitted to specific microenvironments (allopatric selection)[155]. Hence, heterogeneity among distant carcinoma lesions further contributes to the complexity of the problem[156].

Additional mechanisms, such as the epithelial to mesenchymal transition, also render metastatic cancer cells more resistant to treatment[157]. Twist, a transcription factor regulating EMT, was shown to promote paclitaxel resistance by two different mechanisms: upregulating Akt, which led to increased migration and invasion of cancer cells[158], and downregulating

estrogen receptor-α that resulted in loss of ER activity[159]. Clinical dormancy also renders current therapeutics less effective against the metastatic disease. Dormant cells in a quiescent state are likely resistant to the action of cytotoxic agents that exert their activity by disrupting of the mitotic process[160,161]. Additionally, preclinical evidence also suggests that activation of survival mechanisms in disseminated carcinoma cells might confer resistance to treatment[162,163].

1.2.1.4. Therapeutic opportunities for the treatment of metastases

The development of anti-metastatic therapies addresses potential therapeutic targets involved in either metastases initiation or progression. These molecular targets comprise tumor autologous factors involved in signal transduction, adhesion, motility, growth and survival of cancer cells, and microenvironmental factors such as chemokines, angiogenic promoters or stromal components (Figure 1.4 and 1.5).

A number of preclinical studies have explored the potential of blocking the early steps of neoplastic dissemination (Table 1.4). Due to its involvement in extracellular matrix turnover and regulation of signaling pathways controlling cell growth, inflammation, or angiogenesis, matrix metalloproteinases were envisioned as promising targets and led to a number of small-molecule MMP inhibitor drugs in phase III clinical trials[164]. However, these were shown to cause severe side effects and had limited benefit, possibly due to sub-optimally designed clinical studies regarding the stage of cancer, since MMP inhibitors were administered to patients with advanced cancer[164].

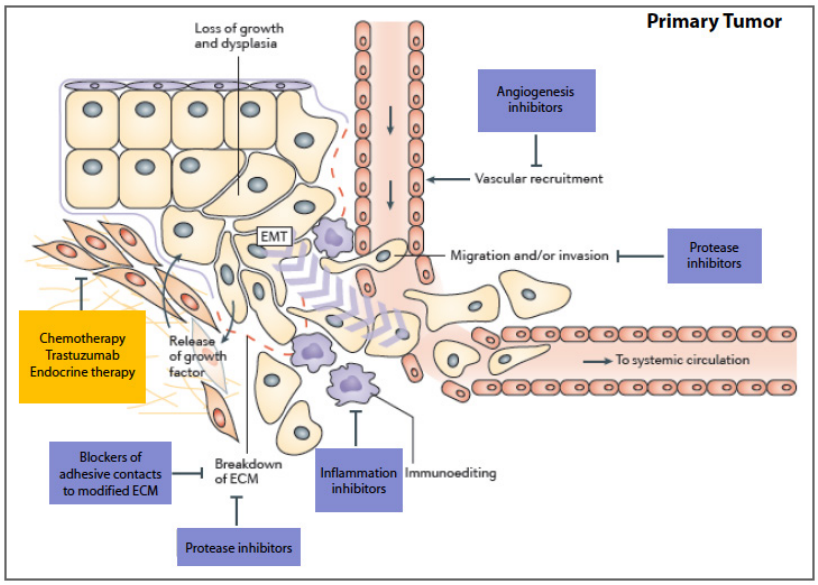

Figure 1.4: Potential targets amenable to therapeutic intervention in the early stages of the metastatic process (adapted and modified from Eckhardt *et al.*, 2012[165]).
Current therapies include chemotherapy, endocrine therapy for estrogen receptor positive tumors and Trastuzumab for HER2 positive cancers. Other possible interventions are shown, including protease inhibitors to block extracellular matrix (ECM) breakdown and tumor cell invasion, angiogenesis inhibitors and inhibitors of inflammation (such as cyclooxygenase 2, COX2) inhibitors.

Notwithstanding, clinically relevant therapeutic agents should be capable to impair established metastases. Although only ~5% of patients present distant metastases at the time of diagnosis[166], breast cancer can relapse years after successful treatment of the primary tumor, likely, as the result from the early dissemination of neoplastic cells[155,167]. Therefore, most patients may have already completed the initial events of the metastatic process. Targeting mechanistic pathways mediating later stages of cancer cell dissemination and supportive microenvironmental factors would represent a more clinically relevant rationale for anti-metastatic therapeutics (Figure 1.5).

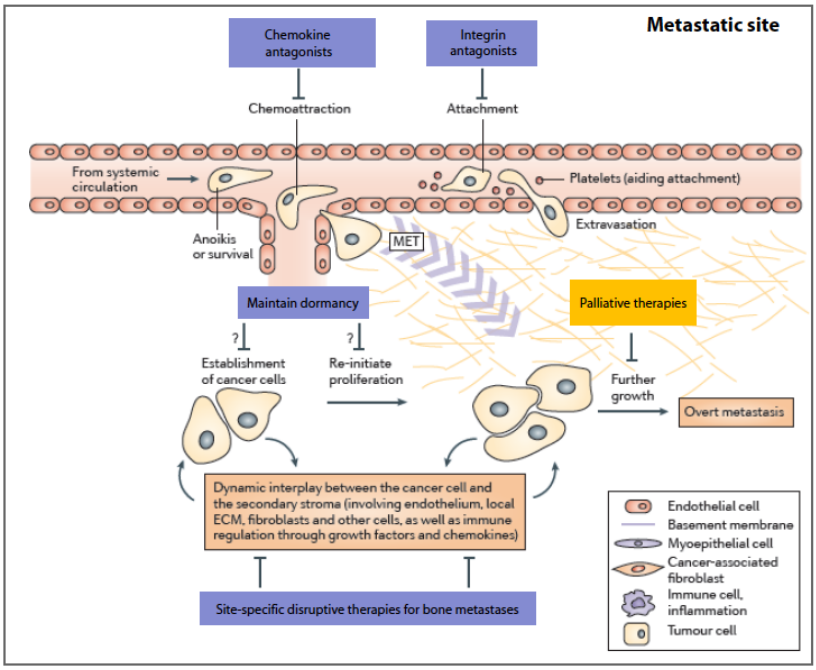

Figure 1.5: Potential targets amenable to therapeutic intervention in the later stages of the metastatic process (adapted and modified from Eckhardt *et al.*, 2012[165]).
At the secondary site, tumor cells can remain dormant in the tissue, either as single cells or as clinically undetectable micrometastases. Only a small fraction of tumor cells develops into overt metastases. How and when dormant cells reacquire growth potential is still unclear but is an attractive stage for therapeutic intervention. For metastases in bone, as depicted here, the common therapeutic option is the administration of bisphosphonates to prevent the release of stimulatory growth factors from the degradation of bone stroma. Denosumab has raised interest as a valuable therapy for bone disease, but other options to prevent osteoclast activation include the administration of recombinant RANKL binding proteins such as osteoprotegerin (OPG) or recombinant RANK-Fc (RANK fused to an Fc fragment of immunoglobulin G). Integrin antagonists that interrupt the interaction of platelets with tumor cells or the binding of tumor cells to endothelial cells (or to the ECM) are also under consideration.

Chemokines and their receptors, which have been implicated in several aspects of tumor progression, including metastatic colonization by promoting evasion to immunosurveillance, represent an amenable target[168]. Likewise, some reports have also evidenced the potential of LOX as an anti-metastatic therapeutic target (Table 1.4). Microenvironment-specific targets, such as the bone, have also been object of interest in the development of therapeutic agents. Patients with breast cancer bone metastases have predominantly osteolytic-type

lesions. These result from cancer cell-mediated deregulation of normal tissue remodeling, through the release of parathyroid hormone-related peptide, or by stimulating RANKL, which induces osteoclastic bone resorption[169]. In this process, TGF-β retained in the bone matrix is released further enhancing bone resorption and providing space for metastatic growth. The implication of macrophage colony-stimulating factor (M-CSF) and its receptor c-FMS in osteoclast differenciation[169], makes them potential targets to block bone metastases (Table 1.4).

Table 1.4: Potential targets and anti-metastatic agents being investigated at the preclinical level.

Target	Therapeutic agent	Mechanism of action	Ref.
miR-10b	*miR-10b* antagomirs	*In vivo* silencing of *miR-10b* inhibited invasion and intravasation of breast cancer cells, but was ineffective at later stages of the metastatic process	170,171
AXL tyrosine kinase	Small molecule R428	Suppressed metastatic seeding from an orthotopic 4T1 mouse breast tumor, and tumor angiogenesis	172,173
Fascin	Migrastatin analogues	Fascin is the main actin filament bundling protein in filopodia; migrastatin analogues targeting fascin were identified as potent inhibitors of carcinoma 4T1 cells migration and invasion	174,175
$CCR4^+$ Tregs	TARC-arp*	A chemokine CCL7-based gene silencing strategy inactivated the immunosuppressivessupressive activity of $CCR4^+$ Tregs and abrogated lung metastases	176
LOX	β-aminoproprionitrile	Treatment of MDA-MB-231 breast tumor-bearing mice with a specific and irreversible inhibitor of LOX enzymatic activity hampered lung metastases without affecting primary tumor growth	177
LOXL2	Functional assay (E0771-shLOXL2 cancer cells)	LOXL2 promoted the formation of a permissive niche in two syngeneic mouse models of breast cancer; LOXL2 silencing in cancer cells was shown to reduce in 90% the development of lung metastases relative to control.	178
c-FMS	Small molecule inhibitor Ki20227	Inhibition of macrophage colony-stimulating factor receptor by Ki20227 suppressed osteoclast-dependent osteolysis in bone metastatic lesions	179

*chemokine CCL17-based strategy that acts as a vehicle for anti-sense oligonucleotide delivery.

RANKL has also been successfully targeted by the monoclonal antibody denusumab. The antibody was compared to the standard of care zoledronic acid[180] for the treatment of bone metastases in a phase III clinical trial[181]. Despite overall survival, and rates of adverse events being comparable, results showed that denosumab was superior to zoledronic acid in delaying skeletal-related events in patients with breast cancer metastatic to the bone[181]. In the setting of adjuvant therapy, denosumab was investigated in postmenopausal, aromatase inhibitor-treated breast cancer patients, where it reduced the risk of clinical fractures without added

toxicity[182]. Currently, several clinical trials involving denosumab are ongoing (NCT02682693, NCT01952054, NCT02051218, NCT01419717, NCT01864798).

Two other drugs currently being investigated in clinical studies are the first-generation tyrosine kinase inhibitor dovitinib, and the human anti-TGFβ-receptor monoclonal antibody fresolimumab. Preclinically, dovitinib inhibited proliferation in fibroblast growth factor receptor 1 (FGFR1)- and 2 (FGFR2)- amplified breast cancer cell lines and had anti-tumor activity in FGFR1-amplified breast cancer xenografts[183]. Treatment with this tyrosine kinase inhibitor as monotherapy was also evaluated in a phase II clinical trial and, overall, the results suggested that targeting FGFR could lead to modest antitumor activity in patients with FGF-pathway–deregulated breast cancer[183]. An ongoing phase II randomized study is investigating dovitinib in combination with endocrine treatment for metastatic breast cancer patients (NCT01528345 and NCT01484041). Fresolimumab is being evaluated for safety in treatment combination with local radiotherapy in metastatic breast cancer (NCT01401062).

1.2.2. Triple-negative breast cancer

The molecular dissection of triple-negative tumors refined our knowledge about the biology underpinning this disease. Furthermore, TNBC subtype-specific profiling facilitated the identification of targetable vulnerabilities within different subsets, and contributed for the development of tailored therapeutic strategies and prediction of benefit to standard chemotherapy.

1.2.2.1. Molecular dissection of the triple-negative breast cancer

Recent studies of gene expression profiling have uncovered the heterogeneous nature of TNBC. Lehmann *el al*. identified seven TNBC subtypes characterized on the basis of gene ontologies and differential gene expression patterns[184]. These subclasses were named as basal-like (BL1 and BL2), immunomodulatory (IM), mesenchymal (M), mesenchymal stem-like (MSL), luminal androgen receptor (LAR), and unstable (UNS) subtypes. Both BL1 and BL2 tumors were enriched for genes associated with proliferation and desoxyribonucleic acid (DNA) damage response. The highly proliferative nature of BL1 tumors was further supported by an elevated Ki-67 assessed by both mRNA expression and immunohistochemical staining analysis. Additionally, the BL2 subtype displayed a gene signature involving growth factor and metabolic signaling, and myoepithelial markers[184]. Tumors in the immunomodulatory subclass were enriched for genes involved in immune and cytokine signal transduction pathways and immune antigens, including T-cell associated genes, immune transcription factors, interferon regulatory factors and tumor necrosis

factor. Interestingly, the immunomodulatory gene signature largely overlapped with the one of medullary breast cancer[185], a rare pathological type of cancer associated with a better prognosis, despite the presence of aggressive features, such as large tumor size and a high nuclear grade[186].

Both the mesenchymal and mesenchymal stem-like subtypes shared an elevated expression of genes engaged in the epithelial-mesenchymal transition and growth factor signaling pathways, such as mechanistic target of rapamycin (mTOR), Wnt/β-catenin, and TGF-β; additionally, mesenchymal stem-like tumors distinguished by a unique gene signature involving growth factor signaling pathways (FGFR, VEGF and platelet-derived growth factor receptor (PDGFR)), decreased expression of proliferation-related genes and enrichment in genes associated with stem cells[184]. The rare and histologically diverse metaplastic breast cancer, characterized by a propensity for distant metastases and resistance to standard chemotherapy, shared similar features with these two molecular defined subtypes[184].

Finally, the luminal androgen receptor group constituted a luminal subtype driven by the androgen receptor signaling and enriched for hormone-regulated pathways[184]. Androgen signaling had been previously reported in ER-negative tumors, coupled with a molecular apocrine gene expression signature and associated to tumors with strong histological apocrine features[187].

Noteworthy, subtype-specific pathological complete responses (pCR) were reported by Masuda *et al*. in a retrospective analysis performed in biopsies from patients who received neoadjuvant chemotherapy. Patients within the basal 1 subtype achieved a higher pCR rate (52%) in contrast to the patients with basal 2 and luminal androgen receptor tumors, which showed the lowest response rates (0% and 10 %, respectively). More recently, other groups confirmed the existence of distinct TNBC molecular profiles and also associated them to different prognoses[188,189].

The Cancer Genome Atlas Network further analyzed the genomic heterogeneity of breast cancers by integrating information across different platforms. *TP53* mutation or deletion was the most common aberration identified in TNBC, being observed in 80% of the cases, followed by genomic aberrations in the PI3K pathway[190]. Abramson *et al*. extended this analysis and validated these findings. Using the DNA sequencing data from the Cancer Genome Atlas Network, 50% of the tumors of the luminal androgen receptor subtype presented phosphatidylinositol-4,5-bisphosphate 3-kinase catalytic subunit alpha (*PIK3CA*) mutations. The basal 2 subtype, in addition to *PIK3CA*, was also enriched in phosphatase and tensin homolog (*PTEN*) and PIK3 regulatory subunit 1 (*PIK3R1*) mutations. Both TNBC subtypes also showed increased levels of phosphorylated Akt[191]. These findings suggested that specific subsets of TNBC displaying increased PI3K pathway activity might benefit from

PI3K inhibitors[192,193].

The high frequency of p53 dysfunction in TNBCs likely results from defects in DNA repair pathway, and is consistent with the significant genomic instability that characterizes these tumors. This feature is also common to tumors carrying mutations in the *BRCA1* gene[194]. Although *BRCA1* mutations in sporadic basal-like breast cancers are rare[195], they display a *BRCAness* immunophenotype, resulting from the impairment of double-strand break repair through homologous recombination[194]. Such dysfunction has important clinical relevance because double-strand break impairment is the basis for specific target treatments[196].

Altogether, these results bear important implications in the way triple-negative breast disease is managed. Gene expression profiling analysis of TNBCs greatly contributed to the exploration of new druggable targets for the treatment of this disease. Furthermore, acknowledging the heterogeneity of this group uncovered the need to align patients to the various therapies according to their triple-negative subtype.

1.2.2.2. Druggable targets in triple-negative breast cancer

The identification of promising molecular targets by molecular profiling of TNBC led to the investigation of novel targeted therapies, which are currently being evaluated in numerous clinical trials.

Poly (adenosine diphosphate-ribose) polymerase (PARP) inhibitors (Table 1.5) have raised great interest in the setting of TNBC due to the *BRCAness* phenotype of these tumors. These inhibitors have shown promising results in *BRCA1/2*-mutant tumors, including in breast cancer[197]. However, clinical studies using Olaparib[198,199] or Veliparib[200], two inhibitors of the PARP enzyme, failed to demonstrate a significant response in patients with TNBC. Additionally, the combination of Iniparib with chemotherapy, which had previously shown to improve survival of patients with metastatic TNBC in a phase II clinical study[201], was not confirmed in the phase III trial[202]. Overall, PARP inhibitors demonstrated limited benefit in *BRCA* unselected TNBC populations, either as a single regimen[199] or in combination with other chemotherapeutics[200,203]. A recent study demonstrated that an increased level of allelic imbalance copy number aberrations and expression of meiosis-associated gene HORMA domain-containing protein 1 (*HORMAD1*) in triple-negative tumors correlated with higher sensitivity to platinum salts and PARP inhibitors[204]. These results clearly underlie the need to identify the subset of patients with triple-negative disease that may benefit from treatment with PARP inhibitors.

Inhibitors targeting the major mediators in the PI3K/Akt/mTOR pathway have also reached clinical trials (Table 1.5). Several studies are ongoing to evaluate the combination of mTOR inhibitors, Everolimus and Temsirolimus (rapamycin analogues), with chemotherapy,

platinum agents or other targeted therapies, in the setting of TNBC. The addition of Everolimus was generally associated with more adverse effects and did not significantly improve clinical response rates[205,206]. Nonetheless, a clinical benefit was demonstrated in a combination of Everolimus and Carboplatin[207]. In respect to PI3K inhibitors, these are relatively new to the clinical landscape, but several compounds have been evaluated in phase I trials[208-211], including in TNBC (Table 1.5). Adding to the spectrum of agents targeting the PI3K pathway, a selective small molecule inhibitor of all three isoforms of Akt, Ipatasertib, enabled a robust antitumor activity in patient-derived xenografts models[212]. Two clinical studies are ongoing to evaluate the efficacy of ipatasertib combined with Paclitaxel in the treatment of early stage (FAIRLANE)[213] and metastatic (LOTUS)[214] TNBC patients. Targeting the PI3K signaling pathway might benefit the subset of TNBCs with mesenchymal/mesenchymal stem-like features[184,215]. Additionally, preclinical data has shown that PI3K suppression may confer sensitivity to PARP inhibition in TNBCs without the *BRCA* mutations, by impairing homologous recombination in DNA repair[216]. This provides a new rationale to combine PI3K and PARP inhibitors in this indication.

The androgen receptor, which has been implicated in breast cancer pathogenesis[217], is expressed in more than 70% of breast tumors, including triple-negative (35%), generating particular interest in this subset of patients[218]. The luminal androgen receptor subtype is heavily enriched in hormonally regulated pathways and, alike the luminal intrinsic subtype, they are less likely to benefit from the current chemotherapy regimens[67]. This suggests that these patients may also benefit from androgen receptor inhibitors or, eventually, a combination of androgen receptor/PI3K inhibitors[192,193]. At present, three anti-androgens are being evaluated in TNBC (Table 1.5), with promising results coming from the treatment with single agent enzalutamide in advanced androgen receptor-positive TNBC[219]. Lastly, preclinical studies have shown that Orteronel, a potent inhibitor of 17,20-lyase enzyme, impairs androgen synthesis[220], and is now under evaluation in androgen receptor-positive TNBC (Table 1.5).

Table 1.5: Targeted therapies being investigated in clinical trials for the treatment of triple-negative breast cancer.

Targeted therapy	Therapeutic combinations	Clinical phase	ClinicalTrial.gov Identifier (Ref.)
PARP inhibitors			
Olaparib (AZD2281)	Monotherapy	II	NCT00494234 ([199])
			NCT00679783 ([198])
	Cediranib Maleate	I/II	NCT01116648
	Paclitaxel	I	NCT00707707 ([203])
Velipalib (ABT888)	Temozolomide	II	NCT01009788 ([200])
Iniparib (BSI-201)	Gemcitabine/Carboplatin	III	NCT00938652 ([202])
	Irinotecan	II	NCT01173497
mTOR inhibitors			
Everolimus (RAD001)	Paclitaxel followed by 5-Fluorouracil/Epirubicin/ Cyclophosphamide	II	NCT00499603 ([206])
	Cisplatin and Paclitaxel	II	NCT00930930 ([205])
	Carboplatin	II	NCT01127763 ([207])
			NCT02531932
Temsirolimus	Erlotinib	I	NCT00998036
	Neratinib	I/II	NCT01111825
	Liposomal doxorubicin/ Bevacizumab	II	NCT02456857
PI3K inhibitors			
BMK120	Capecitabine	II	NCT02000882
GDC-0941	Cisplatin	I/II	NCT01918306
AZD8186	Monotherapy	I	NCT01884285
Akt inhibitors			
Ipatasertib	Paclitaxel	II	NCT02162719 ([214])
			NCT02301988 ([213])
GSK2141795	Trametinib	II	NCT01964924
Androgen receptor/ synthesis inhibitors			
Becalutamide	Monotherapy	II	NCT00468715 ([221])
Enzalutamide	Monotherapy	II	NCT01889238 ([219])
Orteronel	Monotherapy	II	NCT01990209
VEGF/VEGFR inhibitors			
Bevacizumab	Taxane therapy	III	NCT01094184
	Carboplatin/Gemcitabine	II	NCT01201265
	Abraxane	II	NCT00472693
	Carboplatin/Cyclophosphamide or Paclitaxel	II	NCT01898117
Ramucirumab	Capecitabine	II	NCT01234402
Apatinib	Monotherapy	II	NCT01176669 ([222])
Sunitinib	Monotherapy	II	NCT00246571
	Paclitaxel/Carboplatin	I/II	NCT00887575
Sorafenib	Cisplatin followed by Paclitaxel	II	NCT01194869
	Pemetrexed	II	NCT02624700
EGFR inhibitors			
Cetuximab	Cisplatin	II	NCT00463788 ([223])
	Carboplatin	II	NCT00232505 ([224])
	Ixabepilone	II	NCT01097642
			NCT00633464
Erlotinib	Bendamustine	I/II	NCT00834678
	Monotherapy	II	NCT00739063
	Metformin	I	NCT01650506
Panitumumab	Paclitaxel/Carboplatin	II	NCT01009983
			NCT02593175
	Gemcitabine/Carboplatin	II	NCT00894504
HGFR inhibitors			
Tivantinib	Monotherapy	II	NCT01575522 ([225])
FGFR inhibitors			
Dovitinib (TKI-258)	Monotherapy	II	NCT00958971
NOTCH inhibitors			
RO4929097	Paclitaxel/Carboplatin	I	NCT01238133
	Monotherapy	II	NCT01151449
	Vismodegib	I	NCT01071564
JAK2 inhibitors			
Ruxolitinib	Monotherapy	II	NCT01562873
	Paclitaxel	I/II	NCT02041429
Cyclin-dependent kinases inhibitors			
Dinaciclib	Epirubicin	I	NCT01624441
P276-00	Gemcitabine/Carboplatin	I	NCT01333137
MEK1/2 inhibitors			
Trametinib (GSK1120212)	Akt Inhibitor GSK2141795	II	NCT01964924
	Monotherapy		NCT01467310
	BMK-120	I	NCT01155453

VEGF is implicated as the major angiogenic factor in human cancers, contributing to tumor growth and metastases[116]. Compared to other breast tumors, TNBCs were shown to have higher levels of VEGF[226]. The use of anti-angiogenic therapies in TNBC was supported by the results from a three phase III clinical studies in which the addition of Bevacizumab to Paclitaxel resulted in increased response rates and time to progression[227 228,229]. In the setting of metastatic TNBC, subgroup analysis of the RIBBON-2 trial showed marked improvements in progression-free survival with Bevacizumab and a trend towards improved overall survival[230]. Nevertheless, preliminary results from a recently completed clinical trial reported no difference in overall survival with the inclusion of Bevacizumab to adjuvant chemotherapy. Moreover, the use of this monoclonal antibody was associated with increased incidences of grade 3 or worse hypertension, severe cardiac events, and treatment discontinuation[231]. In 2010, the Food and Drug Administration (FDA) withdrew the recommendation for the use of Bevacizumab in the treatment of breast cancer due to safety concerns[232]. Nevertheless, Bevacizumab and other agents targeting VEGF and its receptor are still being evaluated in multiple clinical trials (Table 1.5).

Similar to VEGF, the epidermal growth factor receptor 1 has been addressed as a target in breast cancer, and has long been associated with basal-like TNBC[28,233]. Two completed clinical trials have explored the addition of Cetuximab to platinum agents (Table 1.5). The combination Cetuximab and Cisplatin resulted in increased progression free survival and overall survivals, but the overall response rate compared to Cisplatin alone (20% *vs* 10%, respectively) did not reach statistical significance, failing the primary endpoint of the study[223]. In the TBCRC001 trial limited activity was observed with the combination of Cetuximab and Carboplatin, despite EGFR pathway activation in most TNBC patients recruited for the study, suggesting alternate mechanisms for pathway activation[224]. The combination of Cetuximab with Ixabepilone was also evaluated in early and advanced TNBC. In the first setting, the combination improved the rate of pathological complete response in TNBC patients[234], while it presented a similar level of clinical activity compared to Ixabepilone alone in the second case[235]. These results suggest that a better understanding of the pathways maintaining EGFR activity is still required. An analysis of two randomized phase II trial pointed to a higher expression of *PTEN*, lower expression of alpha basic crystalline (*CRYAB*) and lack of Kirsten ras oncogene homolog (*KRAS*) amplification as potential predictive markers of benefit from Cetuximab for patients with basal-like breast tumors[236].

Janus kinase 2 (JAK2) amplification have been found in residual triple-negative tumors after neoadjuvant chemotherapy[237]. Evidence from preclinical studies suggested that the JAK2/Signal transducer and activator of transcription 3 (STAT3) pathway is preferentially active in a chemotherapy-resistant population of cancer cells and its inhibition in mouse

models resulted in impaired tumors growth[238]. Ruxolitinib, which is already approved by for the treatment of patients with myelofibrosis, is currently being investigated for the treatment of triple-negative inflammatory breast cancer (Table 1.5).

The somewhat disappointing results from these early clinical trials with targeted agents might be partially explained by the heterogeneity inherent to TNBC. These studies were performed in a group of patients with unselected triple-negative tumors, *i.e.*, only selected based on the absence of ER, PR and HER2 by immunohistochemical characterization. However, heterogeneity of TNBC considerably contributes to dilute the effect of a treatment that otherwise could be effective in a molecularly-selected subset of patients.

1.3. Nucleolin: a new perspective on breast cancer needs

Nucleolin participates in various cellular functions controlling different components of RNA and DNA metabolism, including ribosome biogenesis, ribosomal (r)RNA maturation, ribosomal (r)DNA transcription and chromatin structure[239,240]. Therefore, nucleolin is mainly located at the dense fibrillar and granular regions of the nucleolus and nucleoplasm[241]. Nonetheless, different pools of nucleolin, in the cytoplasm and cell membrane, have also been demonstrated to exhibit important functions[240,242,243]. Altogether, nucleolin's biological functions that contribute to cell homeostasis are also responsible for its role in the development of malignant traits under pathological conditions. In this respect, overexpression of nucleolin, and increased localization at the cell membrane, was shown in different cancer cell lines[243-248] and endothelial cells[249,250], as well as in tumors of diverse histological origin[251-259]. Nucleolin overexpression contributes to tumorigenesis and cancer progression by supporting cancer cells proliferation and survival, and by promoting invasion and angiogenesis.

1.3.1. Role of nucleolin in tumorigenesis and metastization

In the nucleolus, nucleolin controls chromatin accessibility and dynamics, thus contributing to the regulation of RNA polymerase I transcription activity[260]. Moreover, its association with unmethylated rRNA genes interferes with the binding of transcription termination factor 1 to promoter-proximal terminator T0, further contributing for the maintenance of an euchromatin state and the subsequent transcription by RNA polymerase I[261,262]. Additionally, nucleolin was also a key factor participating in several steps of the assembly and maturation of pre-rRNA[263-265]. As a result, nucleolin overexpression enables the sustained proliferation of cancer cells by potentiating a high level of protein synthesis.

Nucleolin also promotes oncogenesis, acting as a transcriptional factor through direct binding to promoter region of target genes (in the nucleoplasm), or by regulating

mRNA stability or translation (in the cytoplasm). A complete list of oncogenes and mRNAs under the regulation of nucleolin is summarized in Table 1.6. Among them, nucleolin and the human heterogeneous nuclear ribonucleoprotein K (hnRNP K) bind selectively to the guanosine (G)- and cytosine (C)-rich sequences of *VEGF* promoter region, respectively, acting as transcriptional activators[266]. Nucleolin also participates in human papillomavirus 18 (HPV18)-associated cervical carcinogenesis through the control of HPV18 enhancer chromatin structure. The downregulation of nucleolin protein expression resulted in the inhibition of *E6* and *E7* oncogene transcription and selectively decreased $HPV18^{+}$ cervical cancer cell growth[255].

Table 1.6: Oncogenes, mRNAs and microRNAs regulated by nucleolin protein.

		Nucleolin function	Implication in cancer disease	Ref.
mRNA (protein)	*HIF-1α* (HIF-1α)	mRNA stabilization	Proliferation, invasion, angiogenesis	267,268
	MMP9 (MMP-9)	mRNA translation enhancement; mRNA stabilization	Migration, invasion, angiogenesis	269-271
	MMP2 (MMP-2)	mRNA stabilization	Migration, invasion	271,272
	Egfr (EGFR)	mRNA stabilization	Proliferation, survival, differentiation	273,274
	Il10 (IL-10)	mRNA stabilization	Anti-apoptotic, immunosurveillance	275,276
	BCL2 (BCL2)	mRNA stabilization	Survival (anti-apoptotic)	277-281
	IL2 (IL-2)	mRNA stabilization	Immunosurveillance	282,283
	GAST (Gastrin)	mRNA stabilization	Proliferation, invasion, survival (anti-apoptotic)	284,285
	TP53 (p53)	mRNA translation suppression	Tumor suppressor	286,287
	AKT1 (Akt1)	mRNA translation enhancement	Proliferation, survival (anti-apoptotic)	288,289
	CCN1 (Cyclin 1)	mRNA translation enhancement	Survival (anti-apoptotic)	288
Oncogene (protein)	*Il9r* (IL-9R)	Transcription enhancement	Immunosurveillance	290
	VEGF (VEGF)	Transcription enhancement	Angiogenesis	266
	IRF2 (IRF2)	Transcription enhancement	Proliferation	291
	CD59 (CD59)	Transcription enhancement	Modulation of immune responses (inhibitor of reactive lysis)	292
	BCL221 (Bcl221)	Transcription enhancement	Survival (anti-apoptotic)	292
	MCL1 (Mcl1)	Transcription enhancement	Survival (anti-apoptotic)	292
	E6 and *E7* (E6 and E7)	Transcription enhancement	Target p53 for degradation, maintenance of viral (HPV) episomes	255,293
microRNA	*miR-15a/16*	Biogenesis	Pro-apoptotic	294
	miR-21, miR-103, miR-221, and *miR-222*	Biogenesis	Proliferation, survival (anti-apoptotic), migration, invasion	295

At the mRNA level, nucleolin regulates the expression of several key proteins involved in cancer growth and progression. In this respect, B cell lymphoma 2 (BCL2) protein is probably the most studied. BCL2 overexpression in various cancers results from nucleolin binding to the adenin-uracil (AU)-rich element of *BCL2* mRNA promoting its stability[277,278,280]. Nucleolin also regulates the expression of p53 and Akt1 proteins, by suppressing and enhancing their translation, respectively[286,288]. In another study, the expression of MMP-9 was increased upon binding of nucleolin to the mRNA three prime untranslated region (3'UTR) improving the proteinase translational efficiency[269]. More recently, the modulation of mRNA stability by a truncated form of nucleolin, generated through the action of metalloproteinase 7 (MMP-7), was implicated in the increased expression of several oncogenes, including *MMP9*, and hypoxia inducible factor 1 α (*HIF1α*), while the expression of various tumor suppressors was decreased[270].

Interestingly, VEGF was shown to induce the translocation of nucleolin from the nucleus to the cell membrane, through the activation of a signaling pathway involving receptor protein tyrosine phosphatase β/ζ (RPTPβ/ζ), which culminates in nucleolin phosphorylation by PI3K[296]. Phosphorylation regulates nucleolin's subcellular localization, and has been correlated with metastatic potential in various carcinomas[254]. Pleiotrophin also induced the translocation of nucleolin in a similar manner to that of VEGF[297], in addition to its direct binding to cell surface nucleolin[298,299]. In the cell membrane, nucleolin acts as a receptor to different ligands involved in cancer progression, and mediates their mitogenic, anti-apoptotic, invasive and pro-angiogenic effects (Table 1.7). Cell surface nucleolin also acts as a binding partner for several membrane proteins, such as those of the ErbB tyrosine kinase receptor family (Table 1.7).

Table 1.7: Ligands of cell surface nucleolin and implications of their interaction for cancer development (adapted and modified from Koutsioumpa & Papadimitriou, 2014[300]).

Ligands	Biological function	Ref.
Carcinogenic		
Midkine (MK)	Nucleolin was identified as a low affinity receptor for MK, which is up-regulated in several human carcinomas where it promotes proliferation, survival and migration of cancer cells and angiogenesis.	301-303
Pleiotrophin (PTN)	Nucleolin was identified as a low affinity receptor for PTN and participates in its nuclear translocation promoting PTN-induced endothelial cell migration.	298,299
HGF	Nucleolin was identified as an alternative receptor for HGF, promoting HGF-mediated regulatory interplay between stromal and epithelial cells within the prostate, and possibly also at sites of metastases.	304

(continues on the next page)

P-selectin	Formation of signaling complex containing cell surface nucleolin/PI3K/p38 MAPK that regulates adhesion and spreading of human colon carcinoma cells.	305
VEGF	VEGF stimulates nucleolin translocation from the nucleus to the membrane, promoting nucleolin-mediated endothelial cell migration and formation of capillary-like structures (angiogenesis), and increased metastatic potential of colorectal carcinoma.	254,296,306,307
Fas	Formation of nucleolin/Fas complexes inhibits Fas ligand (FasL) binding, and thus prevents induction of Fas-mediated apoptosis in B-cell lymphomas.	308
ErbB tyrosine kinase receptor family	Association of nucleolin with ErbB receptors induces their dimerization and phosphorylation leading to enhanced anchorage-independent cell growth.	309
Ras proteins	Nucleolin regulates K-Ras cluster formation and activation of the MAPK pathway; interaction facilitates the formation of nucleolin/ErbB1 receptor.	310,311
RPTPβ/ζ / $\alpha_v\beta_3$ integrin	$\alpha_v\beta_3$ expression and β_3 phosphorylation at Tyr^{773}, as a result of the RPTPβ/ζ/c-Src signaling cascade, induces cell surface localization of nucleolin through PI3K phosphorylation and promotes nucleolin-mediated angiogenesis and cancer cell migration.	296,297
uPAR / CK2	uPA stimulates the formation and internalization of a complex comprising uPAR/nucleolin/CK2 that is responsible for uPA mitogenic effect in several cells expressing uPAR; single-chain uPA (scuPA) might also directly bind to cell surface nucleolin.	312,313
Tipα	Nucleolin in gastric cancer cells binds and shuttles Tipα to the nucleus where it induces epithelial to mesenchymal transition and promotes cancer cell migration and invasion.	314,315
Anti-carcinogenic		
Lactoferrin	Nucleolin-mediated binding and nuclear translocation of lactoferrin in breast cancer cells might be responsible for lactoferrin anticancer effects.	316,317
Endostatin	Nucleolin mediates the internalization and nuclear translocation of endostatin; in the nucleus, endostatin inhibits bFGF-stimulated phosphorylation of nucleolin by CK2, which results in the inhibition of endothelial cell proliferation and migration.	318
ADAMTS-2	Nucleolin was identified as a potential receptor mediating the antiangiogenic activity of ADAMTS-2 in vitro, and impaired growth and vascularization of tumors in vivo.	319

1.3.2. Strategies targeting nucleolin for cancer treatment

Accumulating evidence suggesting the implication of nucleolin in mechanisms involved in cancer development, and its expression in human cancers, has raised interest in the field of targeted therapies. Cell-surface nucleolin has been validated as a novel target for anticancer therapy by using several molecules such as the HB-19 and N6L nucant pseudopeptides, the AS1411 aptamer and the F3 tumor-homing peptide.

1.3.2.1. HB-19 and its related nucleolin antagonist pseudopeptide

The HB-19, and its related nucleolin antagonist pseudopeptide (N6L), bind the carboxyl (C)-terminal of arginine-glycine-glycine-rich (RGG) domain of cell-surface expressed nucleolin forming a stable complex[247,320]. The lead compound HB-19 inhibited the growth of several human carcinoma cell lines, and impaired angiogenic-related traits of endothelial cells. *In vivo*, treatment with HB-19 markedly suppressed the progression of established human breast tumor xenografts in mice, while displaying no toxicity to normal tissue[307]. Likewise, in a mouse model of spontaneous melanoma, HB-19 significantly delayed the onset and frequency of cutaneous nodules, and decreased angiogenesis in these tumors, as well as impaired experimental metastization[321]. Further *in vitro* studies demonstrated that HB-19 restored contact inhibition in culture and impaired anchorage-independent growth[321]. Consistent with these results, the N6L pseudopeptide also inhibited the anchorage-dependent and independent growth of tumor cell lines and hampered angiogenesis. N6L induced significant inhibition of tumor growth in mice grafted with human MDA-MB-231 or PC3 cells, and significantly prolonged the survival of mice bearing murine lymphomas[322]. Currently, the N6L pseudopeptide is being explored in a phase I/IIa clinical trial to assess safety, tolerability, pharmacokinetics and preliminary efficacy in advanced solid tumors (NCT01711398).

Treatment of cancer cells with HB-19 and N6L compounds resulted in a drastic downregulation of surface/cytoplasmic nucleolin, without affecting the nuclear pool, producing distinct inhibitory mechanisms depending on the malignant tumor cell type[247]. In epithelial cancer cells, these pseudopeptides inhibited cell adhesion and induced reversion of the malignant phenotype, possibly through a selective inhibitory effect on the expression of genes implicated in tumorigenesis and angiogenesis, such as matrix metalloproteinase 2 (MMP-2) and VEGF[247,323]. Additionally, tissue inhibitor of metalloproteinase 3 (TIMP-3) has also been implicated in N6L-induced inhibition of cell invasion[324]. Others demonstrated that the antiangiogenic action of HB-19 pseudopeptide results from the suppression of c-Src, extracellular signal-regulated protein kinases 1 and 2 (ERK1/2), Akt and focal adhesion kinase (FAK) pathway activation, together with MMP-2 downregulation[325].

Recently, targeting moieties functionalized with the N6L pseudopeptide have been developed and tested preclinically (Table 1.8). Latorre *et al*. described the functionalization of magnetic nanoparticles with N6L for the controlled and selective release of cytotoxic drugs (Doxorubicin and Gemcitabine)[326]. An important characteristic of these nanoparticles is their potential to absorb energy and release heat, which is lethal to tumor cells. Therefore, the additional application of hyperthermia further unfolded a higher cytotoxic potential of these nanoparticles[327].

1.3.2.2. AS1411 aptamer

The AS1411 is a nucleolin-binding guanosine-rich phosphodiester oligodeoxynucleotide aptamer[328], as demonstrated with tumor cells like MCF-7 and MDA-MB-231 breast cancer cells[329] and MV4-11 leukemia cells[330]. The mechanisms underlying the antitumoral activity of AS1411 rely on disruption of the anti-apoptotic pathway of NF-kB[331], *BCL2* mRNA stabilization[329], and maturation of nucleolin-dependent microRNAs (*miR*)[295]. Moreover, the aptamer induces the translocation of the protein arginine methyltransferase 5 (PRMT5)-nucleolin complex from the nucleus to the cytoplasm, leading to the upregulation of tumor suppressors[332]. More recently, the antiproliferative activity of AS1411 against various cancer cells was also associated with its capacity to stimulate macropinocytosis by a nucleolin-dependent mechanism[333,334]. Binding of the aptamer to nucleolin led to a sustained activation of Rac1 and to a type of nonapoptotic cell death (methuosis)[334]. Importantly, Pichiorri *et al*. demonstrated that *in vivo* targeting of nucleolin by AS1411 led to a significant reduction of lung metastases in mice bearing highly aggressive breast cancer tumors, resulting from decreased *miR-103*, *miR-21*, *miR-221*, and *miR-222* mature forms[295]. Given the encouraging preclinical results, AS1411 was selected for a phase I clinical trial in advanced solid tumors (NCT00881244). The findings of this study were promising, but AS1411 showed limited activity in a subsequent Phase II study[335].

Conjugation of this nucleolin-targeting aptamer to different nanotechnology-based vehicles has been extensively explored (Table 1.8). Poly(ethylene glycol) (PEG)-grafted liposomes modified with the AS1411 aptamer, and containing Doxorubicin, presented increased cellular internalization and cytotoxicity against MCF-7 breast cancer cells, and improved antitumor efficacy against MCF-7 breast cancer xenografts in mice, compared to its non-targeted counterparts[336]. AS1411-targeted PEGylated poly(D, L-lactide) nanoparticles containing triptolide also demonstrated antitumor efficacy in a xenograft mouse model of Gemcitabine-resistant human pancreatic cancer (MIA PaCa-2), revealing great potential to reverse drug resistance of pancreatic cancer[337]. Recently, the aptamer has been conjugated to gold nanospheres, presenting promising results in a mouse model of breast cancer[338].

Table 1.8: Delivery strategies targeting cell surface nucleolin (adapted and modified from Sader *et al.*, 2015[339]).

Ligand	Delivery system	Drug delivered	Application	Ref.
AS1411 aptamer				
	Human serum albumin NPs		Breast cancer cells (MCF-7).	340
	Gold nanospheres		Carcinoma, sarcoma, melanoma, and glioblastoma human cells.	341
			MDA-MB-231 breast cancer xenografts.	338
	PEGylated liposomes	Doxorubicin	MCF-7 human breast cancer xenografts.	336
	PEGylated cationic liposomes	siRNA	A375 human melanoma xenografts.	342
	PEGylated poly(D, L-lactic-co-glycolic acid) (PLGA)	Paclitaxel	C6 rat glioma xenografts.	343
		Vinorelbine	Human breast cancer cells (MDA-MB-231).	344
	PEGylated poly(D, L-lactide) (PDLLA)	Triptolide	Gemcitabin-resistant human pancreatic cancer xenografts (MIA PaCa-2).	337
F3 peptide				
	Hydrogel NPs	Doxorubicin	Doxorubicin-resistant cell line (NCI/ADR-RES).	345
		Cisplatin	Human ovarian cancer xenografts.	346
		Photodynamic therapy	Rat glioma (9L and F98) and human breast cancer (MDA-MB-435S) cell lines.	347
	Poly(ethylene glycol)–polylactic acid (PEG–PLA)	Paclitaxel	C6 rat glioma xenografts.	348
	alpha-emitter ^{213}Bi-DTPA-[F3]$_2$		Tumor model of peritoneal carcinomatosis	349
	pH-sensitive liposomes	Doxorubicin	MDA-MB-435S human breast cancer xenografts.	246
		siRNA	Human microvascular endothelial cells (HMEC-1), lung carcinoma (A549) and prostate cancer cells (PC3).	350-353
		Doxorubicin and C6-ceramide	MDA-MB-231, MCF-7 and MDA-MB-435S human breast cancer cells.	245,354
	Carbon nanotubes	Near-infrared laser treatment	MCF-7 human breast cancer cells.	355
N6L peptide				
	Magnetic NPs	Doxorubicin and magnetic hyperthermia	MDA-MB-231 human breast cancer xenografts.	327
	Dimercaptosuccinic acid coated magnetic NPs		MDA-MB-231 human breast cancer xenografts.	356
Non-targeted				
	DNA NPs		Embryonic kidney, bronchial epithelial and cervical human cancer cells.	357
			T lymphocyte, bronchial epithelial and cervical human cancer cells.	358

*NPs, nanoparticles

1.3.2.3. F3 peptide

The 31 aminoacid tumor homing peptide, codenamed F3, was identified as a potential candidate for targeting nucleolin in cancer and endothelial cells. Fluorescein-labeled F3 peptide was shown to bind to HL-60 human myeloid leukemia cells and human MDA-

MB-435 breast cancer cells, being internalized in an energy-dependent manner, followed by nuclear translocation[250]. Upon intravenous injection into mice bearing HL-60 or MDA-MB-435 tumors, F3 peptide accumulated in both cancer and endothelial cells lining tumor blood vessels. Christian *et al*. further identified cell surface-nucleolin as the receptor for F3 peptide on tumor cells and angiogenic endothelial cells[249]. The targeting capability enabled by the F3 peptide motivated the development of therapeutic strategies for the specific deliver of numerous anticancer drugs (Table 1.8). In this respect, several studies have reported the conjugation of the F3 peptide to hydrogel nanoparticles. *In vitro* assessment of these F3 peptide-targeted nanoparticles demonstrated specific binding to cancer and tumor endothelial cells[345-347,359], and cellular uptake was shown to depend on nucleolin expression on the plasma membrane[345]. The therapy demonstrated to be effective in mice bearing ovarian cancer, primarily due to an anti-vascular effect[346]. The tumor homing peptide has also been efficiently coupled to the α-emitter ^{213}Bi-DTPA-$[F3]_2$, showing promising clinical outcomes[349]. Additionally, Moura *et al*. developed a targeted strategy in which the F3 peptide was coupled to pH-sensitive liposomes[246]. These targeted liposomes promoted intracellular and triggered release of Doxorubicin, causing a major impact on primary breast tumor invasiveness. The anti-tumor activity of F3-targeted pH-sensitive liposomes might be mediated by its ability to simultaneously target several tumor cell populations, including cancer stem cells[245].

1.4. State-of-the-art overview and aim of the project

The molecular complexity of breast cancer has changed our view about the biologic diversity of this disease and, particularly, altered the way clinical treatment decisions are made. Both molecular and immunohistochemical panels of biomarkers are currently being applied to predict the benefit of specific therapies such as endocrine and HER2-targeted therapy. However, a subset of women diagnosed with triple-negative (ER^-/ PR^-/ $HER2^-$) breast cancer, do not currently benefit from targeted therapies. Moreover, this subtype is associated with an increased risk of recurrence and death in the first five years following diagnosis. Additionally, therapeutic approaches in the setting of metastatic breast cancer are determined based on the characteristics of the primary tumor. However, heterogeneity between primary tumors and metastases is observed at the molecular level, and is expectable that these strategies might reveal ineffective against the secondary lesions. Hence, it urges the need to find novel targets and develop targeted strategies addressing these needs.

Nucleolin is a protein implicated in tumorigenesis and angiogenesis, and a growing number of evidence also suggests its involvement in the acquisition of metastatic potential. Its overexpression in cancer cells and endothelial cells of tumor-associated blood vessels, including expression at the cell surface, has been generating increased interest in nucleolin as

a therapeutic target, and prompted the development of various strategies targeting nucleolin. In line with this, the previously developed F3 peptide-targeted pH-sensitive liposomes have shown to cause a major impact on primary breast tumor invasiveness.

In the context of the current state-of-the-art, the main goal of this project is to evaluate the therapeutic impact of F3 peptide-targeted pH-sensitive liposomes on metastatic triple-negative breast cancer, and assess the translational value of nucleolin in this breast cancer subtype. In order to accomplish this, the specific aims of the project are:

- To establish the conditions enabling high metastatic take rate of the widespread triple-negative murine 4T1 syngeneic breast cancer model, towards a more reliable pre-clinical screening of anticancer drugs;
- To explore the therapeutic potential of nucleolin in the setting of metastatic breast cancer, using F3 peptide-targeted pH-sensitive liposomes containing Doxorubicin;
- To evaluate nucleolin expression in patient-derived breast tissues, both in primary tumors and corresponding metastases, with particular emphasis on triple-negative carcinomas.

Chapter 2

The effect of inoculated cell density on the growth dynamics and metastatic efficiency of the breast cancer 4T1 murine model

Abstract

The murine 4T1 breast carcinoma cell line has remarkable tumorigenic and invasive characteristics. Owing to its characteristics, 4T1 tumors have been widely used to study stage IV human breast cancer. However, 4T1 metastatic breast cancer model suffers from the liability of fast growing tumors enhanced by the frequent inoculation of a large number of cells, rendering, among several problems, a surprisingly low metastatic take rate. The need of translatable and predictive tumor models is a recognized need for successful drug development. The present work aimed at establishing the conditions enabling high metastatic take rate of the widespread triple-negative murine 4T1 syngeneic breast cancer model, towards a more reliable pre-clinical screening of anticancer drugs. We demonstrated that 4T1 tumors grew in the mammary fat pad of mice when as few as 500 cancer cells were implanted, with 87% tumor incidence. 4T1 cancer cells colonized primarily the lungs with 100% efficiency, and distant lesions were also commonly found in tissues such as the mesentery and pancreas. Drastically reducing the number of inoculated cells resulted in increased tumor doubling times and decreased specific growth rates, following a Gompertzian tumor expansion. Thereby, extending the time frame of primary tumor development, without requiring its excision, was beneficial for metastatic progression. This approach is highly relevant for a better assessment of antimetastatic therapies.

2.1. Introduction

The manifestation of metastases is predictive of poor clinical outcome[360-363], and prevails the one of the most challenging issues faced by cancer treatment today. A continuous effort in dissecting the biological processes behind cancer cell dissemination has been pushing forward our understanding of the disease and uncovering vulnerabilities that may be exploited for the development of novel agents to treat metastatic cancer.

Mouse models are crucial to our comprehensive knowledge on the molecular basis and pathogenesis of cancer disease[364]. Nevertheless, a major impediment for the study of metastases has been the unavailability of suitable mouse models that accurately recapitulate the complexity of human tumor progression[365,366]. To better mimic the development of metastases in humans, several parameters need to be considered in a mouse model, namely location and implantation method of the primary tumor, interaction of cancer cells with the microenvironment at the primary and secondary sites, dissemination routes and time-to-progression of the disease. Subcutaneous transplantation of human (xenograft) and murine (allograft) cell lines into mice, and genetic engineered mice, are widely used for the establishment of pre-clinical models[365,367]. In the subcutaneous model, ectopic location of cancer cells usually fails to produce metastases, owing to the limited tumor microenvironment generated[368]. Furthermore, surgical resection of primary tumors is often imperative in order to prolong mice survival and enable the development of spontaneous metastases[365]. Genetic engineered mouse models surpass some of these constrains, offering the possibility of orthotopic neoplastic generation in immune competent hosts[365,367]. Nevertheless, metastatic lesions may appear only upon long latency periods and generally their incidence is low[365,367]. Even though the existing pre-clinical models still offer valuable information about the biology, molecular basis and therapeutic opportunities, the setting up of spontaneous metastases faces several challenges, and improvement of its modeling remains of major importance[365,366,369].

The murine 4T1 breast carcinoma cell line has remarkable tumorigenic and invasive characteristics. Upon injection in the mammary gland of Balb/c mice, 4T1 cells spontaneously generate tumors and are described to metastasize to the lungs, liver, lymph nodes, brain and bones, in a way that closely resembles human breast cancer[370]. Owing to its characteristics, 4T1 cells have been widely used to study stage IV human breast cancer[371-374]. Moreover, 4T1 murine tumors represent a clinically relevant triple-negative breast cancer model [375-377], which, alongside the cancer cell invasion and metastization, is an important challenge due to its lack of responsiveness to endocrine therapy. However, 4T1 metastatic breast cancer model suffers from the liability of fast growing tumors enhanced by the frequent inoculation of a large number of cells, rendering a tumor microenvironment that does not recapitulate human breast tumors, early mice euthanasia[171,374,378-383], along with a surprisingly

low metastatic take rate.

Notwithstanding the widespread use of the 4T1 animal model, some of the aforementioned issues truly limit its usefulness to understand the biology of metastatic breast cancer and therefore the identification of novel therapeutic opportunities and the corresponding proof of concept. The need of translatable and predictive tumor models is a recognized need for successful drug development. The present work aims at establishing the conditions enabling high metastatic take rate of the widespread triple-negative murine 4T1 syngeneic breast cancer model, towards a more reliable pre-clinical screening of anticancer drugs.

2.2. Results

2.2.1. Metastatic pattern and efficiency

The 4T1 metastatic breast carcinoma model is amply used. However, a large number of cells are often implanted in mice[171,374,378-382] and require primary tumor removal to extend the disease time course, besides presenting a low metastatic efficiency. Herein, we assessed the effect of inoculated 4T1 cell density on the metastatic efficiency, without removal of the primary tumor. Immunocompetent Balb/c female mice were orthotopically injected with four cell densities, ranging from 500 to 1 x 10^6 cells, and tumor incidence, time for tumor onset, and metastatic efficiency were evaluated.

No obvious correlation was detected between tumor incidence and the inoculated 4T1 cell density (Table 2.1). The percentage of mice that developed breast carcinomas varied from 85% to 92%, in animals implanted with 5 x 10^4 and 1x10^6 cells, respectively. However, the mean time for tumor onset was significantly different between the groups inoculated. Palpable tumors were detected at 17.5 and 16.5 d *post* injection of 500 and 2000 cancer cells, respectively, whereas this latency time drastically decreased when 5 x 10^4 (7.6 d, $p < 0.01$) or 1 x 10^6 (3.6 d, $p < 0.0001$) 4T1 cells were implanted (Table 2.1).

Table 2.1: Tumor growth and metastases in 4T1 breast carcinoma-bearing mice.

No. 4T1 cells inoculated	No. of mice with tumors/total mice (%)	Mean tumor onset (days until palpable tumors ± SEM)	No. of mice with detectable lung metastases/no. of mice evaluated (%)
1x10^6	11/12 (92%)	3.6 ± 2.54 [a]	5/11 (45%)
5x10^4	11/13 (85%)	7.6 ± 0.84 [b]	5/11 (45%)
2000	13/15 (87%)	16.5 ± 1.05	7/9 (78%)
500	13/15 (87%)	17.5 ± 0.91	7/7 (100%) [c]

[a] $p < 0.0001$, [b] $p < 0.01$ relative to 500 and 2000 cell densities (nonparametric one-way *ANOVA* with Dunn's multiple comparisons test); [c] $p = 0.0167$, relative to 5x10^4 and 1x10^6 cell densities (two-tailed chi-square test).

The time course of primary tumor growth might have implications on its metastatic efficiency. In fact, the number of mice with detectable lung metastases significantly increased in those groups with the longest tumor onset, achieving 100% efficacy on the group where only 500 cells were inoculated (Table 2.1). In contrast, only 45% of mice developed lung metastases (or metastatic nodules in other tissues), for cell densities superior to 5 x 10^4.

Figure 2.1 shows representative images of 4T1 breast tumors and metastatic lesions in several tissues.

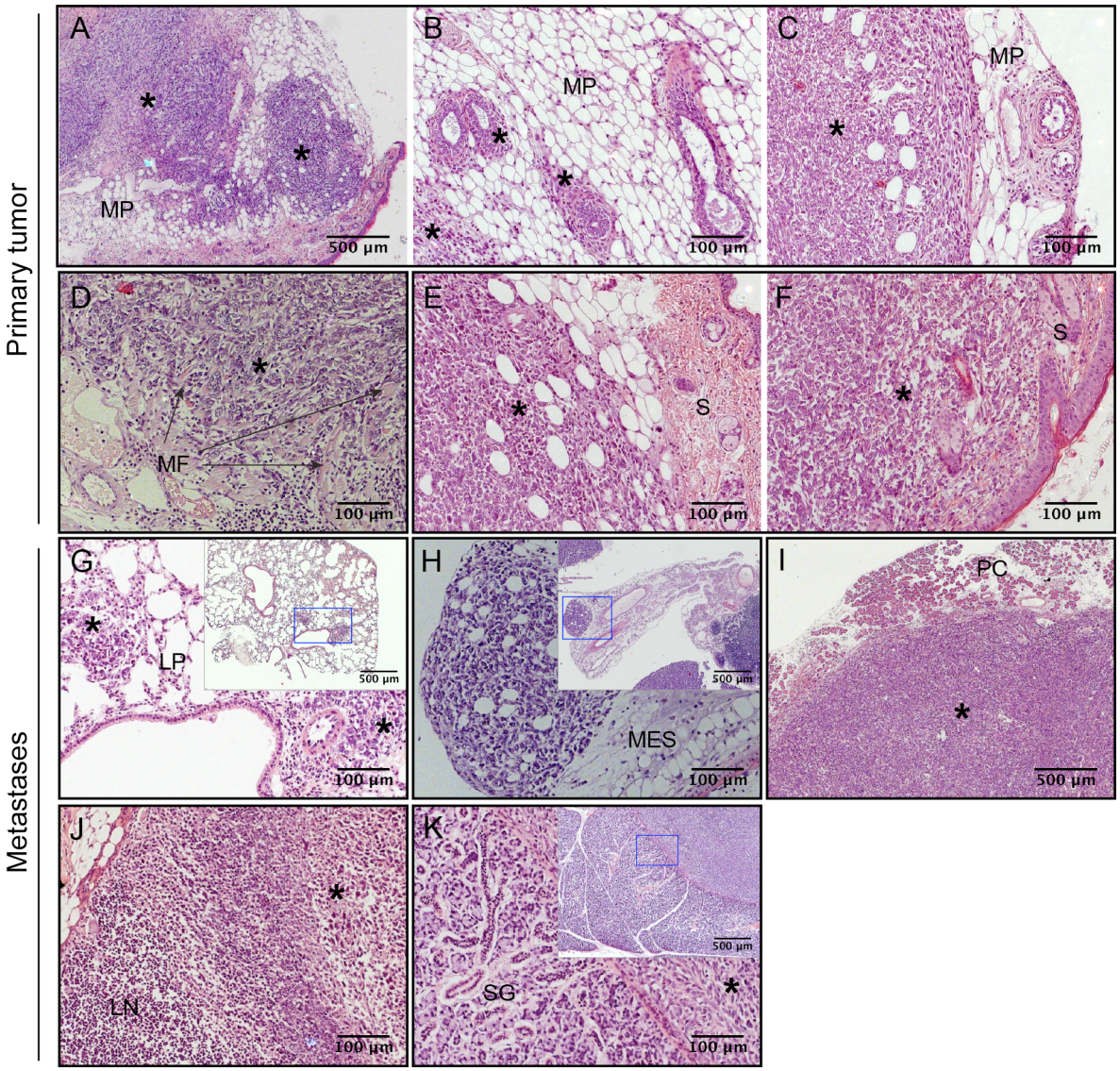

Figure 2.1: Representative sections from orthotopic 4T1 tumors and nodular metastatic deposits.
Tumor cells invading the surrounding mammary parenchyma (A - C), muscle fibers (D) and adjoining skin (E – F) show the highly invasive capacity of 4T1 breast tumors. Examples of metastatic lesions were observed in the lungs (G), mesentery (H), pancreas (I) lymph nodes (J), or salivary gland (K). MP, mammary parenchyma; MF, muscle fibers; S, skin; LP, lung parenchyma; LN, lymph node; MES, mesentery; PC, pancreas; SG, salivary gland; * indicates tumor areas. All images present original magnification x200, except upper left and inset images, x50.

The highly invasive nature of these tumors was confirmed by their capacity to invade neighboring mammary parenchyma (Figure 2.1A - C), muscle fibers (Figure 2.1D) and adjacent skin (Figure 2.1E - F). Macrometastatic lesions in several organs and tissues were also observed (Figure 2.1G - K). In these experiments, 4T1 cells have colonized mainly the lungs (Figure 2.1G), as previously described[378,384], while macrometastases in the liver were rarely observed. As important, macrometastases in the brain were not identified. Metastases in tissues such as the mesentery (Figure 2.1H) and pancreas (Figure 2.1I) were often observed, and occasionally in lymphatic nodes (Figure 2.1J). Less frequently, other tissues, like the salivary gland (Figure 2.1K), were affected. However, the extent of pulmonary and visceral lesions was considerably variable amongst individuals. Different metastatic patterns were observed in mice, particularly on the lowest cell densities: either small lesions extensively spread, or scarce but larger metastatic nodules (data not shown). Therefore it was difficult to establish the metastatic burden based on the number or volume of the lesions. Moreover, it was difficult to perform weight estimates in certain tissues, such as the mesentery.

2.2.2. Dynamics of 4T1 tumor growth

Dynamics of tumor growth were analyzed by two mathematical models commonly used to describe tumor growth: the Exponential and Gompertz models[385]. The first is a simplistic model that assumes that the number of cancer cells doubles during cell cycle, resulting in exponential growth of solid tumors. However, tumor growth involves other biological processes, such as regulation of proliferation, stromal recruitment, escape from immunesurveillance and angiogenesis, thereby being usually explained by the Gompertz model, which considers growth rate decay as tumors become larger[386,387]. Tumor growth curves fitted to the experimental mean tumor volumes over time are presented in Figure 2.2A. The model providing the best fit was chosen based on Akaike's information criteria (AIC) and extra sum-of-squares F test analysis (Figure 2.2B)[388,389]. Tumor growth showed a Gompertz behavior for all groups, except for those generated from inoculation of $1x10^6$ cells, where exponential growth was prevalent (Figure 2.2). Notwithstanding, Gompertzian tumor growth was diverse among the different groups. It was evident that tumors generated from 5×10^4 cells attained the decay phase much earlier than the tumors resulting from the inoculation of lower cell densities (Figure 2.2A).

A

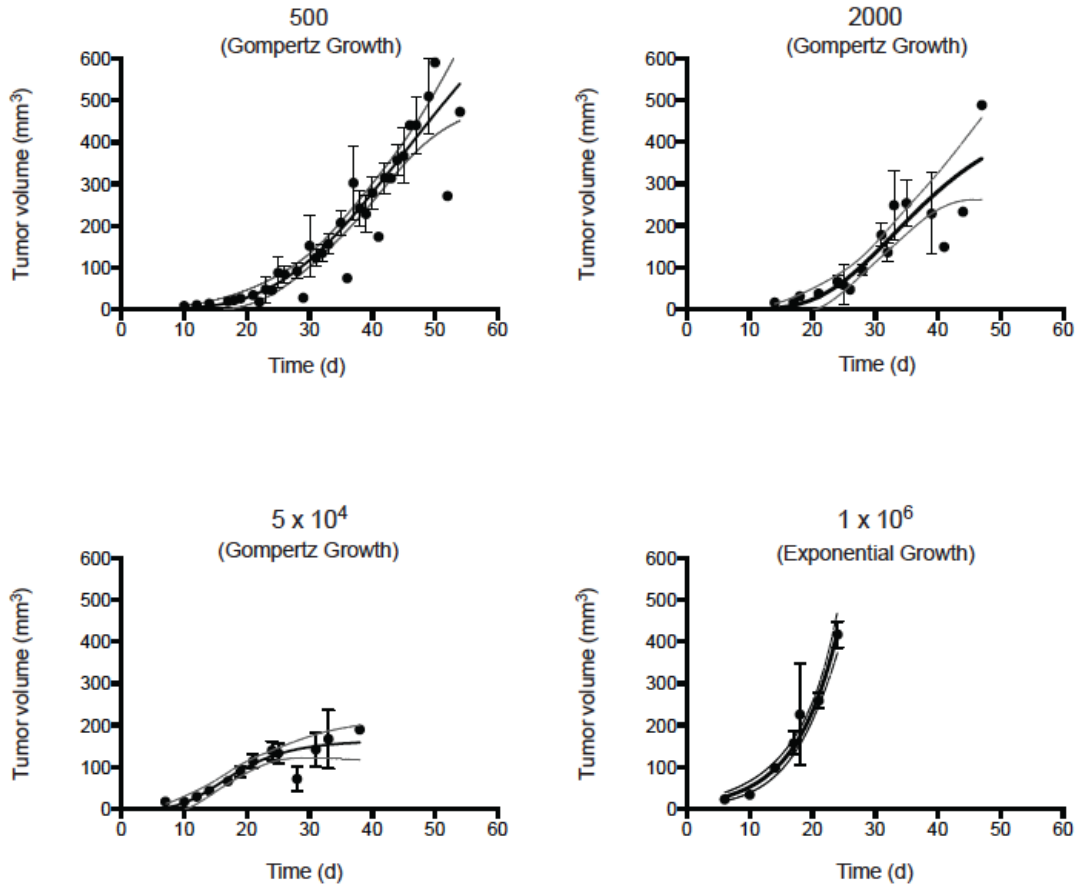

B

No. 4T1 cells inoculated	Best fit model	AIC probability	Extra sum-of squares F test	SGR (%/d) ± SEM	Doubling time (d)
$1x10^6$	Exponential	57.29%	1.758 (p>0.05)	14.9 ± 1.15	4.6
$5x10^4$	Gompertz	99.98%	19.85 (p<0.0001)	16.1 ± 5.06	4.3
2000	Gompertz	88.01%	6.263 (p<0.05)	8.6 ± 3.41	8.1
500	Gompertz	99.88%	15.84 (p<0.0001)	5.1 ± 1.50	13.7

Figure 2.2: Fitting of mathematical growth models to tumor growth experimental data as a function of inoculated cell density.

Exponential and Gompertz models were fitted to the population's tumor growth curves (A) and compared using the Akaike's information criteria (AIC) and the extra sum-of-squares F test (B). Specific growth rates (SGR) and doubling times of each group were determined from the mathematical equations of the best fit (B). Dark symbols represent experimental mean tumor volumes. The solid line represents the best fit for each group with a 95% confidence interval, light lines.

Doubling time (DT) and specific growth rate (SGR), two parameters usually used to quantify and characterize neoplastic growth, were also determined (see *Materials and Methods*). One million and 5 x 10^4 cell density groups averaged growth rates of 14.9% and 16.1% *per* day, with doubling times of 4.6 and 4.3 days, respectively (Figure 2.2B).

2.2.3. 4T1 tumors viable rim area and vasculature

The previous sections have evidenced that the inoculated cell density has a marked influence on the tumor growth dynamics and metastatic efficiency. Tumor necrosis is thought to result from rapidly proliferating cancer cells outpacing their blood supply in certain tumor regions[390,391]. As necrotic cells release pro-inflammatory factors into the tumor microenvironment, which are known to promote tumor growth and dissemination[390,392], it was further questioned whether the altered dynamics would affect the viable rim area and vascular density of primary tumors, and whether it would relate to their metastatic efficiency. Sections from tumors of all groups were stained either with H&E, to determine the viable rim area, or with CD31, to assess vascular density. Additionally, the analysis accounted for differences on tumor volumes, distinguishing between smaller (100 – 200 mm^3) and larger (> 250 mm^3) tumors, within each group of mice. Both the viable rim area and vascular density were independent from tumor volume and cell density inoculated (Figure 2.3 and 2.4A, respectively). Considerable necrotic heterogeneity amongst the neoplastic masses was observed (Figure S2.1). In both classes of tumors analyzed, with a mean size of 100 – 200 mm^3 or higher than 250 mm^3, there were cases with large necrotic areas, thus having decreased viable rim areas, or with low extent of necrosis (and high extent of viable rim regions).

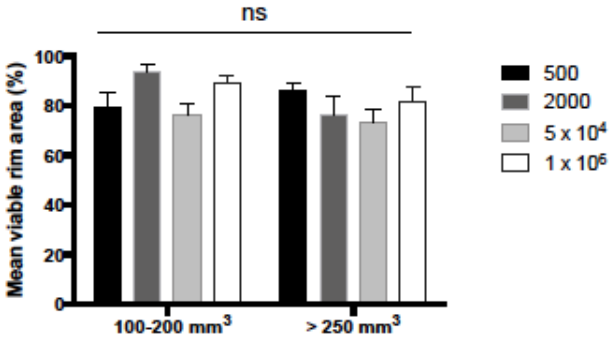

Figure 2.3: Viable rim areas of 4T1 breast tumors as a function of inoculated cell density and primary tumor mean volume.

Quantitative analysis of viable rim areas were assessed in tumors with mean volumes of 100 – 200 mm^3 and > 250 mm^3, based on H&E immunostaining in carcinoma sections derived from 500, 2000, 5 x 10^4 and 1 x 10^6 cancer cells. Data represent mean ± SEM of 3 – 6 independent sections. ns, $p > 0.05$ two-way *ANOVA* with Tukey's multiple comparisons test.

Representative images of tumor sections stained with CD31 (Figure 2.4B) confirmed the high vascularized nature of these tumors, regardless the number of inoculated cells they were generated from. These tumors already entailed a good vascular network at volumes between 100 – 150 mm^3.

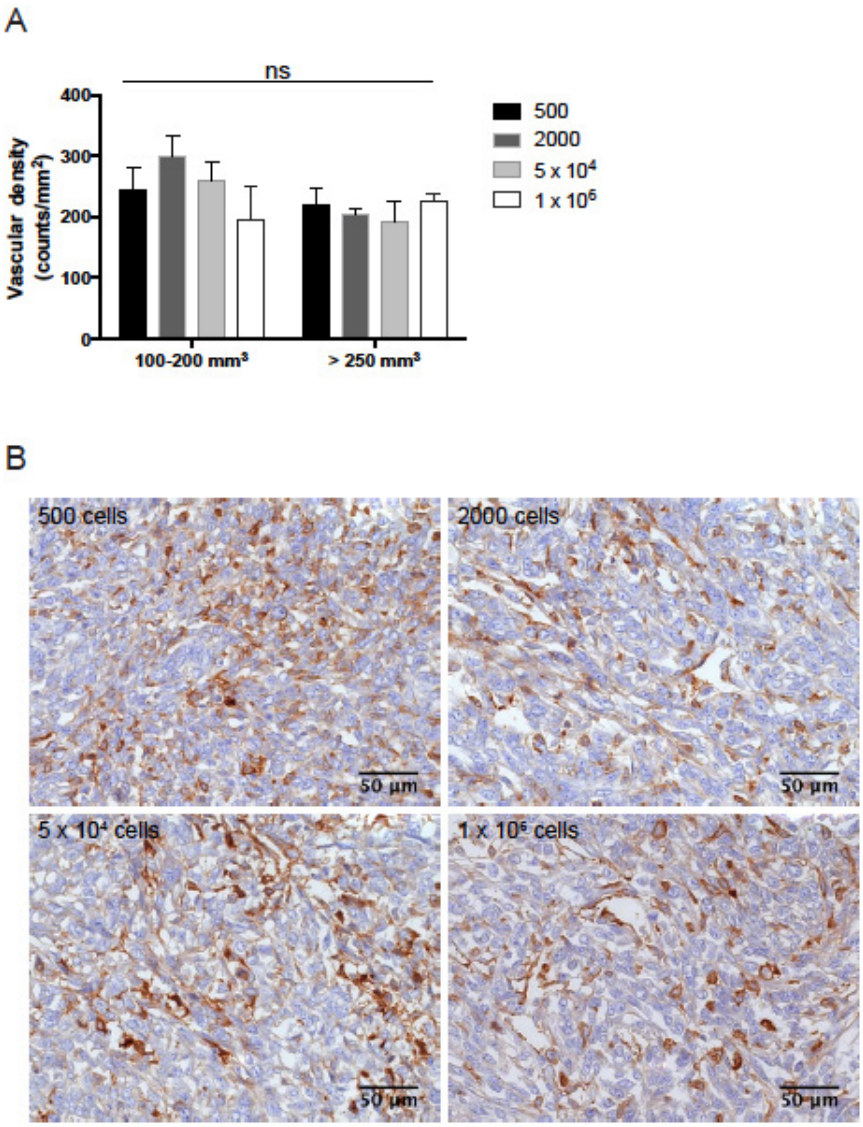

Figure 2.4: Vascular density of 4T1 breast tumors as a function of inoculated cell density and primary tumor mean volume.

Vascular density was assessed in tumors with mean volumes of 100 – 200 mm^3 and > 250 mm^3 (A), based on CD31 immunostaining in carcinoma sections derived from 500, 2000, 5 x 10^4 and 1 x 10^6 cancer cells, original magnification x400 (B). Data represent the mean ± SEM of 3 – 4 independent sections. ns, $p > 0.05$ two-way *ANOVA* with Tukey's multiple comparisons test.

Overall, neither the viable rim area nor the vascular density of tumors originating from the different cell densities correlated with their respective metastatic efficiency. Nevertheless, the inoculation of 500 4T1 cancer cells provided the best metastatic efficiency, possibly due to lower specific growth rates (or extended doubling times), yielding an optimal model to study metastatic breast cancer.

2.3. Discussion

The orthotopic inoculation of cancer cells is extensively used in breast cancer research. The predictive utility of these tumor models relies on their capacity to reproduce human malignancy, and should allow the analysis of human primary tumor growth, including invasion of surrounding tissue, interactions of tumor cells with their stromal components, and metastatic progression[365,367]. Breast cancer originates from genetic and epigenetic transformations in a single cell, progressing to clonal expansion and selection and, ultimately, to metastatic disease[393]. Animal models of breast cancer have provided some understanding of these features, enabling the proposal of new treatments[394]. However, primary breast tumors often originate from the inoculation of a large number of cancer cells, which is associated with a high growth rate, failing to efficiently generate metastases or leading to their surgically resection to prolong survival[365]. Therefore this strategy clearly deviates from the natural history of the disease, resulting in neoplastic tissues that, from our experience, do not resemble the human malignancy. Likewise, the 4T1 breast carcinoma mouse model is frequently implemented upon inoculation of a large number of 4T1 cancer cells in the mammary fat pad of mice, ranging from 1 x 10^4 to more than 1x10^6 cells[171,374,378-383]. However, in the present work it has been demonstrated that the inoculation of such high cell densities compromised the development of an efficient and reproducible model of spontaneous metastases.

It was demonstrated that 4T1 tumors grew in the mammary fat pad of mice when as few as 500 cancer cells were inoculated, being tumor incidence comparable for cell densities ranging from 500 to 1x10^6 (87% and 92%, respectively). However, inoculated cell density influenced significantly the latency period for first palpation and metastatic efficiency (Table 2.1). The indirect correlation between the number of inoculated cancer cells and the time required to proliferate and generate a larger tumor mass, was in contrast with the effect on the metastatic efficiency. Only 45% of mice inoculated with 1x10^6 cells presented macroscopic secondary lesions, which is in contrast with the 100% metastatic efficiency of the group inoculated with 500 cells (Table 2.1). Interestingly, Bailey-Down *et al*.[395] also showed that the reduction of the number of implanted 4T1 cells increased metastatic efficiency. Nevertheless, in animals inoculated with a number of cells equal or lower than 1500, the tumor take rate was lower than 50% and macrometastases were barely observed at five weeks post-implantation[395], in contrast with the results reported herein. In the work of Bailey-Down *et al*., the best compromise between tumor take rate (over 90%) and metastatic efficiency (67% in the lungs) was achieved upon inoculation of 7500 4T1 cells. It is well known that the shedding of cancer cells into the bloodstream is an early event in the process of tumorigenesis[396,397]. Therefore, one could assume that tumors originated from different cell densities would enable

similar metastatic potential. However, in the groups inoculated with the highest cell densities, the time frame between tumor onset and animals euthanasia was strongly shortened by the high tumor burden and subsequent need of primary tumor resection. This short time frame, probably was not sufficient for the progression of the seeded cells into macrometastases. As such, the present results clearly demonstrated that the inoculation of low cell densities surpass the need of primary tumor resection, thus becoming a key methodological aspect to the reproducible development of macrometastases in the 4T1 mouse model.

The results herein presented also highlighted the impact of cancer cell density on the dynamics of the primary tumor development, as reflected by the different growth curves, and specific growth rates and doubling times (Figure 2.2). In fact, tumors originated from $5x10^4$ and $1x10^6$ cells grew at a rate that was approximately 2 and 3 times faster than those from 2000 and 500 cell densities, respectively. These results are in line with the corresponding shortened time for tumor onset (Table 2.1). Two conceptual theories, the Exponential[385] and Gompertz[385,386] growth models, have been used to describe the tumor dynamics. The first one states that primary tumor expansion is purely the result of cell division, resulting in exponential growth of solid tumors, while the second incorporates different growth rates, depending on the stage of tumor development[386]. The cancer cell inoculation titration herein performed was better described by the Gompertz model, but only to a certain extent, as tumors generated from $1x10^6$ cells followed an exponential growth. An old concept to explain the Gompertz model is the insufficient nutrient supply to large solid tumors, which impairs their unlimited expansion[398], thus justifying the decrease of growth rate upon reaching a certain mean volume. Yet, evidence of large tumors (1 – 2 cm^3) with an adequate vascular network[399] has challenged this theory, and is in agreement with the results obtained herein showing similar mean vascular densities (Figure 2.4) and viable rim areas (Figure 2.3), regardless tumor burden and cell densities the tumors were originated from. More recently, the idea of self-seeding[387] as a multidirectional process, whereby cancer cells seed secondary sites and re-infiltrate the primary *foci*, has been validated in several experimental models, including the 4T1 breast cancer model[400]. Self-seeding selects for highly aggressive fractions of circulating tumor cells based on their movement and survival in the bloodstream. The primary tumor homing of this population of cells was shown to further induce angiogenesis and invasion, in addition to the breeding of metastatic progenies in a compatible soil[400]. This process is thought to contribute for the Gompertzian expansion of tumors[387] and might be also contributing for the high metastatic efficiency observed for the lowest 4T1 cell densities.

The higher metastatic efficiency of the 500, 2000 and $5x10^4$ cell density groups may result from other factors as well. 4T1 cancer cells were shown to play an active role in the production and release of a variety of factors that stimulate hematopoiesis, enabling

the recruitment and activation of inflammatory cells, and modulation of the endothelial function[384,401-404]. Although we did not look into systemic and microenvironment local changes, the occurrence of splenomegaly was observed, suggesting that a leukemoid reaction took place (Figure S2.2). These events stimulated primary *foci* progression and, ultimately, metastasization by promoting cancer cell invasion, dissemination, seeding and growth into metastatic lesions[405,406]. Nevertheless, all these processes require a minimum time frame to occur. As such, the time frame requested for the expansion of seeded cells into macrometastases could explain the lower metastatic efficiency of $5x10^4$ cell inoculated group, as compared to the 500 and 2000 counterparts, despite all of them follow the Gompertz growth model.

An inter subject metastatic pattern variability associated with the 4T1 mouse model was also observed, which is more realistic and insightful of metastatic disease. However, this divergent metastatic pattern impeded the accurate determination of the total metastatic burden. It was difficult, and sometimes infeasible, to determine the number of metastatic lesions in tissues extensively affected. Although weighting of organs like the lungs or liver, could surpass this difficulty, this methodology was not appropriate to assess metastatic burden in the mesentery. In this respect, the use of non-invasive techniques as bioluminescence imaging, which enables the longitudinal follow-up of the metastatic spread and quantification of total tumor/metastatic burden, could provide a significant improvement[384,407,408].

2.4. Conclusion

The present study addressed the low metastatic efficacy associated with the orthotopic implementation of the 4T1 metastatic breast cancer cells. Notwithstanding being a widely used animal model to study metastatic breast cancer, the referred problem is barely mentioned in the literature. Herein, it was demonstrated that upon reducing the number of 4T1 mouse breast cancer cells implanted in the mammary fat pad, to a number as low as 500 cells, a 100% metastatic efficiency was established, along with a high primary tumor take rate. The inoculation of a low number of cancer cells significantly increased the tumor doubling time and decreased the specific growth rate, following a Gompertzian tumor expansion. It thus enabled a time frame that permitted the progression of the seeded cells into macrometastases, before reaching a mean volume of the primary tumor demanding surgical removal. This becomes a key methodological aspect towards the reproducible development of macrometastases in the 4T1 mouse model. Extending the time length of tumor development will enable longitudinal studies to follow all the steps of cancer cell dissemination in the same individual, from early seeding to late macroscopic lesions, as well as a better assessment of anti-metastatic therapies.

2.5. Materials and methods

2.5.1. Materials

Ethylenediaminetetraacetic acid disodium salt dihydrate (EDTA), potassium phosphate monobasic (KH_2PO_4), disodium phosphate anhydrous (Na_2HPO_4), potassium chloride (KCl) and sodium chloride (NaCl) were purchase from Sigma-Aldrich (USA).

2.5.2. Cell culture

4T1 mycoplasma-free cells were cultured in RPMI-1640 (Sigma-Aldrich, USA) supplemented with 10% (v/v) heat-inactivated Fetal Bovine Serum (FBS) (Invitrogen, USA), 100 U/ml penicilin, 100 μg/ml streptomycin (Lonza, Switzerland) and maintained at 37ºC in a 5% CO_2 atmosphere.

2.5.3. Animals

Balb/c female mice (Balb/cAnNCrl), 5 – 6 weeks old, were purchased from Charles River Laboratories, France. The animals were housed under controlled environmental conditions (22ºC room temperature, 50 ± 10 % relative humidity, 12 h light – dark rhythm), and fed *at libidum* during the course of the experiments. All animal experiments were conducted according to human standards of animal care (2010/63/EU directive and Portuguese Act 113/2013, for the use of experimental animals).

2.5.4. 4T1 cancer cell inoculation

Sub-confluent 4T1 cells were detached from the flask with dissociation buffer (PBS - 0.02% EDTA), spun down at 200 *g* for 5 min, and resuspended in PBS. Cell count and viability were accessed upon staining with Trypan Blue (Sigma-Aldrich, USA). Cell suspensions were prepared at 5 x 10^3, 2 x 10^4, 5 x 10^5 and 10 x 10^6 cells/mL in PBS, and maintained at room temperature. Mice were inoculated within 40 min after preparation of cell suspension, in the fourth inguinal mammary fat pad (100 μL/mouse).

For the cell titration, mice were assigned to different groups according to the number of 4T1 cells to be injected: *I)* 500, *II)* 2000, *III)* 5 x 10^4 and *IV)* 1 x 10^6. Tumor volume was measured with a caliper every other day, and tumor volume was determined based on the equation $\pi/6(a \times b^2)$, where *a* is the largest tumor diameter and *b* is the smallest[409]. Within each of the aforementioned groups, half of the tumors were allowed to grow between 100 – 200 mm^3 or > 250 mm^3. When tumors reached the specified volumes, corresponding animals were euthanized for necropsy and organs harvested for histological analysis.

2.5.5. Tumor growth curves

Exponential and Gompertz mathematical models[410] were fit to the mean tumor volume data (overtime) of all mice using non-linear regression, and the goodness-of-fit of the models was compared. The goodness-of-fit for each model was determined by the Akaike's Information Criteria (AIC) values and the extra sum-of-squares F test. Specific growth rate (SGR) and doubling time (DT) parameters were determined and given in the output of the fitting analysis.

2.5.6. Histological analysis of primary tumors and metastases

Primary tumors and organs with metastatic lesions were kept on fixative solution (Tissue-Tek® Xpress® Molecular Fixative, Sakura) for 24 h. Tissues were then paraffin embedded, sectioned onto slides (4 μm) and stained with hematoxylin/eosin (H&E). Primary tumors sections were also stained with CD31 (Ventana Medical Systems, Inc., USA) using the BenchMark ULTRA IHC/ISH staining module (Ventana Medical Systems, Inc., USA) to assess the vascular density. Mean vascular density was the mean of CD31 stained blood vessels counted in 4 different fields (400x) of a primary tumor section.

Histological evaluation of metastases and primary tumors invasion of surrounding tissues was performed in sections of the collected organs, stained with H&E. H&E stained sections were visualized in a Axioskop 2 Plus microscope (Zeiss, Germany) and the corresponding area measurements were analyzed with the Fiji software (Life-Line version, 2014 November 25, NIH, USA). Viable rim area was determined in the entire section by excluding necrotic areas, and was represented as a ratio of the total area of that section.

2.5.7. Statistical analysis

Data were analyzed using unpaired nonparametric one-way *ANOVA* with a 95% confidence interval, followed by Dunn's multiple comparisons test. Viable rim area and vessel density for different tumor sizes were analyzed using unmatched two-way *ANOVA* with Tukey's multiple comparisons test.

2.6. Supplementary figures

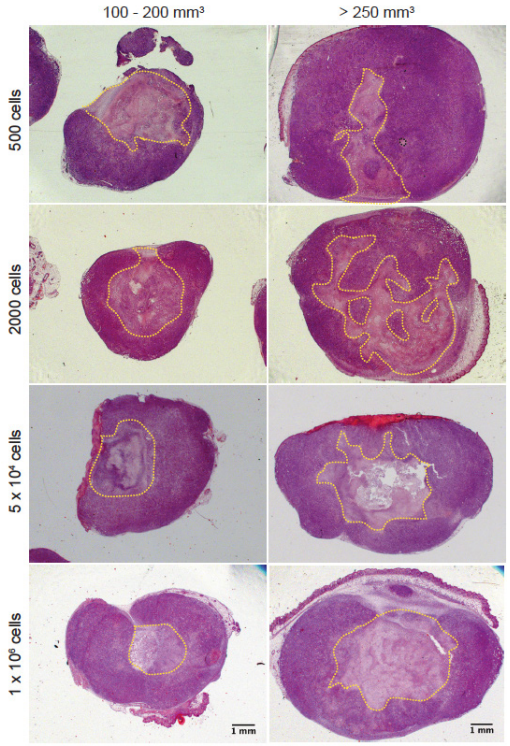

Figure S2.1: Viable rim areas of 4T1 breast tumors as a function of inoculated cell density.

Hematoxylin and eosin staining of representative tumor sections resulting from 500, 2000, 5 x 10^4 and 1 x 10^6 cancer cells inoculated in the mammary fat pad of Balb/c female mice. The images show necrotic and viable rim areas in representative sections of tumors with a mean volume of 100 – 200 mm^3 or larger than 250 mm^3. Necrotic regions correspond to the zones delimited by dashed yellow line. All images present original magnification x12.5.

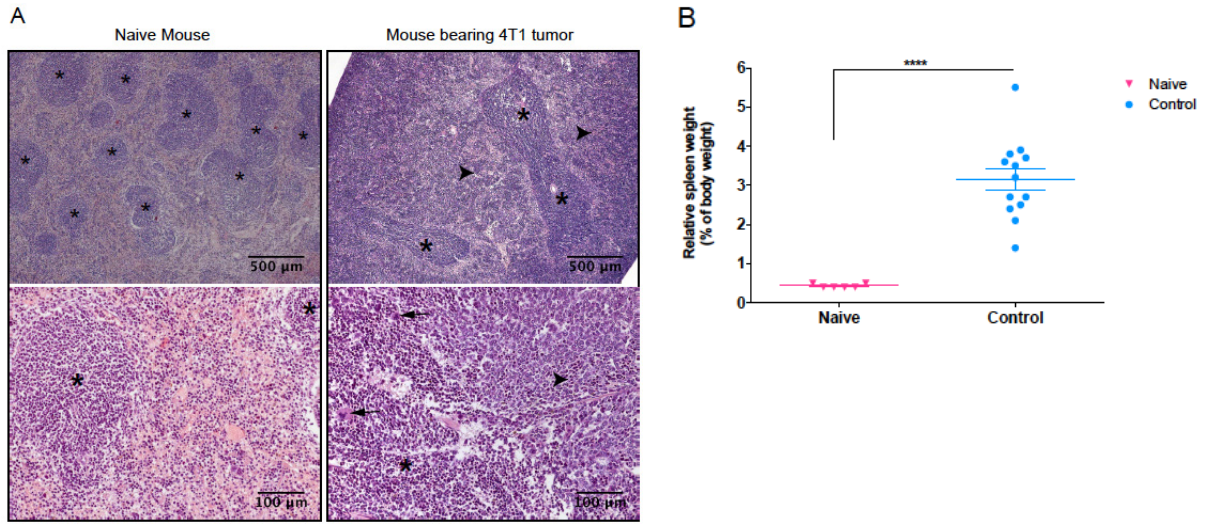

Figure S2.2: Splenic extramedullary hematopoiesis in naïve or 4T1 breast tumor-bearing mice.

Representative images (A) and relative weight (B) of spleens with increased extramedullary hematopoiesis in 4T1 breast tumor-bearing mice, as compared to naïve animals. Well-defined splenic nodules constituting the white pulp (*) were scattered across the spleen section of naïve mice. In contrast, the expansion of hematopoietic cells such as megakaryocytes (arrows), erythroid and myeloid precursor cells through the red pulp (arrowheads) was notably increased in tumor-bearing mice. Data represent mean ± SEM of 6 naïve and 13 tumor-bearing (control) mice. ****, $p < 0.0001$ two-tailed nonparametric Mann-Whitney test.

Chapter 3

Exploring nucleolin as a therapeutic target in a mouse model of metastatic breast cancer

Abstract

The development of targeted therapies capable of tackling metastatic breast cancer has been a difficult challenge. Cell surface nucleolin has emerged as an attractive target in cancer therapy, operating as a binding partner for several ligands with tumorigenic and angiogenic functions, and as a shuttle protein between the nucleus, cytoplasm and cellular membrane. Furthermore, it has been implicated in some mechanisms of metastatic progression. The goal of this work was to explore the therapeutic potential of nucleolin in the setting of metastatic breast cancer, using pH-sensitive liposomes containing Doxorubicin and functionalized with the nucleolin-binding F3 peptide (PEGASEMP™). F3 peptide-targeted liposomes led to 7 to 36-fold increase in cellular association with three metastatic (triple-negative or ER-positive) breast cancer cell lines, compared with non-targeted or targeted by a non-specific peptide counterpart. The increased cellular association enabled a 8.8 to 17-fold augment of cytotoxicity. In the 4T1 model of metastatic breast cancer, however, the therapeutic activity of PEGASEMP™ did not surmount the overall efficacy of Caelyx® (median survival of 46 days and two complete responses), and resulted in only a marginal tumor growth delay relative to non-treated mice. Nevertheless, PEGASEMP™ significantly extended the survival (16 *versus* 28 d, Log-rank p = 0.0015), and reduced the incidence of metastatic nodules in the mesentery (33% *versus* 77%, p = 0.0409) compared with non-treated mice. These results put forward the need to investigate different therapeutic schedules enabling higher systemic exposure of F3 peptide-targeted liposomal Doxorubicin.

3.1. Introduction

Considerable advances in targeted therapy anticipated an important gain on the survival of patients with breast carcinoma. Yet, metastatic breast cancer remains an incurable disease, with a median 5-year survival from diagnosis of only 20 – 26%[411,412], and the majority of patients surviving 20 – 28 months[363,413-415]. Hence, the main goal in the setting of metastatic breast cancer is fundamentally palliation[416].

The development of targeted strategies for hormone- and HER-2-positive breast cancer subtypes, has improved the outcomes in the metastatic setting[417,418]. First-line treatment options for ER/PR-positive breast tumors include the use of aromatase inhibitors, alone or in combination with inhibitors of mTOR (Everolimus) and cyclin-dependent kinases 4/6 (Palbociclib), a context in which tamoxifen still remains a valuable option[21,35,419]. In HER-2-positive breast tumors, the approval of Trastuzumab, followed more recently by other HER2 targeting drugs (Lapatinib, Pertuzumab and Trastuzumab-emtansine), have changed the treatment paradigm and are regarded as standard of care for this subtype of breast carcinoma[21,35,419]. Despite these major achievements, tumor plasticity, both at the cellular and molecular level, will ultimately drive to drug resistance[420-424] and request chemotherapy-based treatments[425,426]. Additionally, triple-negative breast cancer is a subtype for which targeted therapeutic options are still missing at the present time[427]. Therefore, and regardless the limited long-term success and severe side effects that deteriorate the patients quality of life, systemic chemotherapy, alone or in combination with targeted drugs, still rests as the backbone of TNBC and metastatic breast cancer treatment[428]. The encapsulation of chemotherapeutic agents, like anthracyclines, into nanoparticles, has stood as a relevant strategy to significantly improve Doxorubicin (DXR) dose-limiting cardiotoxicity. An example is the pegylated liposomal Doxorubicin (Caelyx®), which is indicated for a variety of solid tumors, including metastatic breast cancer[429,430].

In the case of Caelyx®, the therapeutic efficacy observed in animal models has translated into modest survival benefit in patients[429-432]. Covalent coupling of internalizing targeting ligands onto the surface of pegylated liposomes, arises as a strategy to further improve therapeutic efficacy, while decreasing the extent of drug-associated toxicities[433]. The rationale of this strategy relies on the specific binding to the corresponding receptor overexpressed on the surface of tumor cells, followed by endocytosis and cytosolic delivery of the encapsulated drug payload.

Nucleolin is overexpressed in cancer cells and tumor-associated blood vessels[249,250], and several reports have implicated this protein in various processes supporting tumorigenesis[304,305] and angiogenesis[249,306,434]. Its role in mediating the anti-tumoral and anti-angiogenic activity of endostatin[318,435] has contributed to the emergence of nucleolin as a

relevant therapeutic target in oncology. The involvement of nucleolin in some mechanisms of metastatic progression has also been uncovered[246,266,295,304,305,324]. Moreover, a decrease in metastatic incidence in mouse models of breast[295], melanoma[321] and pancreatic tumors[436] have been reported, upon targeting nucleolin. Along this increased interest, several moieties targeting nucleolin have been developed[247,250]. Covalent attachment of the nucleolin-binding F3 peptide onto pegylated lipid-based nanoparticle[246], revealed to be a promising approach for tumor-targeted delivery of chemotherapeutics to both cancer and endothelial cells. These nanoparticles have shown to suppress tumor invasion in mice-bearing human tumors implanted in the mammary fat pad[246].

In the light of the current state-of-the-art, it is of utmost importance the design of novel therapeutic strategies targeting metastatic sites. We sought to explore nucleolin overexpression as a target to both primary and metastatic lesions, using F3 peptide-targeted liposomes containing Doxorubicin. Following this rationale, the present work aims at assessing the therapeutic impact of F3 peptide-targeted pH-sensitive liposomes containing Doxorubicin in the context of metastatic breast cancer.

3.2. Results

3.2.1. I*n vitro* cellular association with metastatic breast cancer cells

The specificity and extent of interaction of rhodamine-labeled F3 peptide-targeted liposomes was performed upon incubation with metastatic triple-negative (mouse 4T1 and human MDA-MB-231) or estrogen-receptor positive (mouse E0771) breast cancer cells, and further assessed by flow cytometry.

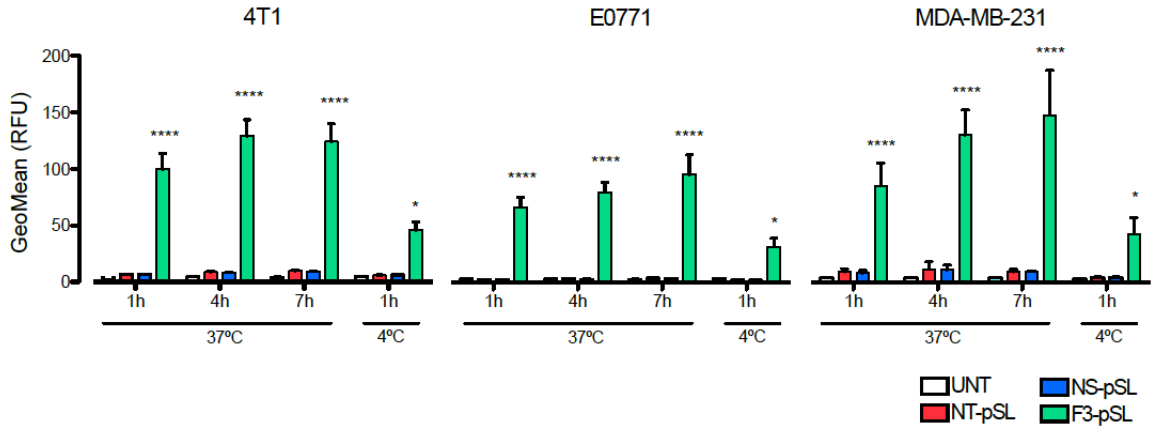

Figure 3.1: Cellular association of different formulations of rhodamine-labeled liposomes by breast cancer cell lines.

Mouse 4T1 and E0771, and human MDA-MB-231 metastatic breast cancer cells, were incubated with rhodamine-labeled pH-sensitive liposomes (at 0.4 mM of total lipid/well), either non-targeted (NT-pSL) or targeted by the F3 peptide (F3-pSL) or a non-specific peptide (NS-pSL), for 1, 4 and 7 h at 37ºC or 1 h at 4ºC. Cell-associated fluorescence was evaluated by

flow cytometry, and the results were expressed as geometric mean of cell-associated rhodamine fluorescence from 3 to 5 independent experiments. ****, $p < 0.0001$; *, $p < 0.05$ two-way *ANOVA* with Tukey's multiple comparisons test.

The extent of cellular association of F3 peptide-targeted liposomes (F3-pSL) was significantly higher than for non-targeted (NT-pSL) or targeted by a non-specific peptide (NS-pSL) counterparts, regardless the cell line and incubation time (Figure 3.1). 4T1 and MDA-MB-231 cells presented the highest absolute values of fluorescence intensity. Notwithstanding, a 28- to 36-fold increase in association of F3 peptide-targeted liposomes by E0771 cells was observed, relative to the tested controls, in contrast with the 12- to 16-fold or 7- to 18-fold increase by 4T1 and MDA-MB-231 cells, respectively. The lower extent of association of NT-pSL and NS-pSL liposomes by E0771 cells, relative to the other cell lines tested, justified the mentioned fold-increase in cellular association of targeted liposomes. Within the time frame assessed, only with 4T1 cancer cells F3 peptide-targeted liposomes seemed to reach their maximum extent of association, following 4 h of incubation at 37ºC. The difference of fluorescence intensity between the experiments at 37ºC and 4ºC, a non-permissive temperature to endocytosis, strongly suggested that an active cellular internalization was taking place.

Overall, these data suggested a ligand-specific interaction between the F3 peptide-targeted liposomes and nucleolin-overexpressing (triple negative and estrogen-receptor positive) breast cancer cells.

3.2.2. I*n vitro* cytotoxicity studies

To evaluate the cytotoxic impact arising from the ligand-specific association of F3 peptide-targeted liposomes, the activity of these nanoparticles encapsulating Doxorubicin (F3-pSL[DXR]) was tested against 4T1 and E0771 mouse breast cancer cell lines, and compared with the activity of free DXR or DXR-encapsulating non-targeted liposomes, either pH-sensitive (NT-pSL[DXR]) or non-pH-sensitive (SL[DXR]), or targeted by a non-specific peptide (NS-pSL[DXR]). Doxorubicin delivered by F3 peptide-targeted liposomes was 8.8 to 10-fold more cytotoxic against 4T1 cells than their non-targeted counterparts or liposomes targeted by a non-specific peptide, respectively (Figure 3.2 and Table 3.1). In the case of E0771 cells, this difference increased to 12.4 to 17-fold.

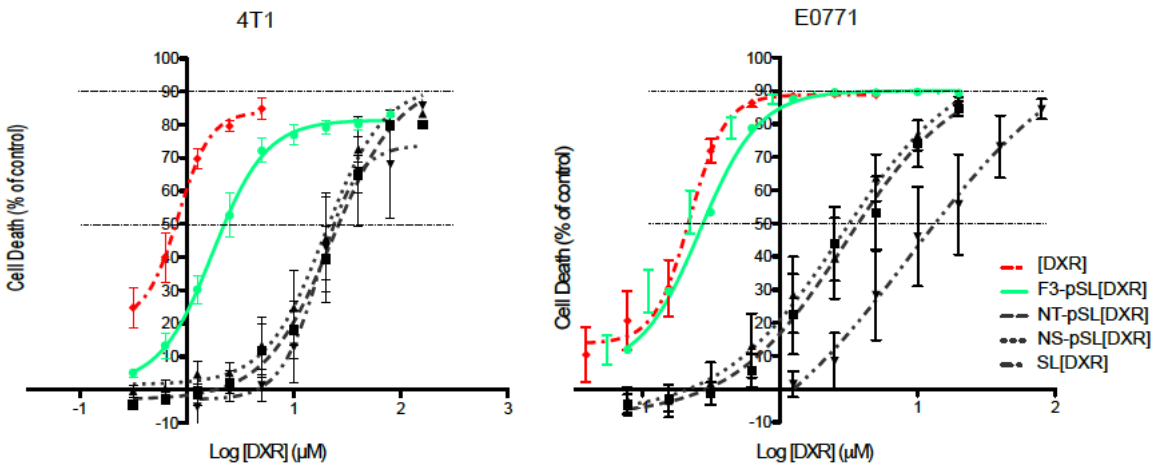

Figure 3.2: Cytotoxicity of different formulations of DXR-encapsulating liposomes against mouse metastatic breast cancer cell lines.

Dose-response curves for 4T1 and E0771 mouse breast cancer cell lines incubated with free doxorubicin (DXR), DXR-encapsulating F3 peptide-targeted (F3-pSL[DXR]) or non-specific peptide-targeted (NS-pSL[DXR]) pH-sensitive liposomes, or non-targeted, pH-sensitive (NT-pSL[DXR]) or non-pH sensitive (SL[DXR]), liposomes for 1 h at 37ºC, followed by additional 95 h in fresh medium (without drug). Cell growth inhibition was determined by the Resazurin Reduction test and represented as percentage of cell death relative to control (untreated cells). Data represent the mean ± SEM of 4 to 6 independent experiments.

Table 3.1: IC_{50} values determined for different DXR-encapsulating liposomal formulations against mouse breast cancer cell lines, following 1 h incubation.

	IC_{50} (μM) ± SEM	
	4T1	E0771
SL[DXR]	18.56 ± 4.044 [a]	5.11 ± 1.023 [a]
NT-pSL[DXR]	17.27 ± 2.838 [a]	3.72 ± 1.021 [b]
NS-pSL[DXR]	19.71 ± 4.521 [a]	4.51 ± 0.809 [a]
F3-pSL[DXR]	1.97 ± 0.371	0.30 ± 0.037
DXR	0.82 ± 0.060	0.21 ± 0.015

IC_{50} values were calculated from the dose-response curves; data represent mean ± SEM of 4 to 6 independent experiments. [a], $p < 0.01$; [b], $p < 0.05$ one-way *ANOVA* with Tukey's multiple comparisons test.

These results were in agreement with the high extent of cellular association of targeted liposomes for 4T1 and E0771 cancer cells, presented in the previous section. Although incubation with free Doxorubicin enabled the highest levels of cytotoxicity (particularly in the case of E0771 cells), one should take into account the high volume of distribution presented by the free drug *in vivo*, upon intravenous administration, responsible for a marked dose-limiting cardiotoxicity and limited efficacy.

3.2.3. Nucleolin expression in cancer cells and MDA-MB-231 and 4T1 tumors

Immunohistochemistry staining with an anti-nucleolin monoclonal antibody was performed in sections from cell blocks from the three cell lines previously used (Figure 3.3), and MDA-MB-231- and 4T1-derived primary tumor tissues, including 4T1-derived metastases (Figure 3.4).

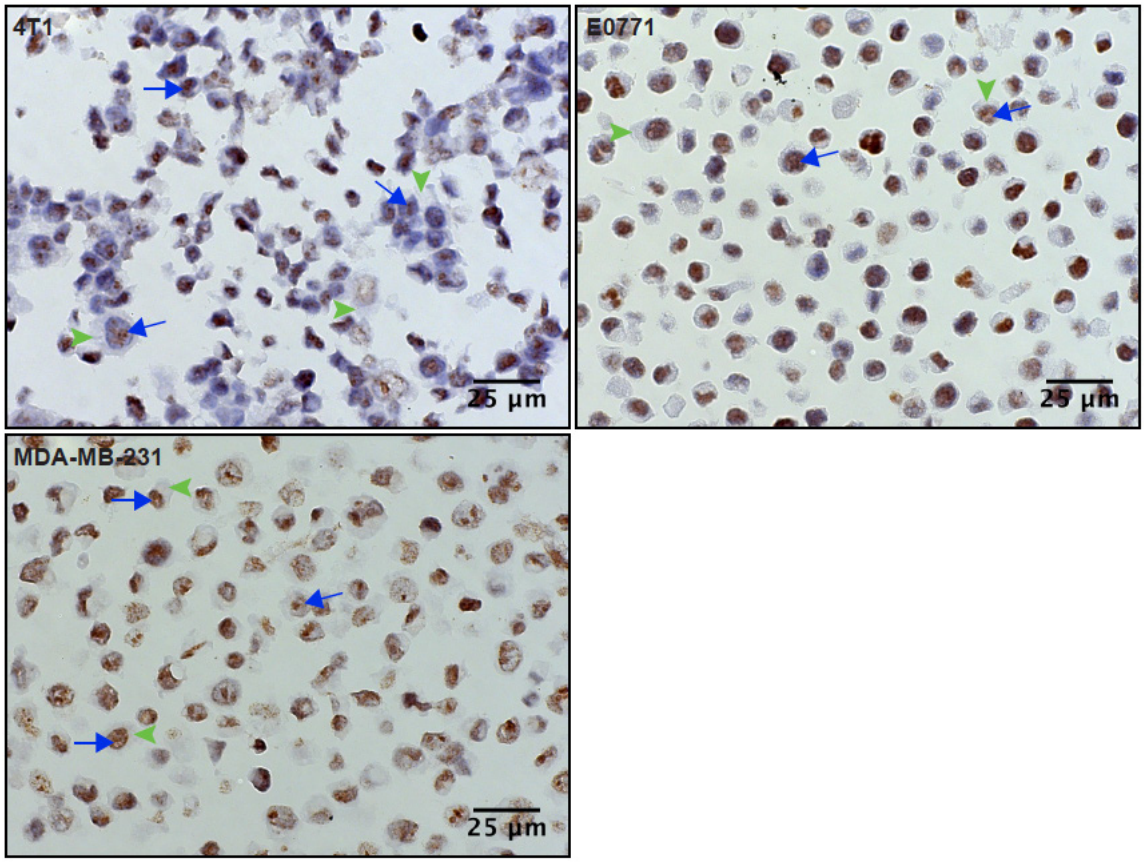

Figure 3.3: Nucleolin expression in breast cancer cell lines.
Immunocytochemistry performed on cell blocks from mouse metastatic breast 4T1 and E0771, and human MDA-MB-231 cancer cells showed positive staining for nucleolin (brown staining), including nuclear/nucleolar staining (blue arrows); green arrowheads indicate (the weaker) cytoplasmatic staining. All images present original magnification x630.

All cancer cells exhibited positive staining for nucleolin, being the pattern of expression mainly nuclear/nucleolar (blue arrows), albeit these cells presented a reduced incidence of cytoplasmic staining (green arrowheads) as well. Interestingly, staining of the cytoplasmic membrane was not identified.

In order to support the targeting strategy towards nucleolin, the protein expression was assessed on 4T1- and MDA-MB-231-derived primary tumors, and 4T1 metastatic lesions. Both primary tumors and metastases overexpressed nucleolin, as illustrated in Figure 3.4. Of notice, a change in the pattern of expression from a nuclear/nucleolar staining in the cell

blocks, to a predominantly cytoplasmic staining in both MDA-MB-231 and 4T1 primary tumors and 4T1 metastases, was observed. Likewise, endothelial cells of tumor blood vessels were also positively stained for nucleolin, confirming results previously reported by others[246,249,250].

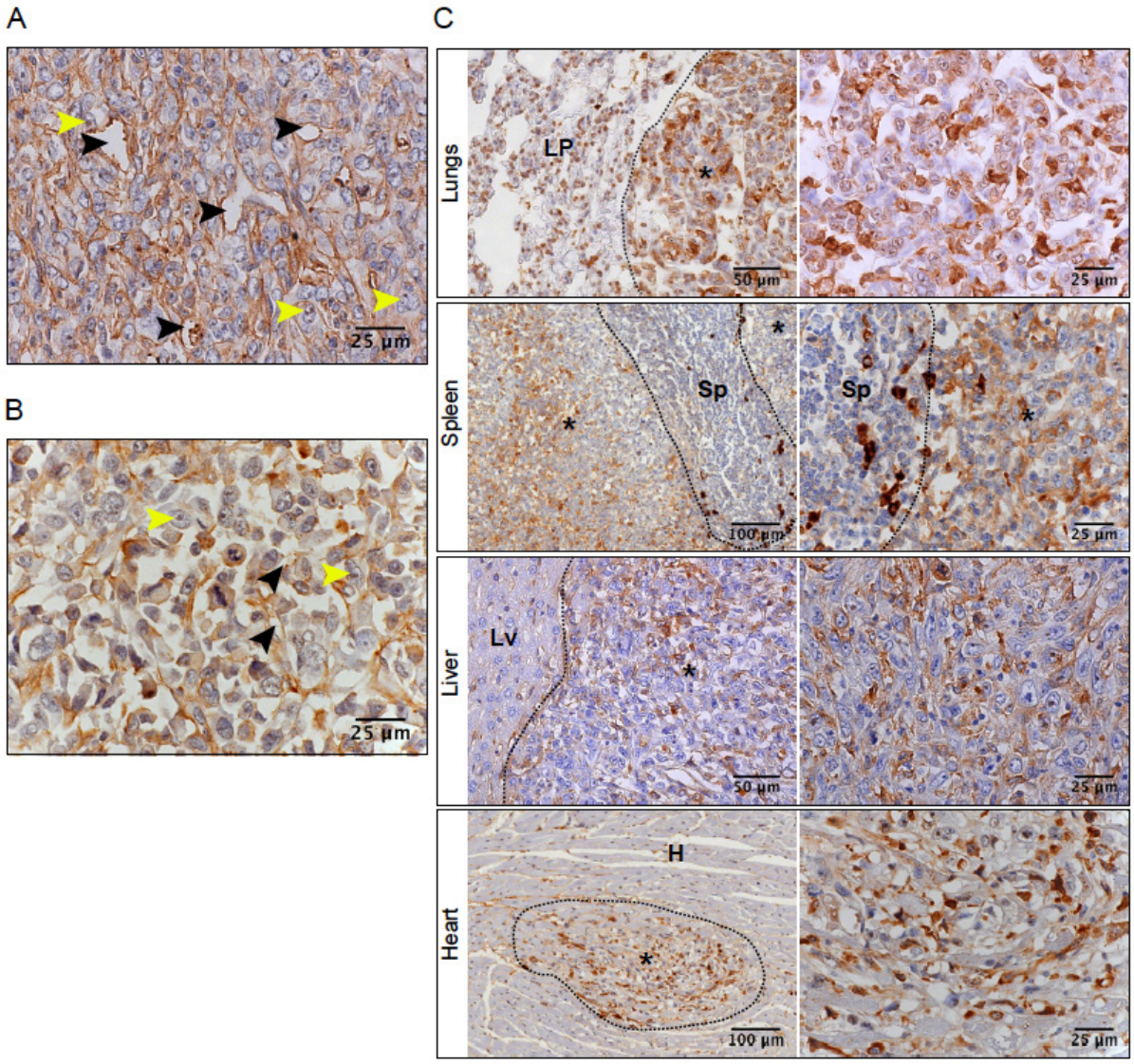

Figure 3.4: Nucleolin expression in representative sections from primary 4T1- and MDA-MB-231-derived tumors and 4T1 nodular metastatic deposits.

The expression of nucleolin was evaluated in 4T1 (A) and MDA-MB-231 (B) orthotopic tumors, original magnification x630. Nucleolin staining observed in both 4T1 and MDA-MB-231 tumors was mostly cytoplasmic, although nucleolar staining was identified in some cells (yellow arrowheads); tumor blood vessels in both mouse models (black arrowheads) were also positively stained for the protein. A positive cytoplasmic expression of nucleolin was also observed in 4T1 metastasis (C). Representative metastatic nodules in the lungs, spleen, liver and heart are illustrated (original magnification x400 and x200, left panel; x630, right panel). LP, normal lung parenchyma; SP, normal spleen tissue; Lv, normal liver tissue; H, normal heart tissue; * indicates tumor areas.

Overall, these data supported the nucleolin-targeted therapeutic rationale towards metastatic breast cancer, for which the 4T1 murine model was used.

3.2.4. Therapeutic activity of F3 peptide-targeted liposomes containing Doxorubicin against 4T1 metastatic breast cancer

To assess the therapeutic impact of the F3 peptide-targeted liposomes containing Doxorubicin, the previously characterized 4T1 metastatic breast carcinoma mouse model was used. As mentioned earlier, this model has the capacity to spontaneously and efficiently metastasize to sites that are a match of the human disease[378,437].

Upon inoculation of 4T1 cancer cells in the mammary fat pad, Balb/c mice were monitored for body weight and symptoms of distress caused by metastatic disease[438,439]. In view of the preceding results, therapeutic protocol was initiated when tumors presented an established vascular network, corresponding to a mean volume of 100 – 150 mm^3. Mice were weekly treated via the lateral tail vein with Caelyx® or F3 peptide-targeted liposomes containing Doxorubicin (codenamed as PEGASEMP™), at 5 mg DXR/kg body, for 5 weeks. A control group was injected with saline. Due to widespread of metastatic disease, not all animals completed this therapeutic regimen. The majority of mice in the control group survived up to the 3rd dose, and only those treated with PEGASEMP™ or Caelyx® managed to achieve the 5th administration (Figure 3.5A). In this experiment, a significant reduction of the primary tumor was observed in three Caelyx®-treated mice, although followed by regrowth, and two complete remissions (Figure 3.5B). The latter remained tumor-free for more than 60 days after the last dose and did not present metastatic nodules upon necropsy. Nevertheless, three animals responded poorly to the therapy with Caelyx® and died from the disease (Figure 3.5B). None of the other treatment groups presented a similar therapeutic response, neither in terms of primary tumor growth inhibition ($p < 0.0001$, Figure 3.5B) nor in terms of overall survival, Figure 3.5C (Log-rank $p = 0.0422$, relative to PEGASEMP™ and $p = 0.0053$, relative to Control). Nevertheless, mice administrated with PEGASEMP™ showed a superior overall survival (Figure 3.5C) compared to non-treated mice (Log-rank $p = 0.0015$). The significant difference of relative tumor weight observed between PEGASEMP™ (8.16 ± 0.84 % of body weight) and Caelyx® (4.28 ± 0.70 % body weight, $p < 0.05$, Figure 3.5D) resulted mainly from the former lower efficiency in inhibiting primary tumor growth (Figure 3.5B). When compared to non-treated mice (4.92 ± 0.67 % of body weight), the difference of relative tumor weight resulted from the extended survival of PEGASEMP™-treated mice (Figure 3.5C), which enabled a longer period for tumor development.

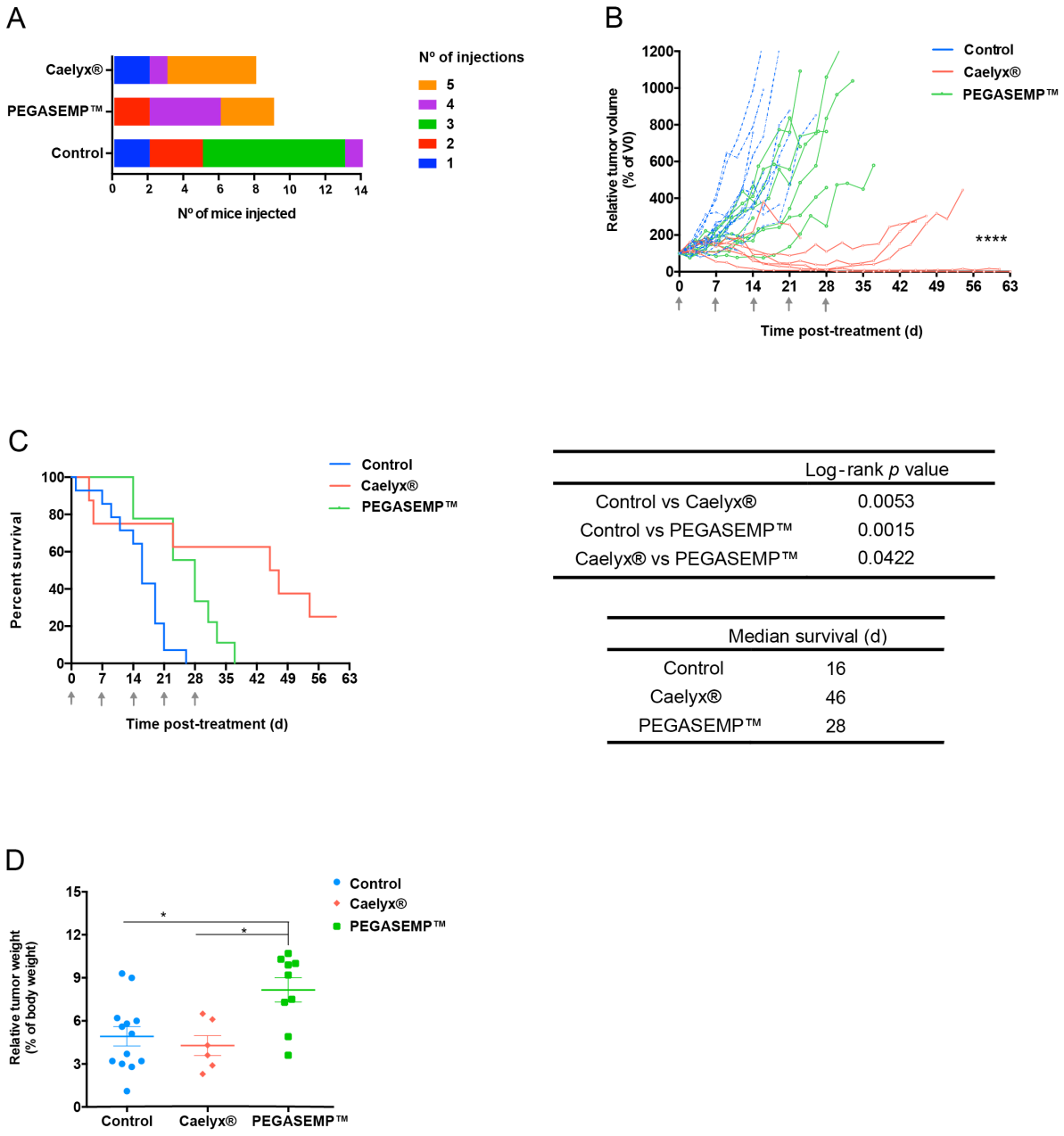

	Log-rank *p* value
Control vs Caelyx®	0.0053
Control vs PEGASEMP™	0.0015
Caelyx® vs PEGASEMP™	0.0422

	Median survival (d)
Control	16
Caelyx®	46
PEGASEMP™	28

Figure 3.5: Therapeutic efficacy of different doxorubicin-encapsulated liposomal formulations in 4T1 metastatic breast cancer model.

Balb/c mice implanted with 500 4T1 cancer cells in the mammary fat pad were treated weekly with Caelyx® or PEGASEMP™, at 5 mg DXR/kg body weight for 5 weeks (indicated by grey arrows). An additional control group included non-treated mice (injected with saline). The number of doses accomplished in each treatment group (A), along with individual tumor growth curves (B), survival curves (C), and relative tumor weight of individual mice (dots) and respective means (D) are illustrated. Data represent individual or mean ± SEM of either control (n=14), Caelyx®- (n=8) or PEGASEMP™-treated (n=9) mice, except in relative tumor weight (n=13 for control and n=6 for Caelyx®). ****, $p < 0.0001$; *, $p < 0.05$ nonparametric one-way ANOVA with Dunn's multiple comparisons test; Log-rank test for the analysis of survival curve.

Histological analysis of the neoplastic tissues confirmed the vast capacity of 4T1 breast cancer cells to invade muscle, skin and surrounding mammary parenchyma (Figure 3.6A). None of the tested treatments had the ability to limit tumoral invasiveness (Figure 3.6A), or induced a significant reduction of the viable rim area as compared to the control non-treated mice (Figure 3.6B).

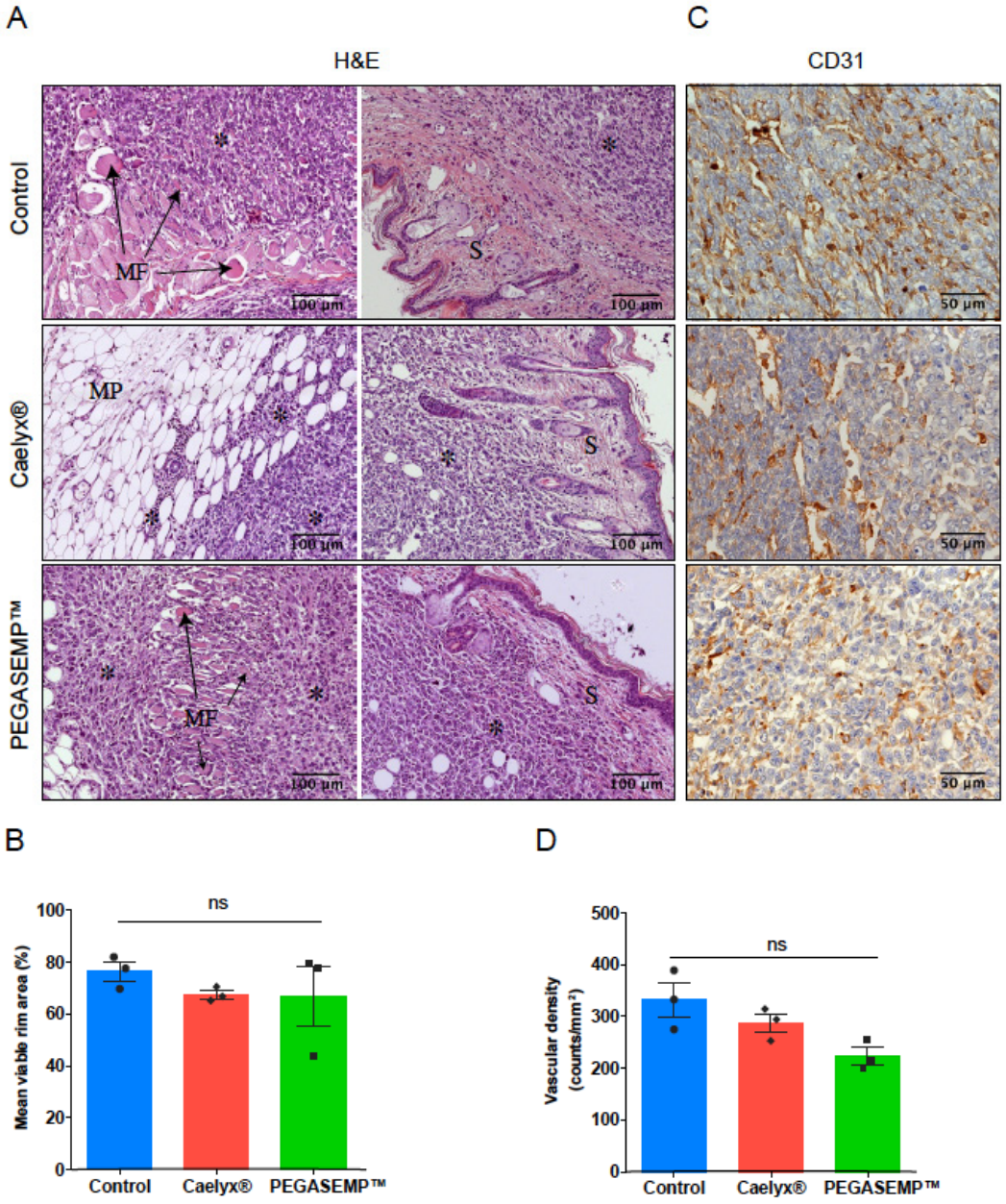

Figure 3.6: Histological analysis of 4T1 primary tumors following treatment with different liposomal formulations. H&E staining (A), quantification of viable rim area (B), CD31 immunostaining (C), and quantification of vascular density (D), on representative sections from 4T1 primary tumors, following treatment either with Caelyx® or PEGASEMP™ (including non-treated mice). Original magnification x200 (H&E), and x400 (CD31). MF, muscle fibers; S, skin; MP, mammary parenchyma; * indicates tumor areas. Data represent mean ± SEM of 3 independent sections. ns, $p > 0.05$ nonparametric one-way ANOVA with Dunn's multiple comparisons test.

This effect was not consistent with the decrease (although non-significant, $p = 0.0709$) of the mean vascular density (Figure 3.6C and D) observed with PEGASEMP™ treatment (223 ± 16.83 counts/mm^2) relative to the control (332 ± 32.91 counts/mm^2).

Secondary metastatic lesions in several organs/tissues were also observed in all animals, with the exception of the two mice that presented a complete response to Caelyx® (Table 3.2). One hundred percent of non-treated and PEGASEMP™-treated animals presented lung metastases. The incidence decreased in Caelyx®-treated mice (75%) owing to disease remission in two mice. Only in the mesentery the incidence of metastatic nodules was significantly reduced in mice under PEGASEMP™ therapy compared to non-treated mice (33% *versus* 77%, respectively; $p = 0.0409$). Noteworthy, the results also pointed to a similar effect relative to Caelyx® (38%, $p = 0.0708$), with the contribution of the two disease-free mice at the end of the experiment (Table 3.2). For the other organs/tissues examined, although statistical differences were not observed, the odds ratio estimates revealed some trends (Figure 3.7). Caelyx® seemed to decrease the incidence of metastization to the pancreas (OR = 0.4444, 95% CI: 0.07207 – 2.741) and diaphragm (OR = 0.3889, 95% CI: 0.05605 – 2.698) compared to non-treated mice. A similar effect was observed in the case of PEGASEMP™-treated animals in pancreatic tissue (OR=0.3556, 95% CI: 0.06083 – 2.078). Although in both cases the odds ratio of metastatic incidence in the liver was inferior to one (OR = 0.2706 and 0.6875, respectively), they were associated with a large confidence interval (95% CI: 0.01143 – 6.403 and 0.05272 – 8.965, respectively), thus with a low level of precision and not regarded as a trend.

Table 3.2: Incidence of metastatic lesions in 4T1 breast carcinoma-bearing mice.

	No. of mice with metastatic lesions /total no. of mice analyzed (%)				
	Lungs	Liver	Pancreas	Mesentery	Diaphragm
Control	13/13 (100%)	2/13 (15%)	9/13 (69%)	10/13 (77%)	6/13 (46%)
Caelyx®	6/8 (75%)[a]	0/8 (0%)	4/8 (50%)	3/8 (38%)[b]	2/8 (25%)
PEGASEMP™	9/9 (100%)	1/9 (11%)	4/9 (44%)	3/9 (33%)[c]	5/9 (56%)

[a], $p = 0.0581$; [b], $p = 0.0708$; [c], $p = 0.0409$ (two-tailed chi-square test analysis)

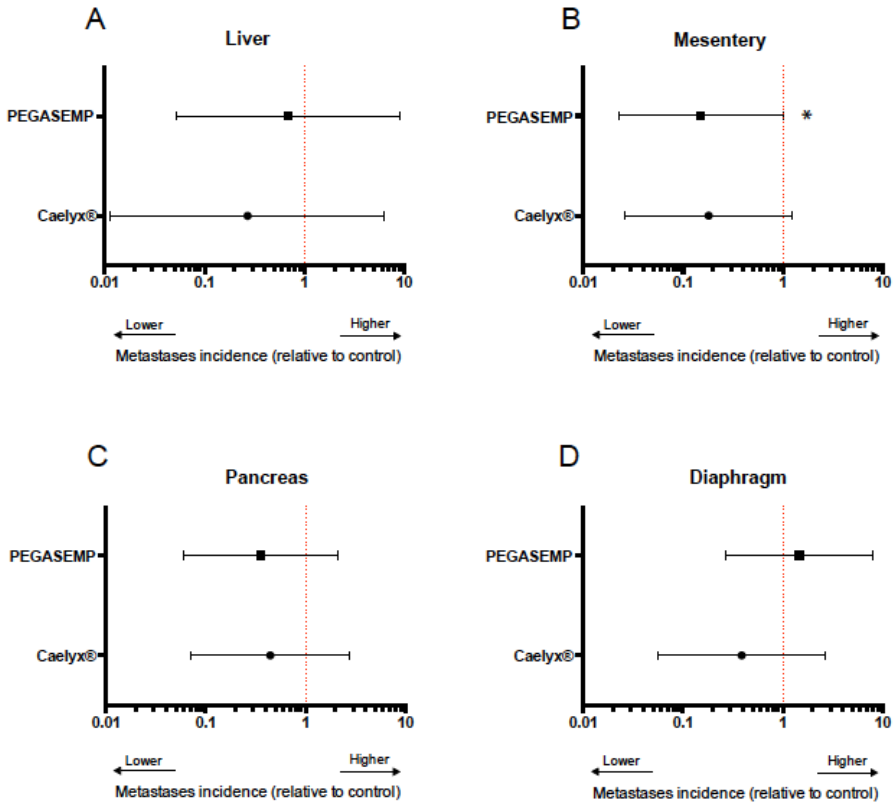

Figure 3.7: Estimates of the odds ratio for metastases incidence.

The forest plot graphs the odds ratios (OR) for incidence of distant lesions in liver (A), mesentery (B), pancreas (C) and diaphragm (D), with a 95% confidence interval (CI). Odds ratios were determined by the analysis of contingency tables comparing the metastatic incidence in organs/tissues from mice exposed to Caelyx® or PEGASEMP™ *versus* non-treated mice. OR=1, treatment does not affect the odds of metastatic incidence (red dashed line); OR<1, treatment is associated with lower odds of metastatic incidence; OR>1, treatment is associated with higher odds of metastatic incidence. *, p = 0.0409 two-tailed chi-square test analysis.

As previously described in chapter 2, the extent of the pulmonary and visceral lesions was considerably variable amongst individuals. Nevertheless, lung metastatic burden was estimated upon organ weight (see *Materials and Methods*). All treatment groups presented comparable mean metastatic burden in the lungs (Figure 3.8). Despite lung metastatic burden of non-treated animals (1.37 0.12) was comparable to the one of PEGASEMP™ group (1.84 ± 0.23), the extent of both survival time (Figure 3.5C) and tumor growth inhibition (Figure 3.5D), were very dissimilar between these two groups. Likewise, Caelyx®-treated mice, with a mean metastatic burden in the lungs of 1.65 ± 0.31 (Figure 3.7), presented the longest survival rate (Figure 3.5C). Despite the significant effect of Caelyx® on primary tumor growth inhibition, the extended survival time of these animals probably enabled a sufficient time frame for metastatic development, already *in site* by the time of treatment initiation.

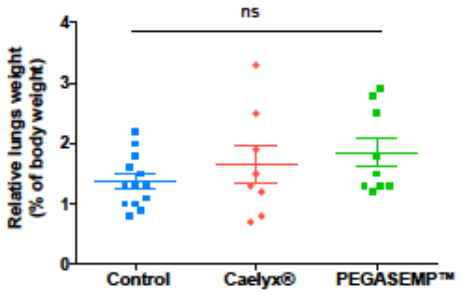

Figure 3.8: Metastatic burden in the lungs following treatment with different liposomal formulations of doxorubicin.
Metastatic burden was determined upon organ weight for individual mice treated either with Caelyx® or PEGASEMP™ (including a control group injected with saline) and further normalized for the whole body weight. Data represent individual (dots) or mean ± SEM of control (n=13), Caelyx® (n=8) and PEGASEMP™ (n=9) mice. ns, $p > 0.05$ nonparametric one-way *ANOVA* with Dunn's multiple comparisons test.

Splenomegaly was confirmed by visual examination and relative organ weight quantification, in all mice bearing 4T1 tumors, as discussed in the previous chapter and in agreement with data from other studies[384,401]. Interestingly, treatments with DXR-containing liposomes resulted in a slight decrease of relative spleen weight, in comparison with non-treated mice (Figure 3.9A). Histological examination of the spleens revealed hyperplasia of the red pulp with a concomitant reduction of the white pulp, with particular emphasis in non-treated mice (Figure 3.9B), and consistent with extramedullary hematopoiesis.

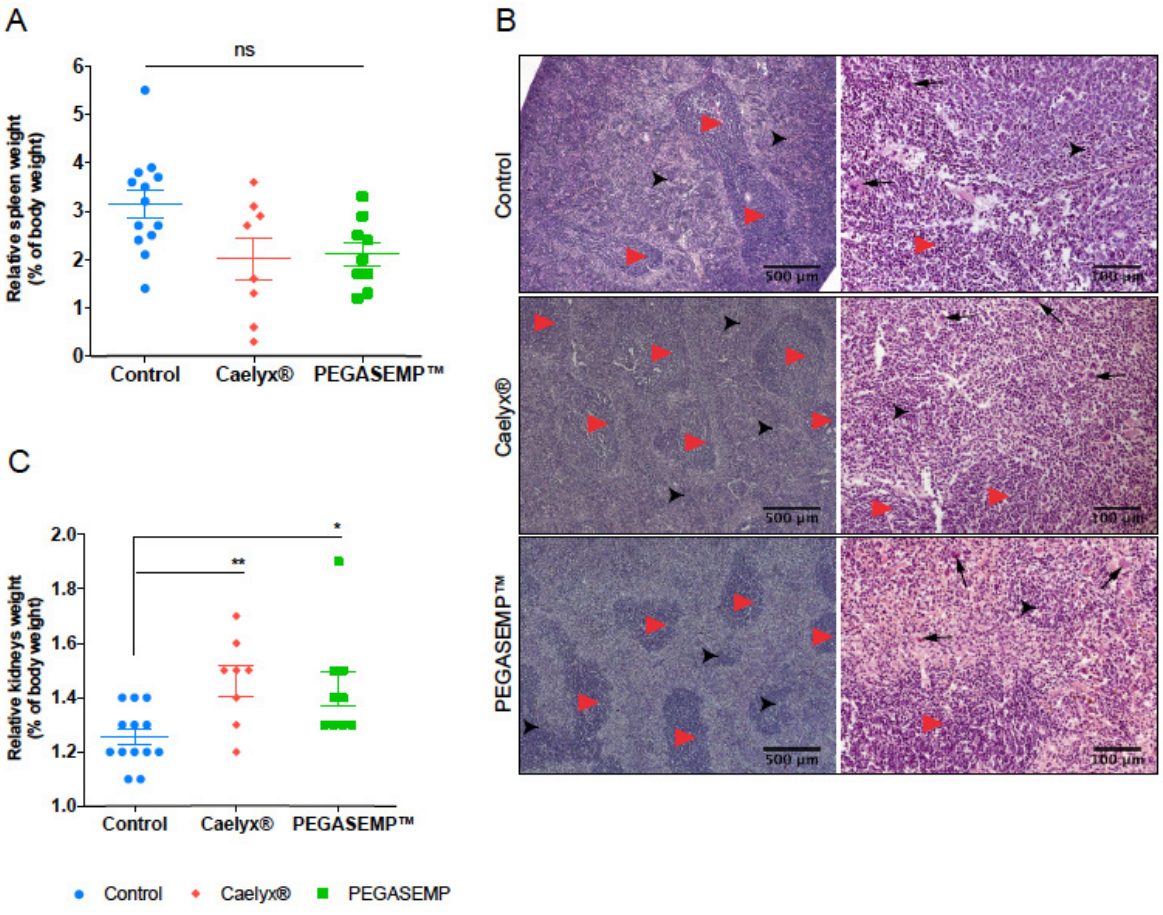

Figure 3.9: Effect of Caelyx® and PEGASEMP™ in the spleen and kidneys of mice bearing 4T1 tumors.
Relative weight (A) and representative H&E images, original magnification x50 (left) or x200 (right) (B) of spleens from mice treated with Caelyx® and PEGASEMP™, including non-treated mice. Images illustrate the red pulp markedly expanded by numerous hematopoietic cells (black arrowheads), including megakaryocytes (black arrows), and myeloid precursor cells, particularly in the controls. Red arrowheads represent white pulp areas with lymphoid nodules. The relative weight of kidneys (C) from Caelyx®- or PEGASEMP™-treated mice, or non-treated control was also analyzed. ns, $p > 0.05$; **, $p < 0.01$; *, $p < 0.05$ nonparametric one-way *ANOVA* with Dunn's multiple comparisons test.

Nonetheless, some degree of toxicity might have occurred given the increase of mean relative kidneys weight, in PEGASEMP™- ($p = 0.0424$) but particularly in Caelyx®-treated animals (p value = 0.0064), relative to non-treated mice (Figure 3.9C). Symptoms of palmar-plantar erythrodysesthesia were not registered in mice treated with Caelyx®, in contrast with previous reports[440], possibly due to a lower dose of Doxorubicin used herein.

3.3. Discussion

Cell surface nucleolin operates as a binding partner for several ligands, and as a shuttle protein between the nucleus, cytoplasm and cell membrane[240]. The shuttling function of nucleolin has been suggested, including the nuclear translocation of ligands like the F3 peptide[249,301,316,318,441]. In the metastatic breast cancer cell lines used herein, the expression pattern was essentially nuclear/nucleolar, although a degree of cytoplasmic staining was also observed (Figure 3.3). This result supported the higher extent of cellular association of liposomes targeted by the nucleolin-binding F3 peptide, relative to either non-targeted liposomes or targeted by non-specific peptide (Figure 3.1), which were in line with the ones previously generated with MDA-MB-435S cancer cells and HMEC-1 endothelial cells, using the same targeting strategy[246,354]. The decreased uptake at 4ºC, was also in agreement with data from Moura *et al*.[246] who demonstrated a relevant extent of active internalization of F3 peptide-targeted liposomes by the clathrin-mediated endocytic pathway. Therefore, the differences on the extent of cellular association among the metastatic breast cancer cell lines tested, could reflect an intrinsic variation in the density of expression and/or recycle rate of cell surface nucleolin. Recent data (personal communication from JN Moreira group) supported a direct relation between density of expression of cell surface nucleolin and the extent of cellular association of F3 peptide-targeted liposomes. Both arguments could also account for the saturation of cellular association observed for the 4T1 cells, following 4 h of incubation at 37ºC, in contrast with the other two cell lines (Figure 3.1). The improved cellular association presented by the F3 peptide-targeted pH-sensitive liposomes was translated into a higher cytotoxicity of encapsulated Doxorubicin, as compared to the non-targeted

controls, including a non-targeted non-pH sensitive formulation. This was likely the result of nucleolin-mediated endocytosis, upon specific binding of F3 peptide, improving the amount and the intracellular bioavailability of Doxorubicin[246]. Overall, these results sustained the rationale of a nucleolin-targeted therapeutic strategy in the setting of metastatic breast cancer. Moreover, in a previous study with nucleolin-overexpressing MDA-MB-435S-derived tumors, F3 peptide-targeted liposomes containing Doxorubicin suppressed tumor invasion in contrast with the non-targeted controls[246], further reinforcing this rationale.

In the study herein presented, the 4T1 cells were used to generate a mouse model of metastatic breast cancer. Globally, no physical signs of toxicity were attained by either treatments, albeit kidneys enlargement was observed in mice treated with Caelyx® and, less extensively, in the PEGASEMP™ cohort (Figure 3.9C). Although none of the Doxorubicin-containing liposomes were proficient in fully preventing metastatic disease (Table 3.2), treatment with Caelyx® presented a superior overall therapeutic response (Figure 3.5B – 5D). Despite PEGASEMP™'s inability to inhibit tumor growth (Figure 3.5E), treatment with this targeted formulation was still able to extend the lifespan of mice, relative to non-treated animals (Figure 3.5D). Therefore, PEGASEMP™ had a therapeutic effect, to some extent, at a level other than the primary tumor growth inhibition. The reduction of primary tumor burden promoted by the treatment with Caelyx® was a differentiating factor relative to PEGASEMP™, and a major contributor for the differences in median overall survival. The expansion of neoplastic masses, within a fairly confined space, generates a high mechanical compressive stress within the tumors, which has been shown to promote cancer progression and metastization[442-445]. Moreover, the tumors growing in the mammary fat pad of mice invaded and started to compress the organs in the peritoneal cavity, often associated with the development of ascites (herein observed), leading to mice euthanasia. Thus, the higher tumor burden observed in animals treated with PEGASEMP™ largely contributed to a shorter median overall survival relative to Caelyx®. Notably, both PEGASEMP™ and Caelyx® reduced the metastatic incidence in the mesentery (Table 3.2 and Figure 3.7). The colonization of the visceral organs by cancer cells in the 4T1 mammary carcinoma model was described to occur later than the lungs[378,384,395]. Therefore it is possible that the liposomal chemotherapy tested herein, limited further dissemination/colonization of tissues of the peritoneal cavity by 4T1 cells, accounting for a lower incidence of metastasis in the mesentery.

Extramedullary hematopoiesis has been shown to play a crucial role in the spontaneous metastization in the 4T1 mouse model[401,446], by contributing to a receptive microenvironment for circulating tumor cells arrest, survival and proliferation in the lungs[401,447,448]. Therefore, the therapeutic activity of both Caelyx® and PEGASEMP™ could be partially exerted by

restricting splenic hematopoiesis, as reflected in a reduced splenomegaly, relative to non-treated mice (Figure 3.9A and B).

The overexpression of nucleolin in endothelial cells of the tumor vasculature, created the expectation that PEGASEMP™ would lead to a significant reduction of tumor vascular density[246,307,318]. Although significant differences were not observed, it was recognizable that PEGASEMP™ induced a partial reduction of vascular density (p = 0.0709), in relation to the other therapeutic cohorts (Figure 3.6D). Such response was in line with the reduction of vessel density also observed by Moura *et al*., though herein the differences were less pronounced, and were not sufficient to induce 4T1 carcinoma growth arrest. Likewise, it has been demonstrated in mouse models of glicosarcoma, neuroblastoma and lung cancer[449,450] that Caelyx® exerted its antitumoral activity in part by the ability to elicit an antivascular effect. This effect was not observed herein with the 4T1 model, possibly due to the aggressiveness of the cancer model used herein and/or dose scheduling. The low extent of the antivascular effect might support the similar tumor viable rim area between mice treated with the Doxorubicin formulations and non-treated mice (Figure 3.6B). Additionally, non-tumoral vessels from surrounding tissues are also expected to provide nutrient and oxygen supplies to cells in the peritumoral region[451,452]. Altogether, these factors likely contributed to the maintenance of viable areas in the tumor mass that fuels its expansion and invasion (Figure 3.6A), and could be responsible for the tumor regrowth observed in some Caelyx®-treated mice.

Several studies[453-456] have reported the accumulation of pH-sensitive nanoparticles, with or without a targeting ligand, in the reticuloendothelial system organs – liver and spleen – leading to a rapid clearance from the bloodstream[457]. Additionally, recent results (personal communication from JN Moreira group) demonstrated that Caelyx® presented a higher systemic exposure than PEGASEMP™, at the same dose level (5 mg of DXR/Kg body weight). The reduction of PEGASEMP™'s blood residence time could result in fewer interactions with its tumor targets (cancer cells and endothelial cells from the tumor vasculature), subsequently limiting the overall extent of intracellular drug delivery and the therapeutic effect as compared to Caelyx®.

The targeting component of strategies like PEGASEMP™ renders them dependent on the overexpression of nucleolin and exposure of this protein at the tumor cells surface. The latter stands as one of the most relevant criteria for the patients' eligibility for many of the targeted therapies in a clinical setting, for which Trastuzumab is a classical example. Its indication is dependent on the HER2 overexpression on cancer cell membrane (IHC), and/or HER2 gene amplification (FISH)[458]. In the present study, a striking observation related with the change of nucleolin pattern of expression in the 4T1 tumor tissues, either primary

or secondary lesions, and in MDA-MB-231 tumors, relative to the corresponding cell lines. It became predominantly cytoplasmic, even though nucleolar staining was seen in some cells (Figure 3.4). The biological significance of this difference remains to be elucidated from a targeting perspective. Nevertheless, subcellular localization of nucleolin *in vivo* might change during carcinogenesis in response to biological factors produced by cancer cells and the tumor microenvironment[253,256]. Vascular endothelial growth factor plays an important role in the localization of nucleolin within the cell. VEGF was shown to stimulate nucleolin expression in the membrane and cytoplasmic fractions of endothelial[306] and colorectal carcinoma cells[459], while decreasing it in the nucleus[254]. The synthesis of nucleolin was also correlated with increased rates of cell division[240]. This matched its increased expression in 4T1 tumors and metastatic nodules relative to adjacent non-malignant tissues. This result further reinforced the rationale of targeting nucleolin, in both primary tumors and their metastases, as a therapeutic strategy to tackle metastatic disease, notwithstanding the presence of cell surface nucleolin was not demonstrated.

In this study, immunohistochemical analysis of the tumor tissues did not demonstrate the presence of cell surface nucleolin. However, cell surface nucleolin represents less than 10% of nuclear nucleolin[460] and undergoes a rapid turnover, with an estimated half-life of less than one hour, compared to more than eight hours in the nucleous[460]. Therefore, it was possible that the immunohistochemistry technique used herein was not able to fully capture this dynamic process. Nevertheless, the presence of cell surface nucleolin in the cancer cell lines used in this study has been recently validated in our lab by other techniques and was directly correlated with the extent of cellular association (personal communication from JN Moreira group). Though *in vitro* cellular association clearly demonstrated a selective and efficient binding of F3-pSL liposomes to 4T1 cells (Figure 3.1), the number of receptors at the cell surface *in vivo* might be different.

3.4. Conclusion

In vitro results indicated a higher cytotoxic effect by the F3 peptide-targeted liposomes in comparison with a non-targeted non-pH-sensitive formulation. However, this was not translated into an *in vivo* therapeutic impact. PEGASEMP™ tumor growth delay was marginal compared to control. Nevertheless, its therapeutic efficacy was conceivably higher, as reflected by a significant extension of survival. Still, the therapeutic benefits of PEGASEMP™ did not surmount the overall efficacy of Caelyx®. In this respect, the results generated with PEGASEMP™ suggested the need to further test therapeutic schedules enabling higher systemic exposure of encapsulated Doxorubicin. Fulfilling this goal is likely crucial to translate the efficient *in vitro* intracellular delivery and cytotoxicity of the encapsulated

payload into an *in vivo* setting of metastatic breast cancer, assuming the appropriateness of nucleolin (cytoplasmic) pattern of expression herein reported in tumor-bearing animals.

3.5. Materials and Methods

3.5.1. Materials

2-(N-Morpholino) ethanesulfonic acid (MES), 4-(2-hydroxyethyl)piperazine-1-ethanesulfonic acid (HEPES), ethylenediaminetetraacetic acid dihydrate (EDTA), Trizma®Base, potassium phosphate monobasic, disodium phosphate anhydrous, potassium chloride, sodium chloride, sodium acetate anhydrous, resazurin sodium salt, 3β-hydroxy-5-cholestene-3-hemisuccinate (CHEMS) and cholesterol (CHOL) were purchased from Sigma-Aldrich (USA). The lipids 1,2-distearoyl-*sn*-glycero-3-phosphocholine (DSPC), 1,2-dioleoyl-*sn*-glycero-3-phosphoethanolamine (DOPE), 1,2-distearoyl-*sn*-glycero-3-phosphoethanolamine-N-[methoxy(polyethylene glycol)-2000] (DSPE-PEG_{2K}), 1,2-distearoyl-*sn*-glycero-3-phosphoethanolamine-N-[maleimide(polyethylene glycol)-2000] (DSPE-PEG_{2K}-maleimide) and L-α-Phosphatidylethanolamine-N-(lissamine rhodamine B sulfonyl) (RhoD-PE) were obtained from Avanti Polar Lipids (USA). Doxorubicin hydrochloride (DXR) was from IdisPharma (UK). F3 peptide (KDEPQRRSARLSAKPAPPKPEPKPKKAPAKK) and the non-specific (NS) peptide $(ARALPSQRSR)^{250}$ were custom synthesized by Genecust (Luxemburg). The rabbit monoclonal antibody against nucleolin [EPR7952] was purchased from Abcam (UK). Caelyx® was kindly provided by the Pharmacy of the University Hospital of Coimbra (Portugal). PEGASEMP™ formulation was produced by Northern lipids Inc (Canada).

3.5.2. Liposome preparation

PEGylated non-pH-sensitive and pH-sensitive liposomes were composed of DSPC:CHOL:DSPE-PEG_{2k} (2:1:0.06 molar ratio) or DOPE:CHEMS:DSPC:CHOL:DSPE-PEG_{2k} (4:2:2:2:0.8 molar ratio), respectively. For some experiments, as mentioned in the Results, rhodamine-PE lipid was incorporated in the lipid mixture at 0.5 mol% of total lipid. Liposomes were prepared by the ethanol injection procedure[350]. The ethanolic lipid mixtures were slowly added to 300 mM ammonium sulfate buffer pH 5.5 or 8.5 at 60ºC, under strong agitation, for the non- and pH-sensitive formulations, respectively. Liposomes were extruded sequentially through 50 nm pore size polycarbonate membranes using a LiposoFast Basic mini extruder (Avestin, Canada). The buffer was exchanged in a Sephadex G-50 gel column (Sigma-Aldrich, USA) equilibrated with a buffer solution of 100 mM $NaCH_3COOH$ and 70 mM NaCL (pH 5.5), for the non-pH sensitive liposomes, or with 25 mM Trizma®base in 10% sucrose

(pH 9), for the pH-sensitive formulation. Remote encapsulation of Doxorubicin (18 mol% of Doxorubicin relative to total lipid) was carried out through the ammonium gradient method[461], upon incubation with the liposomes for 1.5 h at 60ºC. Non-encapsulated Doxorubicin was removed using a Sephadex G-50 gel column equilibrated with 25 mM HEPES, 140 mM NaCl buffer (HBS, pH 7.4) for both formulations.

To further prepare F3 peptide-targeted liposomes, DSPE-PEG_{2k}-F3 conjugate was produced. Briefly, thiolated derivative of F3 peptide was generated by reaction with 2-iminothiolane (Sigma-Aldrich, USA) in 25 mM HEPES, 140 mM NaCl, 1 mM EDTA buffer (pH 8.0), for 1 h at room temperature, in an inert N_2 atmosphere. Thiolated derivatives were then incubated overnight at room temperature with DSPE-PEG_{2k}-maleimide micelles in 25 mM HEPES, 25 mM MES, 140 mM NaCl, 1 mM EDTA (pH 7.0) The resulting micelles of DSPE-PEG_{2k}-peptide conjugates were postinserted[462] onto the liposomal membrane, at 2 mol% relative to total lipid, upon incubation with pre-formed liposomes, for 1 h at 50°C.

3.5.3. Characterization of liposomes

Liposomal mean size and polydispersion index were measured by light scattering with a N5 particle size analyzer (Beckman Coulter, USA). Final total lipid concentrations were determined upon quantification of cholesterol using Infinity® Cholesterol kit (ThermoScientific, USA). Encapsulated Doxorubicin was assayed at 492 nm from a standard curve, after liposomal solubilization with 96% absolute ethanol, and the loading efficiency (%) was further calculated.

3.5.4. Cell culture

The 4T1, E0771 and MDA-MB-231S cell lines were cultured in RPMI-1640 (Sigma-Aldrich, USA) supplemented with 10% (v/v) heat-inactivated Fetal Bovine Serum (FBS) (Invitrogen, USA), 100 U/ml penicilin, 100 μg/ml streptomycin (Lonza, Switzerland) and maintained at 37ºC in a 5% CO_2 atmosphere.

3.5.5. Cellular association

4T1, E0771 and MDA-MB-231 breast cancer cells were incubated with rhodamine-labeled liposomes, either non-targeted (NT-pSL) or targeted by a non-specific (NS-pSL) or F3 (F3-pSL) peptide, for 1, 4 and 7 h at 37ºC or 1 h at 4ºC. Cells were washed with phosphate buffered saline (PBS) pH 7.4, detached with dissociation buffer (PBS – 0.02% EDTA) and immediately analyzed for cell-associated fluorescence (FL2 channel) in FACS

Calibur Flow Cytometer (BD, Biosciences). A total of 20,000 events were collected and data were analyzed with Cell Quest Pro software.

3.5.6. I*n vitro* cytotoxicity

4T1 and E0771 cells were seeded in 96-well plates at a density of 1500 cells *per* well and further incubated with serially diluted concentrations of Doxorubicin (at a maximal concentration of 80 μM), free or encapsulated in liposomes (non-targeted non-pH-sensitive, SL; non-targeted pH-sensitive, NT-pSL; targeted by a non-specific peptide pH-sensitive, NS-pSL; and F3 peptide-targeted pH-sensitive, F3-pSL) for 1 h at 37ºC, in an atmosphere of 95% humidity and 5% CO_2. Following incubation, cells were gently washed with cold PBS pH 7.4 and kept in fresh medium for a total of 96 h. Cell viability was evaluated by the *Resazurin Reduction* test[463], at 570 (reduced form) - 610 (oxidized form) nm in a Spectrophotometer SPECTRA max PLUS 384, as previously described[350]. IC_{50} values were determined from dose-response curves.

3.5.7. Animals

Balb/c female mice (Balb/cAnNCrl), 5 – 6 weeks old, were purchased from Charles River Laboratories, France. The animals were housed under controlled environmental conditions (22ºC, 50 ± 10 % relative humidity, 12 h light – dark rhythm), and fed *at libidum* during the course of the experiments. All animal experiments were conducted according to the 2010/63/EU guideline and the Portuguese Act 113/2013 on animal experimentation.

3.5.8. Therapeutic study

Balb/c female mice were inoculated in the mammary pad with 500 4T1 cancer cells *per* mouse. Mice bearing orthotopically implanted 4T1 tumors, with a mean volume of 100 – 150 mm^3, were weekly treated intravenously with Caelyx® or PEGASEMP™ (produced by Northern lipids Inc) (at 5 mg Doxorubicin/kg body weight) for five weeks. An additional group injected with saline was included. Tumor size was measured with a caliper every other day, and tumor volume was determined based on the equation $\pi/6(a \times b^2)$, where *a* is the largest tumor diameter and *b* is the smallest[409]. Relative tumor volume was expressed as percentage of the tumor volume, at any time during the treatment, relative to its volume at the beginning of the treatment. Relative weight of the tumor or organs was expressed as percentage of body weight at the time of death. The relative weight of the lungs was used as a measure of the metastatic burden to that specific organ[464].

Monitoring of general physical status and body weight of the animals was performed every other day. Given the metastatic nature of 4T1 cells, development of clinical signs of distress caused by the metastatic disease and body weight losses higher than 20% were not consented and were reason for animal euthanasia. Upon necropsy, the organs were removed for histological analysis.

3.5.9. Histological analysis of primary tumors and metastases

Primary tumors and organs with metastatic lesions were kept on fixative solution (Tissue-Tek® Xpress® Molecular Fixative, Sakura) for 24 h and the tissues were further paraffin embedded and sectioned onto slides (4 μm) to be stained with hematoxylin/eosin (H&E). Primary tumors sections were also stained with nucleolin (EPR7952, dilution 1:8000; Abcam, UK) and CD31 (pre-diluted 0.1 – 1.5 μg/mL, Ventana Medical Systems, Inc., USA) to assess vessel density. Automated staining of the antibodies was performed using the BenchMark ULTRA IHC/ISH staining module (Ventana Medical Systems, Inc., USA).

Histological evaluation of metastases and primary tumors invasion of surrounding tissues was performed in sections of the collected organs, stained with H&E, visualized in an Axioskop 2 Plus microscope (Zeiss, Germany). Resulting images were analyzed with the Fiji software (Life-Line version, 2014 November 25, http://fiji.sc/Fiji) for the measurement of necrotic/viable rim areas[465]. Viable rim area was determined in the entire section by excluding necrotic areas, and was normalized to the total area of the corresponding section. Vessel density was based on CD31-stained blood vessels counted and averaged from four different fields (400x) of a primary tumor section.

3.5.10. Statistical analysis

In vitro data were analyzed using unmatched two-way *ANOVA* with Tukey's multiple comparisons test. All *in vivo* data were analyzed using unpaired nonparametric one-way *ANOVA*, followed by Dunn's multiple comparisons test. Log-rank test was applied for the survival curves and metastatic incidence were analyzed with a two-tailed chi-square test. All the analyses were performed with a 95% confidence interval (CI). Forest plots graph the odds ratio (OR) values and respective confidence intervals previously obtained from the chi-square analysis of metastatic incidence. The 95% CI is an estimate of the OR precision, where the low level of precision increases with CI.

Chapter 4

Nucleolin expression in patient-derived breast cancer samples

Abstract

Two major challenges in the management of breast cancer disease are the development of metastases and the treatment of triple-negative cancer. Finding new molecular targets and the design of targeted therapeutic approaches to improve the overall survival and quality of life of these patients is, therefore, of great importance. In this context, nucleolin has emerged as an attractive target for therapeutic intervention in cancer. Its overexpression has been demonstrated in a variety of human neoplasias and was an unfavorable predictor, related to a higher risk of recurrence and worse overall survival of patients. The goal of the present work was to conduct a preliminary evaluation of nucleolin expression in patient-derived breast tumor tissues, both in primary tumors and corresponding metastases, with highlight on triple-negative breast carcinomas. Nucleolin overexpression was observed in primary breast cancer tumors and their matched lymph node metastases, although not all secondary lesions overexpressed the protein. Nucleolin overexpression was evident in 78% of the triple-negative breast cancer biopsies analyzed. Despite both triple-negative and luminal A tumor tissues presented a nuclear protein expression, differences were found on the staining pattern. The former revealed a diffuse nucleoplasm staining, with a clear nucleolar prominence, whereas the latter had a specked distribution of nucleolin throughout the nucleus. No significant associations between nucleolin expression in the triple-negative breast tumors and clinico-pathological factors were identified in this study. However, a significant association was found between nucleolin and CK5/6, with a frequency of nucleolin expression of 89.5% in CK5/6-negative tumors, compared to 60% in CK5/6-positive group ($p = 0.015$). Taken together, these results suggested nucleolin as a valuable therapeutic target in metastatic and/or triple-negative breast cancer, and sustained the rationale of nucleolin-targeted therapeutic approaches for the treatment of this disease.

4.1. Introduction

The development of metastatic lesions and breast tumors with a triple-negative immunohistochemical signature constitute major challenges in breast cancer treatment. Triple-negative breast carcinomas frequently affect young patients and are related to a more aggressive phenotype, sustained by a higher risk of recurrence in the first four years of diagnosis and decreased 5-year survival[29,31,34]. Treatment options are also more limited for this subtype of breast cancer, missing a molecularly tailored therapy, unlike ER-positive or HER2-overexpressing tumors[21,35,36]. Therefore, triple-negative breast cancer (TNBC) has been the focus of attention for the development of targeted therapeutic strategies that improve the overall survival and quality of life of these patients.

Nucleolin is a pleiotropic protein involved in cell proliferation and growth[240,304,305]. Its predominant localization in the nucleus relates to the fundamental role of this protein in RNA and DNA metabolism[239]. At the intracellular level, nucleolin acts as a transcriptional factor of several oncogenes and provides transcriptional regulation for mRNA of pro-tumorigenic proteins[266,267,269,286,290,291,466]. On the cell-surface, nucleolin has been described as a binding partner for ligands with fundamental roles in tumorigenesis and angiogenesis[240,303-305,318,319]. Recent studies have also reported nucleolin overexpression in human-derived tumor tissues as an unfavorable predictor, related to a higher risk of recurrence and worse overall survival of patients, in a variety of neoplasias[253,256,257,259,467,468]. Moreover, the predictive power of nucleolin in a pattern-dependent manner was shown for some types of neoplasias[251,253,254,257,469]. In gastric tumors, both nucleolar and cytoplasmic nucleolin staining was observed, while only nucleolar staining was identified in non-malignant tissues. The subcellular location of the protein reflected differences in the patient's prognosis, where high cytoplasmic staining was associated with a significant recurrence rate and shortened survival rate (log-rank $p < 0.0001$)[253]. Similar results were reported for esophageal squamous cell carcinomas, in which extra-nuclear expression of nucleolin was significantly correlated with metastatic disease and associated with poor overall survival (log-rank $p < 0.000$)[469]. Nevertheless, the pattern of nucleolin staining associated with malignancy and cancer progression is not the same for other types of tumors. The appearance of a specked nucleolin distribution within the cell's nuclei was associated with HPV18 cervical carcinomas, whereas in normal squamous and glandular epithelial cells was homogenously distributed[255]. The abnormal pattern of nuclear positivity also distinguished benign from malignant naevi lesions, and correlated with melanoma progression and a worse prognosis[470]. These results have been supported by other studies in glioma[251] and non-small cell lung carcinoma[257], and highlight the importance of nucleolin expression pattern in addition to its quantitative analysis. Taken together, nucleolin has been increasingly recognized as both prognostic factor and a valuable target

for cancer treatment.

In light of these findings, nucleolin expression, and its potential as a target for the design of tailored therapeutic approaches, remains to be addressed in breast cancer, and might be of particular interest in the triple-negative subtype. Hence, the present work aimed at a preliminary evaluation of nucleolin expression in patient-derived breast tumor tissues, both in primary tumors and corresponding metastases, with emphasis on triple-negative breast carcinomas. This preliminary characterization also included immunohistochemical staining for cytokeratins 5/6, in order to further distinguish between triple-negative tumors of basal ($CK5/6^{+}$) and non-basal ($CK5/6^{-}$) origin[25].

4.2. Results

4.2.1. Expression of nucleolin in patient-derived metastatic breast tumors

The overexpression of nucleolin in primary tumors and metastases was previously demonstrated in mice (chapter 2). To reinforce its therapeutic relevance, nucleolin expression was also assessed in patient-derived breast tumors.

Nucleolin expression was first analysed in a set of ten samples of lymph node metastases and their corresponding primary tumors with diverse clinico-pathological features, from patients with a median age at diagnosis ranging from 33 to 77 (Table 4.1). Nucleolin was identified in all ductal carcinoma of no special type (NTS) samples, independently of breast carcinoma intrinsic subtype (Table 4.1), as illustrated by representative cases of triple-negative, luminal B and luminal A subtypes of breast cancer, Figure 4.1A. In contrast, four lymph node metastases did not express the target protein (one in each breast carcinoma subtype), while the other six were positively stained, as summarized in Table 4.1. Figure 4.1A illustrates representative cases with positive (#1, #3 and #4) and negative (#2, #5 and #10) nucleolin expression in lymph node metastases. Endothelial cells of tumor (luminal A) blood vessels were also positively stained for nucleolin, as depicted in Figure 4.1B, functioning as positive control in breast cancer samples.

Table 4.1: Clinico-pathological characteristics of patients with lymph node metastases.

Characteristics	n (%), n=10
Age at diagnosis, in years	
Median	65.0
Range	36 - 77
Breast cancer subtype	
Luminal A	5 (50.0)
Luminal B	2 (20.0)
HER2	1 (10.0)
Triple-negative	2 (20.0)
Stage (TNM)	
I	0 (0.0)
II	6 (60.0)
III	4 (40.0)
Tumor grade	
1	5 (50.0)
2	3 (30.0)
3	2 (20.0)
Tumor size, in cm	
≤ 2	5 (50.0)
> 2 to ≤ 5	2 (20.0)
> 5	0 (0.00)
Missing data	3 (30.0)
Ki-67 status	
≤ 20%	6 (60.0)
> 20%	3 (30.0)
Missing data	1 (10.0)
Nucleolin expression in primary tumors	
Positive	10 (100.0)
Negative	0 (0.00)
Nucleolin status in metastases	
Positive	6 (60.00)
Negative	4 (40.00)

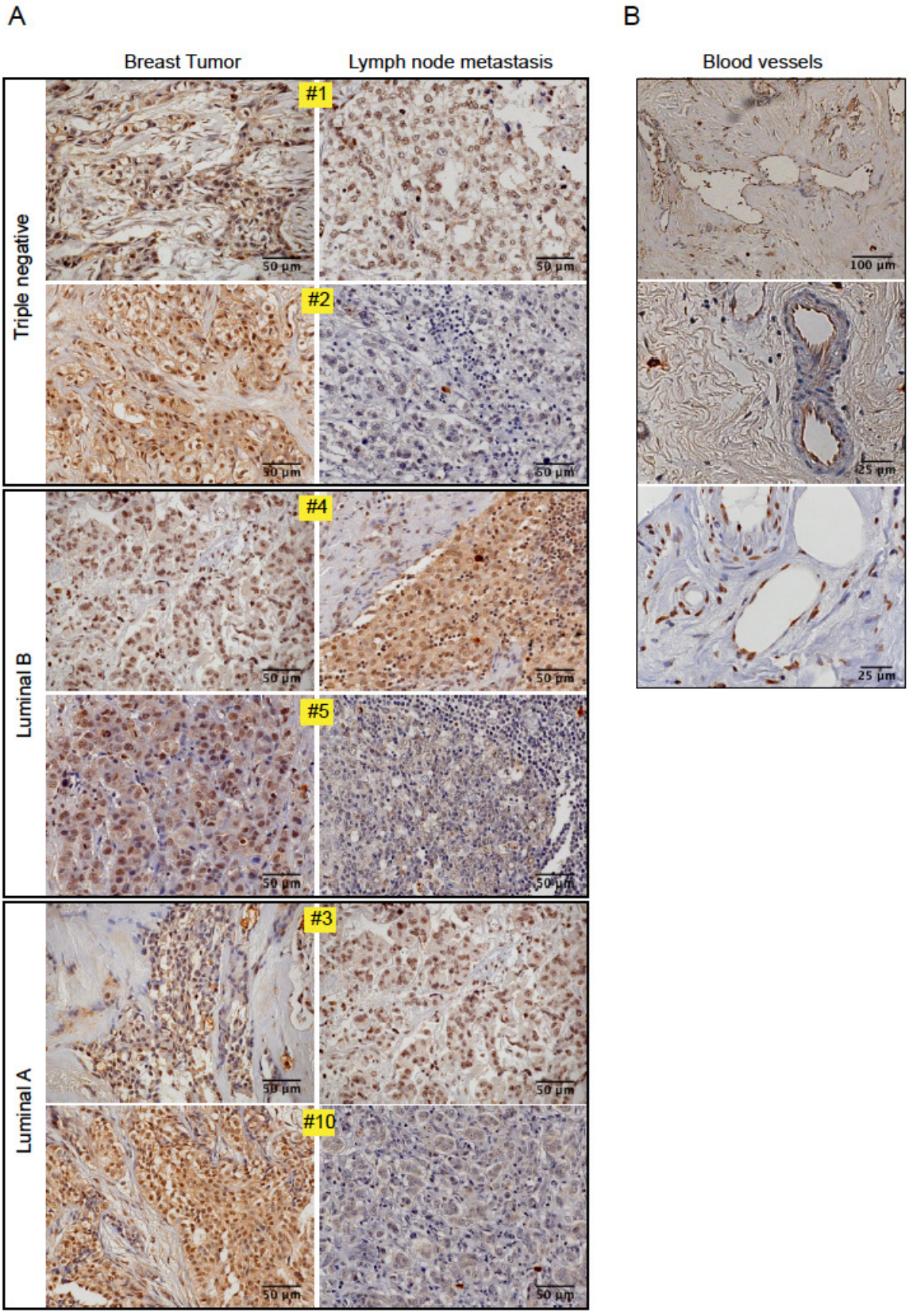

Figure 4.1: Expression of nucleolin in human samples of breast cancer and corresponding lymph node metastases. Patient-derived tumors were stained with an anti-nucleolin antibody. Representative images of nucleolin expression are presented in primary tumors and lymph node metastases of triple-negative, luminal B and luminal A subtypes of breast

cancer (original magnification x400) (A), and endothelial cells of blood vessels in the luminal A breast tumors (original magnification x200, upper image, and x630, lower images) (B).

4.2.2. Pattern of nucleolin expression in luminal A and triple-negative breast cancer

The expression pattern of nucleolin was evaluated in two breast cancer subtypes characterized by distinct expressions of hormone-receptors, Ki-67 and prognosis. Luminal A, characterized by the expression of ER/PR and a lower proliferation index (Ki-67 <20%), represents a subtype with better prognosis, and the triple-negative breast carcinoma, lacking the expression of hormone-receptors and HER2, has the worst prognosis. The aim of this study was to identify possible differences on the pattern of nucleolin expression that could be specific to each breast cancer subtype. The clinico-pathological characteristics of patients in the luminal A and triple-negative cohorts are listed in Tables 4.2 and 4.3, respectively.

Table 4.2: Clinico-pathological characteristics of patients diagnosed with luminal A breast cancer.

Characteristics	n (%), n=8
Age at diagnosis, in years	
Median	64.0
Range	42 - 88
Stage (TNM)	
I	4 (50.0)
II	2 (25.0)
III	1 (12.5)
Missing data	1 (12.5)
Tumor grade	
1	1 (12.5)
2	4 (50.0)
Missing data	3 (37.5)
Tumor dimension, in cm	
≤ 2	5 (62.5)
> 2 to ≤ 5	1 (12.5)
Missing data	2 (25.0)
Ki-67 status	
≤ 20%	5 (62.5)
Missing data	3 (37.5)
Nucleolin expression	
Positive (nuclear)	8 (100.0)
Negative	0 (0.00)

Representative micrographs showing high to low nucleolin expression on breast carcinomas are illustrated in Figure 4.2A. The expression pattern of the protein was different in the two subsets analyzed (Figure 4.2B). In triple-negative breast cancer a diffuse nuclear staining with particular emphasis in the nucleolus was observed, while in luminal A carcinomas the staining was characterized by a nuclear specked pattern (Figure 4.2B). In none of the subsets, cytoplasmic or surface nucleolin expression was identified. Nucleolin expression

was also observed in normal breast tissue adjacent to the tumor (Figure 4.2C), although not all cells were positively stained.

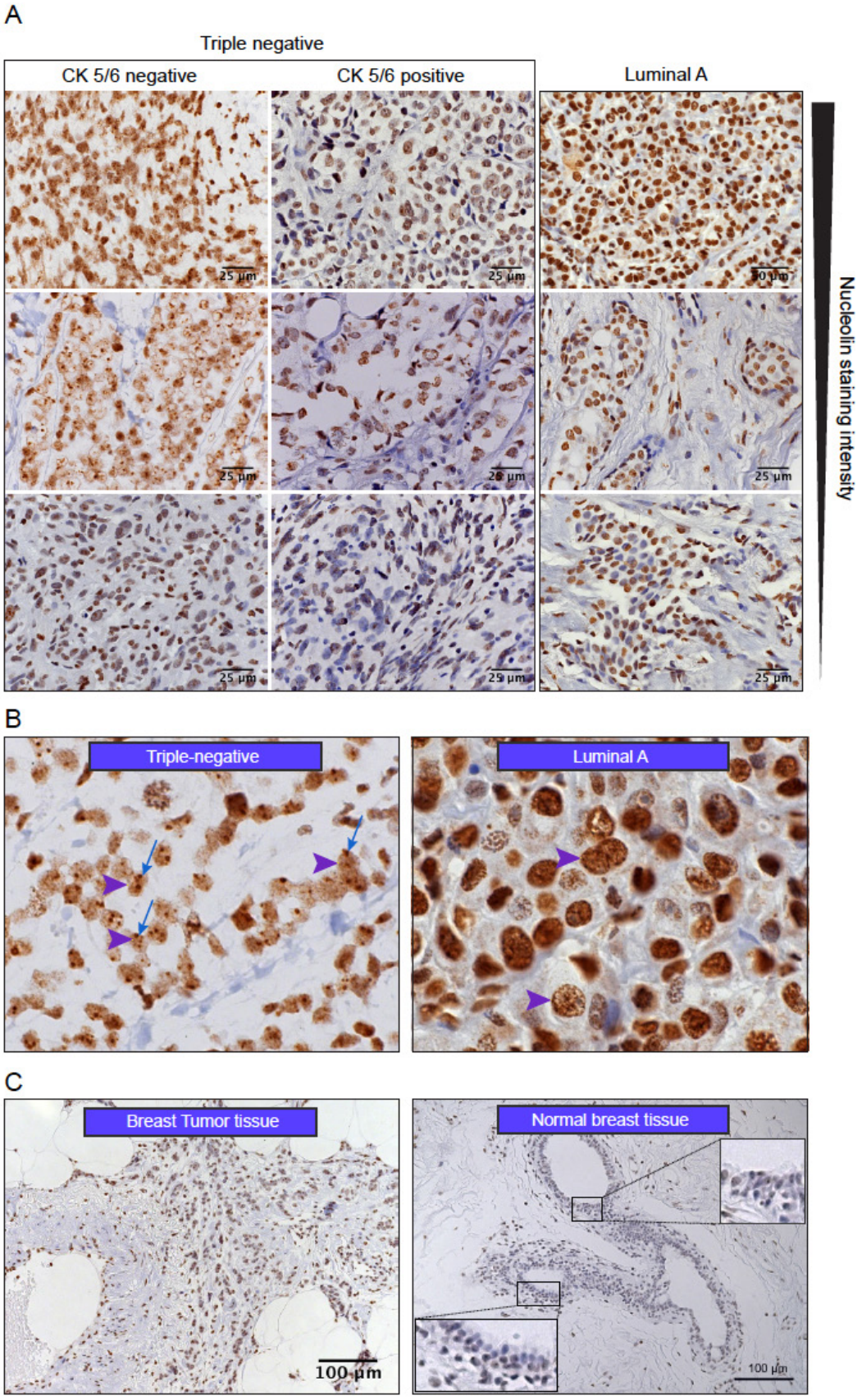

Figure 4.2: Nucleolin expression in patient-derived breast cancer tissues.
Immunostaining of triple-negative (CK 5/6 negative and positive) and luminal A breast carcinoma samples, presenting different intensities and expression patterns of nucleolin (A). In a digital magnification of two representative cases (B) it was visible the nuclear staining in both triple-negative (CK 5/6 negative) and luminal A tumors (purple arrowheads), however with a marked staining of the nucleolus (blue arrows) in the triple-negative, contrasting with the diffuse specked staining in the luminal A sample. Representative immunohistochemical staining of nucleolin in tumor and normal breast tissues (C). Images in A and B present original magnification x630, except upper right image, x400; Images in C present original magnification x200.

4.2.3. Dissecting the prognostic value of nucleolin in triple-negative breast cancer

Breast cancer patients with the triple-negative phenotype constitute a subset of patients with worse prognosis, which is reinforced by the current absence of targeted therapies. Thereby, the identification of new targets with therapeutic value is of great interest. The results from the previous section suggested nucleolin as a possible therapeutic target in triple-negative breast cancer. For that reason, sampling was further extended to seventy-nine women diagnosed with triple-negative breast cancer from the database of the Portuguese Institute of Oncology, Coimbra. Twenty cases missing baseline clinico-pathological characteristics or insufficient material for nucleolin and CK5/6 stainings were excluded. The final study involved a total of 59 triple-negative ductal carcinoma NST samples from patients diagnosed between 2006 and 2012. The median age at diagnosis was 58 years, ranging from 27 to 86 years old, with diverse clinical features (Table 4.3).

Immunohistochemical evaluation of the target protein was performed in core biopsies taken at the time of diagnosis, prior to any therapy. Nucleolin expression was evident in 46 (78%) of primary tumor biopsies (Table 4.3), and 4 of these (8.7%) presented an expression pattern similar to the one obtained in luminal A breast tumors.

Table 4.3: Clinico-pathological characteristics of patients diagnosed with triple-negative breast cancer.

	All samples, n	Nucleolin positive, n (%)	Nucleolin negative, n (%)	*p* value
	59	46 (78.0)	13 (22.0)	
Age at diagnosis, in years				
Median	58.0	58.4	57.9	ns
Range	27 - 86			
Missing data	1			
TNM				
Primary tumor				
T0	4	4 (100.0)	0 (0.0)	ns
T1	6	5 (83.3)	1 (16.7)	
T2	28	18 (64.3)	10 (35.7)	
T3	8	6 (75.0)	2 (25.0)	
T4	8	8 (100.0)	0 (0.0)	
Missing data	5	5 (100.0)	0 (0.0)	
Nodal status				
N0	19	15 (79.0)	4 (21.0)	ns
N1	28	20 (71.4)	8 (28.6)	
N2	6	5 (83.3)	1 (16.7)	
N3	1	1 (100.0)	0 (0.0)	
Missing data	5	5 (100.0)	0 (0.0)	
Metastases				
M0	50	37 (74.0)	13 (26.0)	ns
M1	2	2 (100.0)	0 (0.0)	
Missing data	7	7 (100.0)	0 (0.0)	
Tumor grade				
1	1	1 (100.0)	0 (0.0)	ns
2	16	13 (81.2)	3 (18.8)	
3	23	15 (65.2)	8 (34.8)	
Missing data	19	17 (89.5)	2 (10.5)	
Tumor size, in cm				
≤ 2	28	24 (85.7)	4 (14.3)	ns
> 2to ≤ 5	26	19 (73.1)	7 (26.9)	
> 5	1	1 (100.0)	0 (0.0)	
Missing data	4	2 (50.0)	2 (50.0)	
Ki-67 expression				
≤ 20%	10	9 (90.0)	1 (10.0)	ns
> 20%	49	37 (75.5)	12 (24.5)	
CK5/6 expression				
Positive (nuclear)	20	12 (60.0)	8 (40.0)	0.015
Negative	38	34 (89.5)	4 (10.5)	
Missing data	1	0 (0.0)	1 (100.0)	
Patient				
With active disease	6			
Without active disease	36			
Deceased	12			
Lost to follow-up	5			

No association (p = ns) was identified between nucleolin expression and other clinical factors of prognosis such as age, nodal status, distant metastases, tumor grade and size, or proliferation status. In this set of triple-negative tumors, 64.4% were CK5/6-negative. Interestingly, a statistically significant association between CK5/6 expression status and nucleolin expression was evident. The expression of nucleolin within CK5/6-negative and -positive cohorts was analyzed. A frequency of nucleolin expression of 89.5% was observed in CK5/6-negative tumors, compared to 60% in CK5/6-positive group (p = 0.015).

4.3. Discussion

In addition to its overexpression on a variety of cancer cells[243-247,251-253] and endothelial cells of the tumor vasculature[249,250], nucleolin has been extensively implicated in mechanisms that promote metastatic progression[270,295,304,305,471]. Hence, it has become an attractive target for the therapeutic prevention of metastases. In this respect, a phase II study has been conducted to assess the activity of AS1411, a nucleolin-binding aptamer, for the treatment of metastatic renal cell carcinoma[335]. Although a dramatic and durable response was observed in one patient, a low level of antitumor activity was achieved in the other 34 patients. One reason for these results was the lack of stratification of the subjects enrolled in the study with respect to nucleolin expression, as the trial was not restricted to patients with nucleolin-overexpressing tumors[335].

However studies evaluating the expression of nucleolin in existing human metastatic lesions have been limited, with evidences of overexpression in lymph node and liver metastases of colorectal carcinoma[254]. In our study, positive nucleolin staining in primary breast cancer tumors and their matched lymph node metastases was reported, although not all secondary lesions overexpressed the protein (Table 4.1 and Figure 4.1A). A mismatch status of estrogen, progesterone and HER2 receptors had already been reported between primary breast tumors and their corresponding locoregional and distant metastases[154,472], and reproduced in our samples for two cases (data not shown). Although some lymph node lesions did not overexpressed nucleolin, it could be still inferred that at least a subset of metastatic breast cancer patients expressed the protein, besides the matching primary tumors, thus reinforcing its therapeutic potential. In the future, secondary lesions in other locations where breast cancer cells commonly disseminate to, such as the lungs or bone, should also be object of analysis.

Nucleolin expression has been reported as a putative prognostic factor in several types of cancer[251,253,254,256,259,468]. In addition to its high expression, some studies suggested that the pattern of cellular expression correlated with tumor aggressiveness and a worse prognosis[251,253-255,470]. Increased nucleolin staining and gradual localization of the protein

towards the plasma membrane accompanied increasingly malignancy grade of glioma[251]. Moreover, the detection of cell-surface and cytoplasmic nucleolin in colorectal carcinoma was associated with increased metastatic potential[254] and, in non-small cell lung cancer, nuclear nucleolin was identified as an independent prognostic factor for improved survival[257]. The intracellular redistribution of this protein is known to be regulated by its phosphorylation status[239,254], although glycosylation[473] is also assumed to be responsible for nucleolin localization. In our study, staining of cell surface nucleolin was not observed, in line with data generated with tumors from other histologic origin (pediatric intracranial ependymoma, non-small cell lung cancer, cervical or pancreatic ductal carcinoma)[255,258,259,468]. A literature review on this subject revealed great variability on the immunohistochemical staining pattern of nucleolin, making it difficult to compare results[251,253-259,468,470]. Possible reasons for this might be the lack of antibodies that distinguish between cell-surface, cytoplasmic or nuclear protein. Even the same antibody can enable distinct pattern stainings[253,256,258,259], which might depend on the conditions of incubation (as time, temperature and/or concentration of monoclonal antibody) and antigen retrieval protocol. These differences could also indicate that tumor tissues of diverse origins intrinsically present variable staining patterns. In this study, while all nucleolin-positive tissues presented a nuclear staining, differences on the staining pattern between triple-negative and luminal A breast cancers were observed (Figure 4.2). The former had a diffuse nucleoplasm staining, with a clear nucleolar prominence, whereas the latter revealed a specked distribution of nucleolin throughout the nucleus (Figure 4.2B). This distinct expression pattern by itself could be of prognostic value, since triple-negative breast cancer is associated with aggressive clinical behavior and poorer prognosis than the luminal A subtype[474,475]. In this respect, it would be interesting to further explore whether those triple-negative tumors, with a staining pattern of nucleolin similar to the one of luminal A tumors, would represent a subgroup associated with a better prognosis within triple-negative carcinomas.

The expression of nucleolin in normal breast tissues was observed only in a proportion of epithelial cells. This result is similar to the expression of ER in normal *versus* tumor tissues, in which the positive nuclear staining is observed in a lower percentage of cells in the normal breast[476,477]. This result bear important implications for the establishment of a nucleolin cut-off to be used in future quantitative analysis.

Focusing on tumors with the triple-negative phenotype, a high incidence of positive nucleolin expression was identified (Table 4.3). From a therapeutic point of view, this is an important result because it suggested nucleolin as a valuable target, and that these tumors could potentially benefit from nucleolin-based targeted therapies. The expression of nucleolin in gastric, cervical, pancreatic, and pediatric intracranial ependymoma, was not associated

with clinico-pathological parameters, as gender, age, tumor size or differentiation[253,255,258,259]. However, it has been correlated with tumor size in non-small cell lung cancer[257,468], and with tumor stage and grade, and the serum levels of α-fetoprotein in hepatocellular carcinoma[256]. Herein, no significant associations between nucleolin expression and age at diagnosis, TNM, tumor differentiation and size, and Ki-67 index level were identified in the triple-negative tumor samples (Table 4.3). The triple-negative phenotype accounts for the majority of basal-like breast cancer subtype cases. Seventy four to 84% of these tumors express basal markers (CK5/6 and/or EGFR)[24,25], and one cannot disregard the existence of non-basal-like triple-negative breast cancers. In contrast with this, our sample included mainly CK5/6-negative tumors (64.4%). Nucleolin-expressing tumors were identified in both CK5/6-negative and -positive cohorts, with a higher incidence in the former group (Table 4.3). As previous studies have reported that CK5/6 or EGFR-expressing triple-negative breast tumors were significantly associated with nodal and distant metastases[478], higher histological grade[479], and poorer prognosis[24,480], important therapeutic considerations may be drawn from these results. Specifically, therapies targeting nucleolin may be advantageous in this subset of triple-negative breast cancer patients.

Survival analysis has consistently revealed a high nucleolin expression contribution to poor overall survival and disease-free survival in tumors of histological origin different form breast cancer[253,256-259,468,470]. Work is currently being performed in order to clarify the potential value of nucleolin as a prognostic factor of overall survival in triple-negative breast cancer.

4.4. Conclusion

Many questions remained unanswered, including the relation of nucleolin expression (and pattern of expression) with the metastatic potential of breast tumors, with the therapeutic outcome as a function of the treatment strategy, and with the overall and disease-free survival. Nevertheless, the results obtained herein suggested nucleolin as a relevant therapeutic target in metastatic and/or triple-negative breast cancer, and supported the rationale on nucleolin-based targeting strategies for the treatment of this disease.

4.5. Materials and methods

4.5.1. Materials

The anti-nucleolin mouse monoclonal antibody [ZN004] used for immunostaining of primary breast tumors and lymph node metastases was purchased from Invitrogen (CA, USA). The anti-nucleolin rabbit monoclonal antibody [EPR7952] used for immunostaining of luminal A and triple-negative breast cancer specimens was purchased from Abcam (Cambridge,

UK). Rabbit monoclonal antibodies against estrogen receptor [SP1], progesterone receptor [1E2], HER2 [4B5] and Ki-67 [30-9], and the mouse monoclonal antibody against cytokeratin 5/6 [D5/16B4], were purchased from Ventana Medical Systems, Inc. (Tucson, USA). All ancillary solutions used in the automated immunohistochemistry process were purchased from Ventana Medical Systems, Inc. (Tucson, USA).

4.5.2. Patients and tissue samples

The study was approved by the Ethics Committee of the Portuguese Institute of Oncology, Coimbra. Informed consent was obtained from all of the patients. All samples were handled and made anonymous according to ethical and legal standards.

All tissues used in the study were retrieved from the tissue bank of the Department of Pathology in the Portuguese Institute of Oncology, Coimbra. Specimens included both biopsies and tumor pieces from patients who had not received any form of preoperative chemotherapy or radiotherapy. We retrospectively reviewed the medical records and tissue specimens of 97 patients diagnosed with ductal carcinoma of no special type, between 2006 and 2012. Patient demographics are listed in Tables 4.1 – 4.3. Data collected included patient age and date of diagnosis, histological grade and tumor size, lymph node involvement, details of pre- and postoperative therapy, relapse and disease-specific death. The grade of tumor differentiation was determined according to the criteria of the World Health Organization[481], and tumor staging was assessed by the tumor-node-metastases (TNM) classification of the International Union Against Cancer (UICC)[6]. Hormone-receptor and HER2 status, proliferation (Ki-67) status and cytokeratin 5/6 (CK5/6) were assessed by immunohistochemistry.

4.5.3. Immunohistochemistry analysis

For this study, paraffin-embedded, formalin-fixed breast cancer tissue samples were cut in 4 μm sections. All staining procedures were performed using the automated BenchMark ULTRA IHC/ISH staining module (Ventana Medical Systems, Inc.) following defined protocols.

For nucleolin immunostaining the tissue sections were deparaffinized at 72ºC in a first step. Antigen retrieval occurred by pre-treating these sections with Cell Conditioner 2 (pH 6.0) for 8 min at 96ºC, followed by incubation with ULTRA Cell Conditioner 2 for 24 min at the same temperature. The sections were then incubated 4 min at 36ºC with *ultra*View INHIBITOR to block endogenous peroxidase. Further enzymatic demasking was accomplished by incubating the tissue sections with one drop of Protease 3 for 8 min at 36ºC. Staining with the primary antibody was performed manually, in the case of ZN004

(dilution 1:100), or automatically in the case of EPR7952 (dilution 1:8000), by applying one drop to the tissue and incubating for 32 min at 37ºC. Ventana Amplification Kit was used in conjunction with the Ventana Detection Kit to increase the signal intensity of the primary antibody staining. Sections were then incubated with *ultra*View Horse Radish Peroxidase (HRP) Multimer (8 min), containing a mixture of HRP-labeled goat anti-mouse and anti-rabbit antibodies. Bound antibodies were visualized by incubation in *ultra*View hydrogen peroxide substrate and DAB chromogen (8 min), followed by *ultra*View COPPER solution (4 min) to intensify the color of the stain. The sections were counterstained with haematoxylin for 8 min, blued 4 min, dehydrated and cover slips mounted on the slides.

Immunostaining of the other antibodies (CK5/6, progesterone, estrogen, HER-2 and Ki-67) followed a protocol similar to that of nucleolin, with a few differences. Antigen retrieval was accomplished by applying Cell Conditioner 1 (pH 8.0 – 9.0) to the sections followed by incubation with ULTRA Cell Conditioner 1 for 56 min (CK5/6 and progesterone) or 108 min (estrogen, HER2 and Ki-67). Enzymatic demasking was not necessary. Incubation times with the respective pre-diluted primary antibodies were as follows: CK5/6 (20 min), progesterone (28 min), estrogen (28 min), HER2 (20 min), and Ki-67 (28 min).

Following hematoxylin counterstaining, immunostaining was scored by two independent experienced pathologists, who were blinded to the clinical and pathological parameters and clinical outcomes of the patients. Breast tumors were considered positive for estrogen and progesterone receptors applying a cut-off of > 1% of cells with positively stained nuclei[477]. The staining intensity of HER2 was visually scored and stratified as 0, 1+, 2+ or 3+ according to the staining intensity and membrane delineation[13]. Nuclear staining, plus mitotic figures which are stained by Ki-67, were incorporated into the Ki-67 score that is defined as the percentage of positively stained cells among the total number of malignant cells scored. For luminal A tumors, a Ki-67 cut-off of ≤ 20% was applied. As the cut-off for CK5/6 is not yet standardized, in the present study, the positive *versus* negative expression of the protein (CK5/6) was used. Similarly to cytokeratins 5/6, nucleolin was also evaluated only based on its positive *versus* negative expression status.

4.5.4. Statistical analysis

The association of nucleolin expression (as a categorical variable) with clinical and pathological characteristics was analyzed by one-way ANOVA in the case of continuous variables (age, tumor size and Ki-67) or by Fisher's exact test for categorical variables (TNM, tumor grade and CK5/6). Results were considered statistically significant at an alpha level of 0.05.

Chapter 5

Concluding remarks and future perspectives

Metastases and the triple-negative breast cancer subtype represent two of the major hurdles in breast disease. The development of metastases is the major contributor for the breast cancer-associated deaths and renders this malignancy a treatable but still generally incurable status. Although only ~5% of newly diagnosed breast cancer patients present with metastases to distant organs, the risk of recurrence prevail high in the first four years of diagnosis, particularly for patients with triple-negative disease. Moreover, the benefits of targeted therapies have eluded patients with triple-negative tumors due to the absence of well-defined molecular targets.

In an era where we are stepping towards targeted therapies, finding new markers and therapeutic strategies to specifically address the needs of diseases like triple-negative breast cancer are of enormous importance. For that, the availability of good mouse models that accurately recapitulate the human tumor progression is fundamental. The 4T1 syngeneic model of metastatic breast cancer is a widely used animal model to study metastatic breast cancer. However, the low metastatic efficiency associated with the orthotopic implementation of 4T1 cells is a problem barely referred in the literature. In the present study, this problem was addressed, and the establishment of a 100% metastatic efficiency, along with a high primary tumor take rate, was demonstrated by reducing the density of 4T1 mouse breast cancer cells implanted in the mammary fat pad, to a number as low as 500 cells. This generated tumors with significantly increased doubling times and decreased specific growth rates. The inoculation of a low number of cancer cells extended the time length of tumor development and enabled the progression of the seeded cells into macrometastases, without the need to surgically remove the primary tumor. In addition to the improved metastatic efficiency, the higher reproducibility makes this approach extremely relevant for a better assessment of antimetastatic therapies.

The optimized 4T1 mouse model, was used to investigate the therapeutic potential of a nucleolin-based targeting strategy in the setting of metastatic triple-negative breast cancer. Despite the initial *in vitro* results indicated a higher cytotoxic effect by the F3 peptide-targeted pH-sensitive liposomes (PEGASEMP™) containing Doxorubicin, in comparison with a non-targeted non-pH-sensitive formulation, this was not directly translated into a therapeutic advantage. It enabled a significant augment of survival relative to non-treated mice, but still did not surmount the overall efficacy of Caelyx®. Translating the efficient *in vitro* intracellular delivery and cytotoxicity of the encapsulated payload into an *in vivo* setting of metastatic breast cancer will likely depend on therapeutic schedules that enable a higher systemic exposure of encapsulated Doxorubicin.

In a preliminary study, the expression of nucleolin was further validated in patient-derived breast cancer tissues, both primary breast tumors and their matched lymph node

metastases. Additionally, its expression was also confirmed in triple-negative breast tumors, uncovering the existence of distinct expression patterns for this protein, depending on hormone-receptor status. Furthermore, the results in the triple-negative tumors revealed a significant association of nucleolin expression with the absence of CK5/6 biomarker of the basal phenotype.

Overall, the results generated in this work presented a key methodological aspect towards the reproducible development of macrometastases in the 4T1 mouse model. Extending the time length of tumor development will enable longitudinal studies to follow all the steps of cancer cell dissemination in the same individual, from early seeding to late macroscopic lesions, as well as a better assessment of anti-metastatic therapies. Importantly, the results herein supported nucleolin as a relevant therapeutic target in metastatic and/or triple-negative breast cancer, and the rationale on nucleolin-based targeting strategies for the treatment of this disease. In respect to the use of F3 peptide-targeted pH-sensitive liposomes containing Doxorubicin, further test of therapeutic schedules enabling a higher systemic exposure of encapsulated Doxorubicin is still required. Additionally, many questions remained unanswered, including the relation of nucleolin expression (and pattern of expression, as well) with the metastatic potential of breast tumors, with the therapeutic outcome as a function of the treatment strategy, and with the overall and disease-free survival.

References

List of bibliographic references

1. Torre, L.A.*, et al.* Global cancer statistics, 2012. *CA: A Cancer Journal for Clinicians* **65**, 87-108 (2015).

2. Tavassoli, F.A. *Pathology of the Breast*, (McGraw Hill Professional, 1999).

3. Carter, C.L., Allen, C. & Henson, D.E. Relation of tumor size, lymph node status, and survival in 24,740 breast cancer cases. *Cancer* **63**, 181-187 (1989).

4. Fisher, B.*, et al.* Relation of number of positive axillary nodes to the prognosis of patients with primary breast cancer. An NSABP update. *Cancer* **52**, 1551-1557 (1983).

5. Le Doussal, V.*, et al.* Prognostic value of histologic grade nuclear components of Scarff-Bloom-Richardson (SBR). An improved score modification based on a multivariate analysis of 1262 invasive ductal breast carcinomas. *Cancer* **64**, 1914-1921 (1989).

6. Sobin, L.H., Gospodarowicz, M.K. & Wittekind, C. *TNM classification of malignant tumours*, (John Wiley & Sons, 2011).

7. D'Eredita, G., Giardina, C., Martellotta, M., Natale, T. & Ferrarese, F. Prognostic factors in breast cancer: the predictive value of the Nottingham Prognostic Index in patients with a long-term follow-up that were treated in a single institution. *European Journal of Cancer* **37**, 591-596 (2001).

8. Balslev, I.*, et al.* The Nottingham prognostic index applied to 9,149 patients from the studies of the Danish Breast Cancer Cooperative Group (DBCG). *Breast cancer research and treatment* **32**, 281-290 (1994).

9. Sinn, H.-P. & Kreipe, H. A brief overview of the WHO classification of breast tumors. *Breast Care* **8**, 149-154 (2013).

10. Elston, C.W., Ellis, I.O. & Pinder, S.E. Pathological prognostic factors in breast cancer. *Critical reviews in oncology/hematology* **31**, 209-223 (1999).

11. Mohsin, S.K.*, et al.* Progesterone receptor by immunohistochemistry and clinical outcome in breast cancer: a validation study. *Modern pathology* **17**, 1545-1554 (2004).

12. Harvey, J.M., Clark, G.M., Osborne, C.K. & Allred, D.C. Estrogen receptor status by immunohistochemistry is superior to the ligand-binding assay for predicting response to adjuvant endocrine therapy in breast cancer. *Journal of Clinical Oncology* **17**, 1474-1474 (1999).

13. Wolff, A.C.*, et al.* Recommendations for human epidermal growth factor receptor 2 testing in breast cancer: American Society of Clinical Oncology/College of American Pathologists clinical practice guideline update. *Journal of Clinical Oncology* **31**, 3997-4013 (2013).

14. Perou, C.M.*, et al.* Molecular portraits of human breast tumours. *Nature* **406**, 747-752 (2000).

15. Sørlie, T.*, et al.* Gene expression patterns of breast carcinomas distinguish tumor subclasses with clinical implications. *Proc Natl Acad Sci USA* **98**, 10869-10874 (2001).

16. Sørlie, T.*, et al.* Repeated observation of breast tumor subtypes in independent gene expression data sets. *Proceedings of the National Academy of Sciences* **100**, 8418-8423 (2003).

17. Hu, Z.*, et al.* The molecular portraits of breast tumors are conserved across microarray platforms. *BMC genomics* **7**, 96 (2006).

18. Goldhirsch, A.*, et al.* Strategies for subtypes—dealing with the diversity of breast cancer: highlights of the St Gallen International Expert Consensus on the Primary Therapy of Early Breast Cancer 2011. *Annals of oncology*, mdr304 (2011).

19. Cheang, M.C.U.*, et al.* Ki67 index, HER2 status, and prognosis of patients with luminal B breast cancer. *Journal of the National Cancer Institute* **101**, 736-750 (2009).

20. Inwald, E.C.*, et al.* 4-IHC classification of breast cancer subtypes in a large cohort of a clinical cancer registry: use in clinical routine for therapeutic decisions and its effect on survival. *Breast cancer research and treatment* **153**, 647-658 (2015).

21. Coates, A.S.*, et al.* Tailoring therapies—improving the management of early breast cancer: St Gallen International Expert Consensus on the Primary Therapy of Early Breast Cancer 2015. *Annals of Oncology* **26**, 1533-1546 (2015).

22. Prat, A.*, et al.* Prognostic significance of progesterone receptor–positive tumor cells within immunohistochemically defined luminal A breast cancer. *Journal of Clinical Oncology*, JCO. 2012.2043. 4134 (2012).

23. Goldhirsch, A.*, et al.* Personalizing the treatment of women with early breast cancer: highlights of the St Gallen International Expert Consensus on the Primary Therapy of Early Breast Cancer 2013. *Annals of Oncology* **24**, 2206-2223 (2013).

24. Tischkowitz, M.*, et al.* Use of immunohistochemical markers can refine prognosis in triple negative breast cancer. *BMC cancer* **7**, 134 (2007).

25. Rao, C., Shetty, J. & Prasad, K.H.L. Immunohistochemical Profile and Morphology in Triple–Negative Breast Cancers. *Journal of clinical and diagnostic research: JCDR* **7**, 1361 (2013).

26. Prat, A.*, et al.* Molecular characterization of basal-like and non-basal-like triple-negative breast cancer. *The oncologist* **18**, 123-133 (2013).

27. Pogoda, K., Niwinska, A., Murawska, M., Olszewski, W. & Nowecki, Z. The outcome of special histologic types of triple-negative breast cancer (TNBC). in *ASCO Annual Meeting Proceedings*, Vol. 32 1122 (2014).

28. Nielsen, T.O.*, et al.* Immunohistochemical and clinical characterization of the basal-like subtype of invasive breast carcinoma. *Clinical Cancer Research* **10**, 5367-5374 (2004).

29. Cossetti, R.J.D., Tyldesley, S.K., Speers, C.H., Zheng, Y. & Gelmon, K.A. Comparison of breast cancer recurrence and outcome patterns between patients treated from 1986 to 1992 and from 2004 to 2008. *Journal of Clinical Oncology*, JCO. 2014.2057. 2461 (2014).

30. Kennecke, H.F.*, et al.* Late risk of relapse and mortality among postmenopausal women with estrogen responsive early breast cancer after 5 years of tamoxifen. *Annals of Oncology* **18**, 45-51 (2007).

31. Metzger-Filho, O.*, et al.* Patterns of Recurrence and Outcome According to Breast Cancer Subtypes in Lymph Node–Negative Disease: Results From International Breast Cancer Study Group Trials VIII and IX. *Journal of Clinical Oncology*, JCO. 2012.2046. 1574 (2013).

32. Kennecke, H.*, et al.* Metastatic behavior of breast cancer subtypes. *Journal of clinical oncology* **28**, 3271-3277 (2010).

33. Smid, M.*, et al.* Subtypes of breast cancer show preferential site of relapse. *Cancer research* **68**, 3108-3114 (2008).

34. Kim, K., Lee, E., Lee, J. & Bae, J. Clinicopathologic Signature of TNBC Patients with Good Prognosis. *Cancer Research* **69**, 4065-4065 (2009).

35. Cardoso, F.*, et al.* ESO-ESMO 2nd international consensus guidelines for advanced breast cancer (ABC2). *The Breast* **23**, 489-502 (2014).

36. Senkus, E.*, et al.* Primary breast cancer: ESMO Clinical Practice Guidelines for diagnosis, treatment and follow-up. *Annals of Oncology* **26**(2015).

37. Neuman, H.B.*, et al.* Stage IV breast cancer in the era of targeted therapy. *Cancer* **116**, 1226-1233 (2010).

38. Rashaan, Z.M.*, et al.* Surgery in metastatic breast cancer: patients with a favorable profile seem to have the most benefit from surgery. *European Journal of Surgical Oncology (EJSO)* **38**, 52-56 (2012).

39. Ly, B.H., Vlastos, G., Rapiti, E., Vinh-Hung, V. & Nguyen, N.P. Local-regional radiotherapy and surgery is associated with a significant survival advantage in metastatic breast cancer patients. *Tumori* **96**, 947e954 (2010).

40. Morrow, M. & Goldstein, L. Surgery of the primary tumor in metastatic breast cancer: closing the barn door after the horse has bolted? *Journal of clinical oncology* **24**, 2694-2696 (2006).

41. Pritchard, K.I. Endocrine Therapy of Advanced Disease Analysis and Implications of the Existing Data. *Clinical cancer research* **9**, 460s-467s (2003).

42. Lumachi, F.*, et al.* Endocrine therapy of breast cancer. *Current medicinal chemistry* **18**, 513-522 (2011).

43. Olson, E. & Mullins, D.A. When standard therapy fails in breast cancer: current and future options for HER2-positive disease. *Journal of clinical trials* **3**, 1000129 (2013).

44. Singh, J.C., Jhaveri, K. & Esteva, F.J. HER2-positive advanced breast cancer: optimizing patient outcomes and opportunities for drug development. *British journal of cancer* **111**, 1888-1898 (2014).

45. Twelves, C., Jove, M., Gombos, A. & Awada, A. Cytotoxic chemotherapy: Still the mainstay of clinical practice for all subtypes metastatic breast cancer. *Critical Reviews in Oncology/Hematology* (2016).

46. Li, B.T., Wong, M.H. & Pavlakis, N. Treatment and prevention of bone metastases from breast cancer: a comprehensive review of evidence for clinical practice. *Journal of clinical medicine* **3**, 1-24 (2014).

47. Ellis, M.J.*, et al.* Randomized phase II neoadjuvant comparison between letrozole, anastrozole, and exemestane for postmenopausal women with estrogen receptor–rich stage 2 to 3 breast cancer: clinical and biomarker outcomes and predictive value of the baseline PAM50-based intrinsic subtype—ACOSOG Z1031. *Journal of clinical oncology* **29**, 2342-2349 (2011).

48. Cataliotti, L.*, et al.* Comparison of anastrozole versus tamoxifen as preoperative therapy in postmenopausal women with hormone receptor-positive breast cancer. *Cancer* **106**, 2095-2103 (2006).

49. Davidson, N.E.*, et al.* Chemoendocrine therapy for premenopausal women with axillary lymph node–positive, steroid hormone receptor–positive breast cancer: results from INT 0101 (E5188). *Journal of clinical oncology* **23**, 5973-5982 (2005).

50. LHRH-agonists in Early Breast Cancer Overview group. Use of luteinising-hormone-releasing hormone agonists as adjuvant treatment in premenopausal patients with hormone-receptor-positive breast cancer: a meta-analysis of individual patient data from randomised adjuvant trials. *The Lancet* **369**, 1711-1723 (2007).

51. Francis, P.A.*, et al.* Adjuvant ovarian suppression in premenopausal breast cancer. *New England Journal of Medicine* **372**, 436-446 (2015).

52. McGuire, W.L. Steroid receptors in human breast cancer. *Cancer research* **38**, 4289-4291 (1978).

53. Dowsett, M.*, et al.* Prognostic value of Ki67 expression after short-term presurgical endocrine therapy for primary breast cancer. *Journal of the National Cancer Institute* **99**, 167-170 (2007).

54. Dunbier, A.K.*, et al.* Association between breast cancer subtypes and response to neoadjuvant anastrozole. *Steroids* **76**, 736-740 (2011).

55. Paik, S.*, et al.* Gene expression and benefit of chemotherapy in women with node-negative, estrogen receptor–positive breast cancer. *Journal of clinical oncology* **24**, 3726-3734 (2006).

56. Albain, K.S.*, et al.* Prognostic and predictive value of the 21-gene recurrence score assay in postmenopausal women with node-positive, oestrogen-receptor-positive breast cancer on chemotherapy: a retrospective analysis of a randomised trial. *The lancet oncology* **11**, 55-65 (2010).

57. Dowsett, M.*, et al.* Relationship between quantitative estrogen and progesterone receptor expression and human epidermal growth factor receptor 2 (HER-2) status with recurrence in the Arimidex, Tamoxifen, Alone or in Combination trial. *Journal of clinical oncology* **26**, 1059-1065 (2008).

58. Johnston, S.*, et al.* Lapatinib combined with letrozole versus letrozole and placebo as first-line therapy for postmenopausal hormone receptor–positive metastatic breast cancer. *Journal of Clinical Oncology* **27**, 5538-5546 (2009).

59. Kaufman, B.*, et al.* Trastuzumab plus anastrozole versus anastrozole alone for the treatment of postmenopausal women with human epidermal growth factor receptor 2–positive, hormone receptor–positive metastatic breast cancer: Results from the randomized phase III TAnDEM study. *Journal of Clinical Oncology* **27**, 5529-5537 (2009).

60. Koeberle, D.*, et al.* Combination of trastuzumab and letrozole after resistance to sequential trastuzumab and aromatase inhibitor monotherapies in patients with estrogen receptor-positive, HER-2-positive advanced breast cancer: a proof-of-concept trial (SAKK 23/03). *Endocrine-related cancer* **18**, 257-264 (2011).

61. Vogel, C.L.*, et al.* Efficacy and safety of trastuzumab as a single agent in first-line treatment of HER2-overexpressing metastatic breast cancer. *Journal of Clinical Oncology* **20**, 719-726 (2002).

62. Gianni, L.*, et al.* Treatment with trastuzumab for 1 year after adjuvant chemotherapy in patients with HER2-positive early breast cancer: a 4-year follow-up of a randomised controlled trial. *The lancet oncology* **12**, 236-244 (2011).

63. Perez, E.A.*, et al.* Trastuzumab plus adjuvant chemotherapy for human epidermal growth factor receptor 2–positive breast cancer: planned joint analysis of overall survival from NSABP B-31 and NCCTG N9831. *Journal of Clinical Oncology* **32**, 3744-3752 (2014).

64. Slamon, D.*, et al.* Adjuvant trastuzumab in HER2-positive breast cancer. *New England Journal of Medicine* **365**, 1273-1283 (2011).

65. Tan-Chiu, E.*, et al.* Assessment of cardiac dysfunction in a randomized trial comparing doxorubicin and cyclophosphamide followed by paclitaxel, with or without trastuzumab as adjuvant therapy in node-positive, human epidermal growth factor receptor 2–overexpressing breast cancer: NSABP B-31. *Journal of Clinical Oncology* **23**, 7811-7819 (2005).

66. Liedtke, C.*, et al.* Response to neoadjuvant therapy and long-term survival in patients with triple-negative breast cancer. *Journal of Clinical Oncology* **26**, 1275-1281 (2008).

67. Rouzier, R.*, et al.* Breast cancer molecular subtypes respond differently to preoperative chemotherapy. *Clinical Cancer Research* **11**, 5678-5685 (2005).

68. Carey, L.A.*, et al.* The triple negative paradox: primary tumor chemosensitivity of breast cancer subtypes. *Clinical Cancer Research* **13**, 2329-2334 (2007).

69. Peshkin, B.N., Alabek, M.L. & Isaacs, C. BRCA1/2 mutations and triple negative breast cancers. *Breast disease* **32**(2010).

70. Byrski, T.*, et al.* Pathologic complete response rates in young women with BRCA1-positive breast cancers after neoadjuvant chemotherapy. *Journal of Clinical Oncology* **28**, 375-379 (2010).

71. Gronwald, J.*, et al.* Neoadjuvant therapy with cisplatin in BRCA1-positive breast cancer patients. in *ASCO Annual Meeting Proceedings*, Vol. 27 502 (2009).

72. Leone, J.P.*, et al.* Neoadjuvant platinum-based chemotherapy (CT) for triple-negative locally advanced breast cancer (LABC): retrospective analysis of 125 patients. in *ASCO Annual Meeting Proceedings*, Vol. 27 625 (2009).

73. Sirohi, B.*, et al.* Platinum-based chemotherapy in triple-negative breast cancer. *Annals of oncology*, mdn395 (2008).

74. Liu, M.*, et al.* Platinum–based chemotherapy in triple–negative breast cancer: A meta–analysis. *Oncology letters* **5**, 983-991 (2013).

75. Tevaarwerk, A.J.*, et al.* Survival in patients with metastatic recurrent breast cancer after adjuvant chemotherapy: Little evidence for improvement over the past three decades. *Cancer* **119**, 1140--1148 (2013).

76. Chaffer, C.L. & Weinberg, R.A. A perspective on cancer cell metastasis. *Science* **331**, 1559-1564 (2011).

77. van Zijl, F., Krupitza, G. & Mikulits, W. Initial steps of metastasis: cell invasion and endothelial transmigration. *Mutation Research/Reviews in Mutation Research* **728**, 23-34 (2011).

78. Friedl, P. & Wolf, K. Tumour-cell invasion and migration: diversity and escape mechanisms. *Nature Reviews Cancer* **3**, 362-374 (2003).

79. Thiery, J.P., Acloque, H., Huang, R.Y.J. & Nieto, M.A. Epithelial-mesenchymal transitions in development and disease. *Cell* **139**, 871-890 (2009).

80. Bonde, A.-K., Tischler, V., Kumar, S., Soltermann, A. & Schwendener, R.A. Intratumoral macrophages contribute to epithelial-mesenchymal transition in solid tumors. *BMC cancer* **12**, 35 (2012).

81. Nishimura, K., Semba, S., Aoyagi, K., Sasaki, H. & Yokozaki, H. Mesenchymal stem cells provide an advantageous tumor microenvironment for the restoration of cancer stem cells. *Pathobiology* **79**, 290-306 (2012).

82. Labelle, M., Begum, S. & Hynes, R.O. Direct signaling between platelets and cancer cells induces an epithelial-mesenchymal-like transition and promotes metastasis. *Cancer cell* **20**, 576-590 (2011).

83. Lamouille, S., Xu, J. & Derynck, R. Molecular mechanisms of epithelial–mesenchymal transition. *Nature reviews. Molecular cell biology* **15**, 178 (2014).

84. Mani, S.A.*, et al.* The epithelial-mesenchymal transition generates cells with properties of stem cells. *Cell* **133**, 704-715 (2008).

85. Morel, A.-P.*, et al.* Generation of breast cancer stem cells through epithelial-mesenchymal transition. *PloS one* **3**, e2888 (2008).

86. Li, X.*, et al.* Intrinsic resistance of tumorigenic breast cancer cells to chemotherapy. *Journal of the National Cancer Institute* **100**, 672-679 (2008).

87. Creighton, C.J.*, et al.* Residual breast cancers after conventional therapy display mesenchymal as well as tumor-initiating features. *Proceedings of the National Academy of Sciences* **106**, 13820-13825 (2009).

88. Singh, A. & Settleman, J. EMT, cancer stem cells and drug resistance: an emerging axis of evil in the war on cancer. *Oncogene* **29**, 4741-4751 (2010).

89. Mani, S.A.*, et al.* Mesenchyme Forkhead 1 (FOXC2) plays a key role in metastasis and is associated with aggressive basal-like breast cancers. *Proceedings of the National Academy of Sciences* **104**, 10069-10074 (2007).

90. Sarrió, D.*, et al.* Epithelial-mesenchymal transition in breast cancer relates to the basal-like phenotype. *Cancer research* **68**, 989-997 (2008).

91. Reya, T. & Clevers, H. Wnt signalling in stem cells and cancer. *Nature* **434**, 843-850 (2005).

92. Arce, L., Yokoyama, N.N. & Waterman, M.L. Diversity of LEF/TCF action in development and disease. *Oncogene* **25**, 7492-7504 (2006).

93. Cavallaro, U. & Christofori, G. Cell adhesion and signalling by cadherins and Ig-CAMs in cancer. *Nature Reviews Cancer* **4**, 118-132 (2004).

94. Kessenbrock, K., Plaks, V. & Werb, Z. Matrix metalloproteinases: regulators of the tumor microenvironment. *Cell* **141**, 52-67 (2010).

95. Boyd, N.F.*, et al.* Heritability of mammographic density, a risk factor for breast cancer. *New England Journal of Medicine* **347**, 886-894 (2002).

96. Provenzano, P.P.*, et al.* Collagen density promotes mammary tumor initiation and progression. *BMC medicine* **6**, 11 (2008).

97. Levental, K.R.*, et al.* Matrix crosslinking forces tumor progression by enhancing integrin signaling. *Cell* **139**, 891-906 (2009).

98. Gilkes, D.M.*, et al.* Procollagen lysyl hydroxylase 2 is essential for hypoxia-induced breast cancer metastasis. *Molecular Cancer Research* **11**, 456-466 (2013).

99. Wyckoff, J.B.*, et al.* Direct visualization of macrophage-assisted tumor cell intravasation in mammary tumors. *Cancer research* **67**, 2649-2656 (2007).

100. Carmeliet, P. & Jain, R.K. Molecular mechanisms and clinical applications of angiogenesis. *Nature* **473**, 298-307 (2011).

101. Reymond, N.*, et al.* Cdc42 promotes transendothelial migration of cancer cells through β1 integrin. *The Journal of cell biology* **199**, 653-668 (2012).

102. Sonoshita, M.*, et al.* Suppression of colon cancer metastasis by Aes through inhibition of Notch signaling. *Cancer cell* **19**, 125-137 (2011).

103. Chambers, A.F., Groom, A.C. & MacDonald, I.C. Dissemination and Growth of Cancer Cells in Metastatic Sites. *Rev. Cancer* **2**, 563ā (2002).

104. Douma, S.*, et al.* Suppression of anoikis and induction of metastasis by the neurotrophic receptor TrkB. *Nature* **430**, 1034-1039 (2004).

105. Jaiswal, S.*, et al.* CD47 is upregulated on circulating hematopoietic stem cells and leukemia cells to avoid phagocytosis. *Cell* **138**, 271-285 (2009).

106. Chan, K.S.*, et al.* Identification, molecular characterization, clinical prognosis, and therapeutic targeting of human bladder tumor-initiating cells. *Proceedings of the National Academy of Sciences* **106**, 14016-14021 (2009).

107. Chao, M.P.*, et al.* Anti-CD47 antibody synergizes with rituximab to promote phagocytosis and eradicate non-Hodgkin lymphoma. *Cell* **142**, 699-713 (2010).

108. Chao, M.P.*, et al.* Therapeutic antibody targeting of CD47 eliminates human acute lymphoblastic leukemia. *Cancer research* **71**, 1374-1384 (2011).

109. Rendtlew Danielsen, J.M., Knudsen, L.M., Dahl, I.M., Lodahl, M. & Rasmussen, T. Dysregulation of CD47 and the ligands thrombospondin 1 and 2 in multiple myeloma. *British journal of haematology* **138**, 756-760 (2007).

110. Baccelli, I.*, et al.* Identification of a population of blood circulating tumor cells from breast cancer patients that initiates metastasis in a xenograft assay. *Nature biotechnology* **31**, 539-544 (2013).

111. Zhang, X.H.-F.*, et al.* Latent bone metastasis in breast cancer tied to Src-dependent survival signals. *Cancer cell* **16**, 67-78 (2009).

112. Chen, Q., Zhang, X.H.-F. & Massagué, J. Macrophage binding to receptor VCAM-1 transmits survival signals in breast cancer cells that invade the lungs. *Cancer cell* **20**, 538-549 (2011).

113. Sosa, M.S., Bragado, P. & Aguirre-Ghiso, J.A. Mechanisms of disseminated cancer cell dormancy: an awakening field. *Nature Reviews Cancer* **14**, 611-622 (2014).

114. Hanahan, D. & Weinberg, R.A. Hallmarks of cancer: the next generation. *Cell* **144**, 646-674 (2011).

115. Hanahan, D. & Folkman, J. Patterns and emerging mechanisms of the angiogenic switch during tumorigenesis. *cell* **86**, 353-364 (1996).

116. Hicklin, D.J. & Ellis, L.M. Role of the vascular endothelial growth factor pathway in tumor growth and angiogenesis. *Journal of clinical oncology* **23**, 1011-1027 (2005).

117. Welti, J., Loges, S., Dimmeler, S. & Carmeliet, P. Recent molecular discoveries in angiogenesis and antiangiogenic therapies in cancer. *The Journal of clinical investigation* **123**, 3190-3200 (2013).

118. Raza, A., Franklin, M.J. & Dudek, A.Z. Pericytes and vessel maturation during tumor angiogenesis and metastasis. *American journal of hematology* **85**, 593-598 (2010).

119. Gerhardt, H. & Semb, H. Pericytes: gatekeepers in tumour cell metastasis? *Journal of molecular medicine* **86**, 135-144 (2008).

120. Lin, E.Y.*, et al.* Vascular endothelial growth factor restores delayed tumor progression in tumors depleted of macrophages. *Molecular oncology* **1**, 288-302 (2007).

121. Qian, B.-Z. & Pollard, J.W. Macrophage diversity enhances tumor progression and metastasis. *Cell* **141**, 39-51 (2010).

122. Murdoch, C., Muthana, M., Coffelt, S.B. & Lewis, C.E. The role of myeloid cells in the promotion of tumour angiogenesis. *Nature Reviews Cancer* **8**, 618-631 (2008).

123. Schoppmann, S.F.*, et al.* Tumor-associated macrophages express lymphatic endothelial growth factors and are related to peritumoral lymphangiogenesis. *The American journal of pathology* **161**, 947-956 (2002).

124. Nozawa, H., Chiu, C. & Hanahan, D. Infiltrating neutrophils mediate the initial angiogenic switch in a mouse model of multistage carcinogenesis. *Proceedings of the National Academy of Sciences* **103**, 12493-12498 (2006).

125. Pahler, J.C.*, et al.* Plasticity in tumor-promoting inflammation: impairment of macrophage recruitment evokes a compensatory neutrophil response. *Neoplasia* **10**, 329-IN322 (2008).

126. Coussens, L.M.*, et al.* Inflammatory mast cells up-regulate angiogenesis during squamous epithelial carcinogenesis. *Genes & development* **13**, 1382-1397 (1999).

127. Du, R.*, et al.* HIF1α induces the recruitment of bone marrow-derived vascular modulatory cells to regulate tumor angiogenesis and invasion. *Cancer cell* **13**, 206-220 (2008).

128. Olumi, A.F.*, et al.* Carcinoma-associated fibroblasts direct tumor progression of initiated human prostatic epithelium. *Cancer research* **59**, 5002-5011 (1999).

129. Dumont, N.*, et al.* Breast fibroblasts modulate early dissemination, tumorigenesis, and metastasis through alteration of extracellular matrix characteristics. *Neoplasia* **15**, 249-IN247 (2013).

130. Kalluri, R. & Zeisberg, M. Fibroblasts in cancer. *Nature Reviews Cancer* **6**, 392-401 (2006).

131. Marsh, T., Pietras, K. & McAllister, S.S. Fibroblasts as architects of cancer pathogenesis. *Biochimica et Biophysica Acta (BBA)-Molecular Basis of Disease* **1832**, 1070-1078 (2013).

132. Calvo, F.*, et al.* Mechanotransduction and YAP-dependent matrix remodelling is required for the generation and maintenance of cancer-associated fibroblasts. *Nature cell biology* **15**, 637-646 (2013).

133. Tang, D.*, et al.* Cancer-associated fibroblasts promote angiogenesis in gastric cancer through galectin-1 expression. *Tumor Biology*, 1-11 (2015).

134. Fukumura, D.*, et al.* Tumor induction of VEGF promoter activity in stromal cells. *Cell* **94**, 715-725 (1998).

135. Erez, N., Truitt, M., Olson, P. & Hanahan, D. Cancer-associated fibroblasts are activated in incipient neoplasia to orchestrate tumor-promoting inflammation in an NF-κB-dependent manner. *Cancer cell* **17**, 135-147 (2010).

136. Zhang, X.H.-F*., et al.* Selection of bone metastasis seeds by mesenchymal signals in the primary tumor stroma. *Cell* **154**, 1060-1073 (2013).

137. Paget, S. The distribution of secondary growths in cancer of the breast. *The Lancet* **133**, 571-573 (1889).

138. Sceneay, J., Smyth, M.J. & Möller, A. The pre-metastatic niche: finding common ground. *Cancer and Metastasis Reviews* **32**, 449-464 (2013).

139. Kaplan, R.N*., et al.* VEGFR1-positive haematopoietic bone marrow progenitors initiate the pre-metastatic niche. *Nature* **438**, 820-827 (2005).

140. Quail, D.F. & Joyce, J.A. Microenvironmental regulation of tumor progression and metastasis. *Nature medicine* **19**, 1423-1437 (2013).

141. Wyckoff, J*., et al.* A paracrine loop between tumor cells and macrophages is required for tumor cell migration in mammary tumors. *Cancer research* **64**, 7022-7029 (2004).

142. Palumbo, J.S*., et al.* Platelets and fibrin (ogen) increase metastatic potential by impeding natural killer cell–mediated elimination of tumor cells. *Blood* **105**, 178-185 (2005).

143. Nieswandt, B., Hafner, M., Echtenacher, B. & Männel, D.N. Lysis of tumor cells by natural killer cells in mice is impeded by platelets. *Cancer research* **59**, 1295-1300 (1999).

144. Schumacher, D., Strilic, B., Sivaraj, K.K., Wettschureck, N. & Offermanns, S. Platelet-derived nucleotides promote tumor-cell transendothelial migration and metastasis via P2Y 2 receptor. *Cancer cell* **24**, 130-137 (2013).

145. Ostrand-Rosenberg, S. & Sinha, P. Myeloid-derived suppressor cells: linking inflammation and cancer. *The Journal of Immunology* **182**, 4499-4506 (2009).

146. Hiratsuka, S., Watanabe, A., Aburatani, H. & Maru, Y. Tumour-mediated upregulation of chemoattractants and recruitment of myeloid cells predetermines lung metastasis. *Nature cell biology* **8**, 1369-1375 (2006).

147. Hiratsuka, S*., et al.* The S100A8–serum amyloid A3–TLR4 paracrine cascade establishes a pre-metastatic phase. *Nature cell biology* **10**, 1349-1355 (2008).

148. Cheng, P*., et al.* Inhibition of dendritic cell differentiation and accumulation of myeloid-derived suppressor cells in cancer is regulated by S100A9 protein. *The Journal of experimental medicine* **205**, 2235-2249 (2008).

149. Xiang, X*., et al.* Induction of myeloid-derived suppressor cells by tumor exosomes. *International Journal of Cancer* **124**, 2621-2633 (2009).

150. Peinado, H*., et al.* Melanoma exosomes educate bone marrow progenitor cells toward a pro-metastatic phenotype through MET. *Nature medicine* **18**, 883-891 (2012).

151. Escudier, B*., et al.* Vaccination of metastatic melanoma patients with autologous dendritic cell (DC) derived-exosomes: results of thefirst phase I clinical trial. *Journal of translational medicine* **3**, 10 (2005).

152. Lugini, L.*, et al.* Immune surveillance properties of human NK cell-derived exosomes. *The Journal of Immunology* **189**, 2833-2842 (2012).

153. Stoecklein, N.H. & Klein, C.A. Genetic disparity between primary tumours, disseminated tumour cells, and manifest metastasis. *International journal of cancer* **126**, 589-598 (2010).

154. Aurilio, G.*, et al.* A meta-analysis of oestrogen receptor, progesterone receptor and human epidermal growth factor receptor 2 discordance between primary breast cancer and metastases. *European Journal of Cancer* **50**, 277 - 289 (2014).

155. Klein, C.A. Parallel progression of primary tumours and metastases. *Nature Reviews Cancer* **9**, 302-312 (2009).

156. Almendro, V.*, et al.* Genetic and phenotypic diversity in breast tumor metastases. *Cancer Research* **74**, 1338–1348 (2014).

157. Smith, B.N. & Bhowmick, N.A. Role of EMT in metastasis and therapy resistance. *Journal of clinical medicine* **5**, 17 (2016).

158. Cheng, G.Z.*, et al.* Twist transcriptionally up-regulates AKT2 in breast cancer cells leading to increased migration, invasion, and resistance to paclitaxel. *Cancer research* **67**, 1979-1987 (2007).

159. Vesuna, F.*, et al.* Twist contributes to hormone resistance in breast cancer by downregulating estrogen receptor-α. *Oncogene* **31**, 3223-3234 (2012).

160. Naumov, G.N.*, et al.* Ineffectiveness of doxorubicin treatment on solitary dormant mammary carcinoma cells or late-developing metastases. *Breast cancer research and treatment* **82**, 199-206 (2003).

161. Braun, S.*, et al.* Lack of effect of adjuvant chemotherapy on the elimination of single dormant tumor cells in bone marrow of high-risk breast cancer patients. *Journal of Clinical Oncology* **18**, 80-80 (2000).

162. Weaver, V.M.*, et al.* β4 integrin-dependent formation of polarized three-dimensional architecture confers resistance to apoptosis in normal and malignant mammary epithelium. *Cancer cell* **2**, 205-216 (2002).

163. Fu, Y., Li, J. & Lee, A.S. GRP78/BiP inhibits endoplasmic reticulum BIK and protects human breast cancer cells against estrogen starvation–induced apoptosis. *Cancer research* **67**, 3734-3740 (2007).

164. Coussens, L.M., Fingleton, B. & Matrisian, L.M. Matrix metalloproteinase inhibitors and cancer—trials and tribulations. *Science* **295**, 2387-2392 (2002).

165. Eckhardt, B.L., Francis, P.A., Parker, B.S. & Anderson, R.L. Strategies for the discovery and development of therapies for metastatic breast cancer. *Nature Reviews Drug Discovery* **11**, 479-497 (2012).

166. Valastyan, S. & Weinberg, R.A. Tumor Metastasis: Molecular Insights and Evolving Paradigms. *Cell* **147**, 275-292 (2011).

167. Hartkopf, A.D.*, et al.* Prognostic relevance of disseminated tumour cells from the bone marrow of early stage breast cancer patients–results from a large single-centre analysis. *European Journal of Cancer* **50**, 2550-2559 (2014).

168. Tanaka, T.*, et al.* Chemokines in tumor progression and metastasis. *Cancer science* **96**, 317-322 (2005).

169. Roodman, G.D. Mechanisms of bone metastasis. *New England Journal of Medicine* **350**, 1655-1664 (2004).

170. Ma, L., Teruya-Feldstein, J. & Weinberg, R.A. Tumour invasion and metastasis initiated by microRNA-10b in breast cancer. *Nature* **449**, 682-688 (2007).

171. Ma, L.*, et al.* Therapeutic silencing of miR-10b inhibits metastasis in a mouse mammary tumor model. *Nat Biotech* **28**, 341-347 (2010).

172. Holland, S.J.*, et al.* R428, a selective small molecule inhibitor of Axl kinase, blocks tumor spread and prolongs survival in models of metastatic breast cancer. *Cancer research* **70**, 1544-1554 (2010).

173. Linger, R.M.A., Keating, A.K., Earp, H.S. & Graham, D.K. TAM receptor tyrosine kinases: biologic functions, signaling, and potential therapeutic targeting in human cancer. *Advances in cancer research* **100**, 35-83 (2008).

174. Jansen, S.*, et al.* Mechanism of actin filament bundling by fascin. *Journal of Biological Chemistry* **286**, 30087-30096 (2011).

175. Chen, L., Yang, S., Jakoncic, J., Zhang, J.J. & Huang, X.-Y. Migrastatin analogues target fascin to block tumour metastasis. *Nature* **476**, 240-240 (2011).

176. Biragyn, A.*, et al.* Inhibition of lung metastasis by chemokine CCL17-mediated in vivo silencing of genes in CCR4+ Tregs. *Journal of immunotherapy (Hagerstown, Md.: 1997)* **36**, 258 (2013).

177. Erler, J.T.*, et al.* Lysyl oxidase is essential for hypoxia-induced metastasis. *Nature* **440**, 1222-1226 (2006).

178. Canesin, G.*, et al.* Lysyl oxidase-like 2 (LOXL2) and E47 EMT factor: novel partners in E-cadherin repression and early metastasis colonization. *Oncogene* **34**, 951-964 (2015).

179. Ohno, H.*, et al.* A c-fms tyrosine kinase inhibitor, Ki20227, suppresses osteoclast differentiation and osteolytic bone destruction in a bone metastasis model. *Molecular cancer therapeutics* **5**, 2634-2643 (2006).

180. Body, J.-J. Breast cancer: bisphosphonate therapy for metastatic bone disease. *Clinical cancer research* **12**, 6258s-6263s (2006).

181. Stopeck, A.T.*, et al.* Denosumab compared with zoledronic acid for the treatment of bone metastases in patients with advanced breast cancer: a randomized, double-blind study. *Journal of Clinical Oncology* **28**, 5132-5139 (2010).

182. Gnant, M.*, et al.* Adjuvant denosumab in breast cancer (ABCSG-18): a multicentre, randomised, double-blind, placebo-controlled trial. *The Lancet* **386**, 433-443 (2015).

183. André, F.*, et al.* Targeting FGFR with dovitinib (TKI258): preclinical and clinical data in breast cancer. *Clinical Cancer Research* **19**, 3693-3702 (2013).

184. Lehmann, B.D.*, et al.* Identification of human triple-negative breast cancer subtypes and preclinical models for selection of targeted therapies. *The Journal of clinical investigation* **121**, 2750 (2011).

185. Bertucci, F.*, et al.* Gene expression profiling shows medullary breast cancer is a subgroup of basal breast cancers. *Cancer Research* **66**, 4636-4644 (2006).

186. Marginean, F., Rakha, E.A., Ho, B.C., Ellis, I.O. & Lee, A.H.S. Histological features of medullary carcinoma and prognosis in triple-negative basal-like carcinomas of the breast. *Modern Pathology* **23**, 1357-1363 (2010).

187. Farmer, P.*, et al.* Identification of molecular apocrine breast tumours by microarray analysis. *Oncogene* **24**, 4660-4671 (2005).

188. Burstein, M.D.*, et al.* Comprehensive genomic analysis identifies novel subtypes and targets of triple-negative breast cancer. *Clinical Cancer Research* **21**, 1688-1698 (2015).

189. Jézéquel, P.*, et al.* Gene-expression molecular subtyping of triple-negative breast cancer tumours: importance of immune response. *Breast Cancer Res* **17**, 43 (2015).

190. The Cancer Genome Atlas Network (TCGA). Comprehensive molecular portraits of human breast tumours. *Nature* **490**, 61-70 (2012).

191. Abramson, V.G., Lehmann, B.D., Ballinger, T.J. & Pietenpol, J.A. Subtyping of triple-negative breast cancer: Implications for therapy. *Cancer* **121**, 8-16 (2015).

192. Gonzalez-Angulo, A.M.*, et al.* Androgen receptor levels and association with PIK3CA mutations and prognosis in breast cancer. *Clinical Cancer Research* **15**, 2472-2478 (2009).

193. Lehmann, B.D.*, et al.* PIK3CA mutations in androgen receptor-positive triple negative breast cancer confer sensitivity to the combination of PI3K and androgen receptor inhibitors. *Breast Cancer Res* **16**, 406 (2014).

194. De Summa, S.*, et al.* BRCAness: a deeper insight into basal-like breast tumors. *Annals of oncology* **24**, viii13-viii21 (2013).

195. Kenemans, P., Verstraeten, R.A. & Verheijen, R.H.M. Oncogenic pathways in hereditary and sporadic breast cancer. *Maturitas* **49**, 34-43 (2004).

196. Audeh, M.W. Novel treatment strategies in triple-negative breast cancer: specific role of poly (adenosine diphosphate-ribose) polymerase inhibition. *Pharmacogenomics and personalized medicine* **7**, 307 (2014).

197. Fong, P.C.*, et al.* Inhibition of poly (ADP-ribose) polymerase in tumors from BRCA mutation carriers. *New England Journal of Medicine* **361**, 123-134 (2009).

198. Gelmon, K.A.*, et al.* Olaparib in patients with recurrent high-grade serous or poorly differentiated ovarian carcinoma or triple-negative breast cancer: a phase 2, multicentre, open-label, non-randomised study. *The lancet oncology* **12**, 852-861 (2011).

199. Tutt, A.*, et al.* Oral poly (ADP-ribose) polymerase inhibitor olaparib in patients with BRCA1 or BRCA2 mutations and advanced breast cancer: a proof-of-concept trial. *The Lancet* **376**, 235-244 (2010).

200. Isakoff, S.J.*, et al.* A phase II trial of the PARP inhibitor veliparib (ABT888) and temozolomide for metastatic breast cancer. in *ASCO Annual Meeting Proceedings*, Vol. 28 1019 (2010).

201. O'Shaughnessy, J.*, et al.* Iniparib plus chemotherapy in metastatic triple-negative breast cancer. *New England Journal of Medicine* **364**, 205-214 (2011).

202. O'Shaughnessy, J.*, et al.* Phase III study of iniparib plus gemcitabine and carboplatin versus gemcitabine and carboplatin in patients with metastatic triple-negative breast cancer. *Journal of Clinical Oncology*, JCO. 2014.2055. 2984 (2014).

203. Dent, R.A., *et al.* Phase I trial of the oral PARP inhibitor olaparib in combination with paclitaxel for first- or second-line treatment of patients with metastatic triple-negative breast cancer. *Breast Cancer Res* **15**, R88 (2013).

204. Watkins, J., *et al.* Genomic complexity profiling reveals that HORMAD1 overexpression contributes to homologous recombination deficiency in triple-negative breast cancers. *Cancer discovery* **5**, 488-505 (2015).

205. Mayer, I.A., *et al.* Abstract PD1-6: A randomized phase II neoadjuvant study of cisplatin, paclitaxel with or without everolimus (an mTOR inhibitor) in patients with stage II/III triple-negative breast cancer (TNBC). *Cancer Research* **73**, PD1-6-PD1-6 (2013).

206. Gonzalez-Angulo, A.M., *et al.* Open label, randomized clinical trial of standard neoadjuvant chemotherapy with paclitaxel followed by FEC (T-FEC) versus the combination of paclitaxel and RAD001 followed by FEC (TR-FEC) in women with triple receptor-negative breast cancer (TNBC). in *ASCO Annual Meeting Proceedings*, Vol. 29 1016 (2011).

207. Singh, J.C., *et al.* Phase 2 trial of everolimus and carboplatin combination in patients with triple negative metastatic breast cancer. *Breast Cancer Res* **16**, R32 (2014).

208. Edelman, G., *et al.* A phase I dose-escalation study of XL147 (SAR245408), a PI3K inhibitor administered orally to patients with advanced malignancies. *ASCO Meet Abstracts* **28**, 3004 (2010).

209. Jimeno, A., *et al.* Final results from a phase I, dose-escalation study of PX-866, an irreversible, pan-isoform inhibitor of PI3 kinase. in *ASCO Annual Meeting Proceedings*, Vol. 28 3089 (2010).

210. Patnaik, A., *et al.* A first-in-human phase I study of intravenous PI3K inhibitor BAY 80-6946 in patients with advanced solid tumors: Results of dose-escalation phase. in *ASCO Annual Meeting Proceedings*, Vol. 29 3035 (2011).

211. Von Hoff, D.D., *et al.* A phase I dose-escalation study to evaluate GDC-0941, a pan-PI3K inhibitor, administered QD or BID in patients with advanced or metastatic solid tumors. in *ASCO annual meeting proceedings*, Vol. 29 3052 (2011).

212. Lin, J., *et al.* Targeting activated Akt with GDC-0068, a novel selective Akt inhibitor that is efficacious in multiple tumor models. *Clinical Cancer Research* **19**, 1760-1772 (2013).

213. Oliveira, M., *et al.* FAIRLANE: A phase II randomized, double-blind, study of the Akt inhibitor ipatasertib (Ipat, GDC-0068) in combination with paclitaxel (Pac) as neoadjuvant treatment for early stage triple-negative breast cancer (TNBC). in *ASCO Annual Meeting Proceedings*, Vol. 33 TPS1112 (2015).

214. Kim, S., *et al.* LOTUS: A randomized, phase II, multicenter, placebo-controlled study of ipatasertib (Ipat, GDC-0068), an inhibitor of Akt, in combination with paclitaxel (Pac) as front-line treatment for patients (pts) with metastatic triple-negative breast cancer (TNBC). in *ASCO Annual Meeting Proceedings*, Vol. 33 TPS1111 (2015).

215. Hennessy, B.T., *et al.* Characterization of a naturally occurring breast cancer subset enriched in epithelial-to-mesenchymal transition and stem cell characteristics. *Cancer research* **69**, 4116-4124 (2009).

216. Ibrahim, Y.H., *et al.* PI3K inhibition impairs BRCA1/2 expression and sensitizes BRCA-proficient triple-negative breast cancer to PARP inhibition. *Cancer discovery* **2**, 1036-1047 (2012).

217. McNamara, K.M., Moore, N.L., Hickey, T.E., Sasano, H. & Tilley, W.D. Complexities of androgen receptor signalling in breast cancer. *Endocrine-related cancer* **21**, T161-T181 (2014).

218. Park, S.*, et al.* Expression of androgen receptors in primary breast cancer. *Annals of Oncology* **21**, 488-492 (2010).

219. Traina, T.A.*, et al.* Results from a phase 2 study of enzalutamide (ENZA), an androgen receptor (AR) inhibitor, in advanced AR+ triple-negative breast cancer (TNBC). in *ASCO Annual Meeting Proceedings*, Vol. 33 1003 (2015).

220. Yamaoka, M.*, et al.* Orteronel (TAK-700), a novel non-steroidal 17, 20-lyase inhibitor: effects on steroid synthesis in human and monkey adrenal cells and serum steroid levels in cynomolgus monkeys. *The Journal of steroid biochemistry and molecular biology* **129**, 115-128 (2012).

221. Gucalp, A.*, et al.* Phase II trial of bicalutamide in patients with androgen receptor–positive, estrogen receptor–negative metastatic breast cancer. *Clinical Cancer Research* **19**, 5505-5512 (2013).

222. Hu, X.*, et al.* Multicenter phase II study of apatinib, a novel VEGFR inhibitor in heavily pretreated patients with metastatic triple‐negative breast cancer. *International Journal of Cancer* **135**, 1961-1969 (2014).

223. Baselga, J.*, et al.* Randomized phase II study of the anti–epidermal growth factor receptor monoclonal antibody cetuximab with cisplatin versus cisplatin alone in patients with metastatic triple-negative breast cancer. *Journal of clinical oncology* **31**, 2586-2592 (2013).

224. Carey, L.A.*, et al.* TBCRC 001: randomized phase II study of cetuximab in combination with carboplatin in stage IV triple-negative breast cancer. *Journal of Clinical Oncology* **30**, 2615-2623 (2012).

225. Tolaney, S.M.*, et al.* Phase II study of tivantinib (ARQ 197) in patients with metastatic triple-negative breast cancer. *Investigational New Drugs* **33**, 1108-1114 (2015).

226. Linderholm, B.K.*, et al.* Significantly higher levels of vascular endothelial growth factor (VEGF) and shorter survival times for patients with primary operable triple-negative breast cancer. *Annals of oncology*, mdp062 (2009).

227. Miller, K.*, et al.* Paclitaxel plus bevacizumab versus paclitaxel alone for metastatic breast cancer. *New England Journal of Medicine* **357**, 2666-2676 (2007).

228. Robert, N.J.*, et al.* RIBBON-1: randomized, double-blind, placebo-controlled, phase III trial of chemotherapy with or without bevacizumab (B) for first-line treatment of HER2-negative locally recurrent or metastatic breast cancer (MBC). in *ASCO Annual Meeting Proceedings*, Vol. 27 1005 (2009).

229. Miles, D.*, et al.* Randomized, double-blind, placebo-controlled, phase III study of bevacizumab with docetaxel or docetaxel with placebo as first-line therapy for patients with locally recurrent or metastatic breast cancer (mBC): AVADO. in *ASCO Annual Meeting Proceedings*, Vol. 26 LBA1011 (2008).

230. Brufsky, A.*, et al.* Impact of bevacizumab (BEV) on efficacy of second-line chemotherapy (CT) for triple-negative breast cancer (TNBC): Analysis of RIBBON-2. in *ASCO Annual Meeting Proceedings*, Vol. 29 1010 (2011).

231. Cameron, D.*, et al.* Adjuvant bevacizumab-containing therapy in triple-negative breast cancer (BEATRICE): primary results of a randomised, phase 3 trial. *The lancet oncology* **14**, 933-942 (2013).

232. Carpenter, D., Kesselheim, A.S. & Joffe, S. Reputation and precedent in the bevacizumab decision. *New England Journal of Medicine* **365**, e3 (2011).

233. Livasy, C.A.*, et al.* Phenotypic evaluation of the basal-like subtype of invasive breast carcinoma. *Modern Pathology* **19**, 264-271 (2006).

234. De Luca, A.*, et al.* Evaluation of the pharmacokinetics of ixabepilone for the treatment of breast cancer. *Expert opinion on drug metabolism & toxicology* (2015).

235. Trédan, O.*, et al.* Ixabepilone alone or with cetuximab as first-line treatment for advanced/metastatic triple-negative breast cancer. *Clinical breast cancer* **15**, 8-15 (2015).

236. Carey, L.*, et al.* Potential Predictive Markers of Benefit from Cetuximab in Metastatic Breast Cancer: An Analysis of Two Randomized Phase 2 Trials. *Cancer Research* **69**, 2014-2014 (2009).

237. Balko, J.M.*, et al.* Molecular profiling of the residual disease of triple-negative breast cancers after neoadjuvant chemotherapy identifies actionable therapeutic targets. *Cancer discovery* **4**, 232-245 (2014).

238. Marotta, L.L.C.*, et al.* The JAK2/STAT3 signaling pathway is required for growth of CD44+ CD24–stem cell–like breast cancer cells in human tumors. *The Journal of clinical investigation* **121**, 2723-2735 (2011).

239. Ginisty, H., Sicard, H., Roger, B. & Bouvet, P. Structure and functions of nucleolin. *J Cell Sci* **112 (Pt 6)**, 761-772 (1999).

240. Srivastava, M. & Pollard, H.B. Molecular dissection of nucleolin's role in growth and cell proliferation: new insights. *FASEB J* **13**, 1911-1922 (1999).

241. Lischwe, M.A., Richards, R.L., Busch, R.K. & Busch, H. Localization of phosphoprotein C23 to nucleolar structures and to the nucleolus organizer regions. *Experimental cell research* **136**, 101-109 (1981).

242. Borer, R.A., Lehner, C.F., Eppenberger, H.M. & Nigg, E.A. Major nucleolar proteins shuttle between nucleus and cytoplasm. *Cell* **56**, 379-390 (1989).

243. Semenkovich, C.F., Ostlund Jr, R.E., Olson, M.O.J. & Yang, J.W. A protein partially expressed on the surface of HepG2 cells that binds lipoproteins specifically is nucleolin. *Biochemistry* **29**, 9708-9713 (1990).

244. Turck, N.*, et al.* Effect of laminin-1 on intestinal cell differentiation involves inhibition of nuclear nucleolin. *Journal of Cellular Physiology* **206**, 545-555 (2006).

245. Fonseca, N.A.*, et al.* Nucleolin overexpression in breast cancer cell sub-populations with different stem-like phenotype enables targeted intracellular delivery of synergistic drug combination. **69**, 76-88 (2015).

246. Moura, V.*, et al.* Targeted and intracellular triggered delivery of therapeutics to cancer cells and the tumor microenvironment: impact on the treatment of breast cancer. *Breast Cancer Research and Treatment* (2011).

247. Krust, B., El Khoury, D., Nondier, I., Soundaramourty, C. & Hovanessian, A.G. Targeting surface nucleolin with multivalent HB-19 and related Nucant pseudopeptides results in distinct inhibitory mechanisms depending on the malignant tumor cell type. *BMC Cancer* **11**, 333 (2011).

248. Benedetti, E.*, et al.* Nucleolin antagonist triggers autophagic cell death in human glioblastoma primary cells and decreased in vivo tumor growth in orthotopic brain tumor model. *Oncotarget* **6**, 42091-42104 (2015).

249. Christian, S.*, et al.* Nucleolin expressed at the cell surface is a marker of endothelial cells in angiogenic blood vessels. *J Cell Biol* **163**, 871-878 (2003).

250. Porkka, K., Laakkonen, P., Hoffman, J.A., Bernasconi, M. & Ruoslahti, E. A fragment of the HMGN2 protein homes to the nuclei of tumor cells and tumor endothelial cells in vivo. *Proc Natl Acad Sci U S A* **99**, 7444-7449 (2002).

251. Galzio, R.*, et al.* Glycosilated nucleolin as marker for human gliomas. **113**, 571-579 (2012).

252. Hoja-Łukowicz, D.*, et al.* The new face of nucleolin in human melanoma. *Cancer Immunology, Immunotherapy* **58**, 1471-1480 (2009).

253. Qiu, W.*, et al.* Overexpression of nucleolin and different expression sites both related to the prognosis of gastric cancer. *APMIS* **121**, 919-925 (2013).

254. Wu, D.-M.*, et al.* Phosphorylation and changes in the distribution of nucleolin promote tumor metastasis via the PI3K/Akt pathway in colorectal carcinoma. **588**, 1921-1929 (2014).

255. Grinstein, E.*, et al.* Nucleolin as Activator of Human Papillomavirus Type 18 Oncogene Transcription in Cervical Cancer. *The Journal of Experimental Medicine* **196**, 1067-1078 (2002).

256. Guo, X.D.*, et al.* Increased level of nucleolin confers to aggressive tumor progression and poor prognosis in patients with hepatocellular carcinoma after hepatectomy. *Diagnostic pathology* **9**, 1-7 (2014).

257. Xu, J.-Y.*, et al.* Prognostic significance of nuclear or cytoplasmic nucleolin expression in human non-small cell lung cancer and its relationship with DNA-PKcs. *Tumor Biology*, 1-8 (2016).

258. Peng, L.*, et al.* High Levels of Nucleolar Expression of Nucleolin Are Associated with Better Prognosis in Patients with Stage II Pancreatic Ductal Adenocarcinoma. *Clinical Cancer Research* **16**, 3734-3742 (2010).

259. Ridley, L.*, et al.* Multifactorial analysis of predictors of outcome in pediatric intracranial ependymoma. *Neuro-Oncology* **10**, 675-689 (2008).

260. Angelov, D.*, et al.* Nucleolin is a histone chaperone with FACT-like activity and assists remodeling of nucleosomes. *The EMBO journal* **25**, 1669-1679 (2006).

261. Rickards, B., Flint, S.J., Cole, M.D. & LeRoy, G. Nucleolin is required for RNA polymerase I transcription in vivo. *Molecular and cellular biology* **27**, 937-948 (2007).

262. Cong, R.*, et al.* Interaction of nucleolin with ribosomal RNA genes and its role in RNA polymerase I transcription. *Nucleic acids research* **40**, 9441-9454 (2012).

263. Ginisty, H.*, et al.* Interaction of nucleolin with an evolutionarily conserved pre-ribosomal RNA sequence is required for the assembly of the primary processing complex. *Journal of Biological Chemistry* **275**, 18845-18850 (2000).

264. Bouvet, P., Diaz, J.-J., Kindbeiter, K., Madjar, J.-J. & Amalric, F. Nucleolin interacts with several ribosomal proteins through its RGG domain. *Journal of Biological Chemistry* **273**, 19025-19029 (1998).

265. Roger, B., Moisand, A., Amalric, F. & Bouvet, P. Nucleolin provides a link between RNA polymerase I transcription and pre-ribosome assembly. *Chromosoma* **111**, 399-407 (2003).

266. Uribe, D.J., Guo, K., Shin, Y.J. & Sun, D. Heterogeneous nuclear ribonucleoprotein K and nucleolin as transcriptional activators of the vascular endothelial growth factor promoter through interaction with secondary DNA structures. *Biochemistry* **50**, 3796-3806 (2011).

267. Cheng, D.-D., Zhao, H.-G., Yang, Y.-S., Hu, T. & Yang, Q.-C. GSK3β negatively regulates HIF1α mRNA stability via nucleolin in the MG63 osteosarcoma cell line. *Biochemical and biophysical research communications* **443**, 598-603 (2014).

268. Semenza, G.L. Defining the role of hypoxia-inducible factor 1 in cancer biology and therapeutics. *Oncogene* **29**, 625-634 (2010).

269. Fähling, M.*, et al.* Role of nucleolin in posttranscriptional control of MMP-9 expression. *Biochim Biophys Acta* **1731**, 32-40 (2005).

270. Hsu, T.I.*, et al.* MMP7-mediated cleavage of nucleolin at Asp255 induces MMP9 expression to promote tumor malignancy. *Oncogene* **34**, 826-837 (2015).

271. Gialeli, C., Theocharis, A.D. & Karamanos, N.K. Roles of matrix metalloproteinases in cancer progression and their pharmacological targeting. *FeBS Journal* **278**, 16-27 (2011).

272. Jin, H.*, et al.* Divergent behaviors and underlying mechanisms of cell migration and invasion in non-metastatic T24 and its metastatic derivative T24T bladder cancer cell lines. *Oncotarget* **6**, 522 (2015).

273. Xie, Q.*, et al.* p85α promotes nucleolin transcription and subsequently enhances EGFR mRNA stability and EGF-induced malignant cellular transformation. *Oncotarget* (2016).

274. Normanno, N.*, et al.* Epidermal growth factor receptor (EGFR) signaling in cancer. *Gene* **366**, 2-16 (2006).

275. Hsu, T.-I.*, et al.* Positive feedback regulation between IL10 and EGFR promotes lung cancer formation. *Oncotarget* (2016).

276. Changkija, B. & Konwar, R. Role of interleukin-10 in breast cancer. *Breast cancer research and treatment* **133**, 11-21 (2012).

277. Ishimaru, D.*, et al.* Regulation of Bcl-2 expression by HuR in HL60 leukemia cells and A431 carcinoma cells. *Molecular Cancer Research* **7**, 1354-1366 (2009).

278. Ishimaru, D.*, et al.* Mechanism of regulation of bcl-2 mRNA by nucleolin and A+ U-rich element-binding factor 1 (AUF1). *Journal of Biological Chemistry* **285**, 27182-27191 (2010).

279. Willimott, S. & Wagner, S.D. Post-transcriptional and post-translational regulation of Bcl2. *Biochemical Society transactions* **38**, 1571-1575 (2010).

280. Sengupta, T.K., Bandyopadhyay, S., Fernandes, D.J. & Spicer, E.K. Identification of nucleolin as an AU-rich element binding protein involved in bcl-2 mRNA stabilization. *Journal of Biological Chemistry* **279**, 10855-10863 (2004).

281. Zhang, B.*, et al.* Nucleolin/C23 is a negative regulator of hydrogen peroxide-induced apoptosis in HUVECs. *Cell Stress and Chaperones* **15**, 249-257 (2010).

282. Chen, C.-Y.*, et al.* Nucleolin and YB-1 are required for JNK-mediated interleukin-2 mRNA stabilization during T-cell activation. *Genes & development* **14**, 1236-1248 (2000).

283. Boyman, O. & Sprent, J. The role of interleukin-2 during homeostasis and activation of the immune system. *Nature Reviews Immunology* **12**, 180-190 (2012).

284. Lee, P.-T., Liao, P.-C., Chang, W.-C. & Tseng, J.T. Epidermal growth factor increases the interaction between nucleolin and heterogeneous nuclear ribonucleoprotein K/poly (C) binding protein 1 complex to regulate the gastrin mRNA turnover. *Molecular biology of the cell* **18**, 5004-5013 (2007).

285. Ferrand, A. & Wang, T.C. Gastrin and cancer: a review. *Cancer letters* **238**, 15-29 (2006).

286. Takagi, M., Absalon, M.J., McLure, K.G. & Kastan, M.B. Regulation of p53 translation and induction after DNA damage by ribosomal protein L26 and nucleolin. *Cell* **123**, 49-63 (2005).

287. Muller, P.A.J. & Vousden, K.H. Mutant p53 in cancer: new functions and therapeutic opportunities. *Cancer cell* **25**, 304-317 (2014).

288. Abdelmohsen, K.*, et al.* Enhanced translation by Nucleolin via G-rich elements in coding and non-coding regions of target mRNAs. *Nucleic acids research*, gkr488 (2011).

289. Hers, I., Vincent, E.E. & Tavaré, J.M. Akt signalling in health and disease. *Cellular signalling* **23**, 1515-1527 (2011).

290. Shang, Y.*, et al.* Interleukin-9 receptor gene is transcriptionally regulated by nucleolin in T-Cell lymphoma cells. *Molecular carcinogenesis* **51**, 619-627 (2012).

291. Masumi, A.*, et al.* Nucleolin is involved in interferon regulatory factor-2-dependent transcriptional activation. *Oncogene* **25**, 5113-5124 (2006).

292. Tediose, T.*, et al.* Interplay between REST and nucleolin transcription factors: a key mechanism in the overexpression of genes upon increased phosphorylation. *Nucleic acids research*, gkq013 (2010).

293. Oh, S.T., Longworth, M.S. & Laimins, L.A. Roles of the E6 and E7 proteins in the life cycle of low-risk human papillomavirus type 11. *Journal of virology* **78**, 2620-2626 (2004).

294. Pickering, B.F., Yu, D. & Van Dyke, M.W. Nucleolin protein interacts with microprocessor complex to affect biogenesis of microRNAs 15a and 16. *Journal of Biological Chemistry* **286**, 44095-44103 (2011).

295. Pichiorri, F.*, et al.* In vivo NCL targeting affects breast cancer aggressiveness through miRNA regulation. *J Exp Med* **210**, 951-968 (2013).

296. Koutsioumpa, M.*, et al.* Receptor protein tyrosine phosphatase beta/zeta is a functional binding partner for vascular endothelial growth factor. *Molecular cancer* **14**, 1 (2015).

297. Koutsioumpa, M.*, et al.* Interplay between αvβ3 integrin and nucleolin regulates human endothelial and glioma cell migration. *Journal of Biological Chemistry* **288**, 343-354 (2013).

298. Koutsioumpa, M.*, et al.* Pleiotrophin expression and role in physiological angiogenesis in vivo: potential involvement of nucleolin. *Vascular cell* **4**, 1 (2012).

299. Said, E.A.*, et al.* Pleiotrophin inhibits HIV infection by binding the cell surface-expressed nucleolin. *FEBS Journal* **272**, 4646-4659 (2005).

300. Koutsioumpa, M. & Papadimitriou, E. Cell surface nucleolin as a target for anti-cancer therapies. *Recent patents on anti-cancer drug discovery* **9**, 137-152 (2014).

301. Said, E.A., *et al.* The Anti-HIV Cytokine Midkine Binds the Cell Surface-expressed Nucleolin as a Low Affinity Receptor. *Journal of Biological Chemistry* **277**, 37492-37502 (2002).

302. Kadomatsu, K. & Muramatsu, T. Midkine and pleiotrophin in neural development and cancer. *Cancer letters* **204**, 127-143 (2004).

303. Take, M., *et al.* Identification of nucleolin as a binding protein for midkine (MK) and heparin-binding growth associated molecule (HB-GAM). *Journal of biochemistry* **116**, 1063-1068 (1994).

304. Tate, A., *et al.* Met-Independent Hepatocyte Growth Factor-mediated regulation of cell adhesion in human prostate cancer cells. *BMC Cancer* **6**, 197 (2006).

305. Reyes-Reyes, E.M. & Akiyama, S.K. Cell-surface nucleolin is a signal transducing P-selectin binding protein for human colon carcinoma cells. *Exp Cell Res* **314**, 2212-2223 (2008).

306. Huang, Y., *et al.* The angiogenic function of nucleolin is mediated by vascular endothelial growth factor and nonmuscle myosin. *Blood* **107**, 3564-3571 (2006).

307. Destouches, D., *et al.* Suppression of tumor growth and angiogenesis by a specific antagonist of the cell-surface expressed nucleolin. *PLoS One* **3**, e2518 (2008).

308. Wise, J.F., *et al.* Nucleolin inhibits Fas ligand binding and suppresses Fas-mediated apoptosis in vivo via a surface nucleolin-Fas complex. *Blood* **121**, 4729-4739 (2013).

309. Di Segni, A., Farin, K. & Pinkas-Kramarski, R. Identification of nucleolin as new ErbB receptors-interacting protein. *PloS one* **3**, e2310 (2008).

310. Inder, K.L., *et al.* Nucleophosmin and nucleolin regulate K-Ras plasma membrane interactions and MAPK signal transduction. *Journal of Biological Chemistry* **284**, 28410-28419 (2009).

311. Farin, K., *et al.* Oncogenic synergism between ErbB1, nucleolin, and mutant Ras. *Cancer research* **71**, 2140-2151 (2011).

312. Dumler, I., *et al.* Urokinase-induced mitogenesis is mediated by casein kinase 2 and nucleolin. *Current Biology* **9**, 1468-1476 (1999).

313. Stepanova, V., *et al.* Nuclear translocation of urokinase-type plasminogen activator. *Blood* **112**, 100-110 (2008).

314. Watanabe, T., *et al.* Nucleolin as cell surface receptor for tumor necrosis factor-α inducing protein: a carcinogenic factor of Helicobacter pylori. *Journal of cancer research and clinical oncology* **136**, 911-921 (2010).

315. Watanabe, T., *et al.* Epithelial–mesenchymal transition in human gastric cancer cell lines induced by TNF-α-inducing protein of Helicobacter pylori. *International Journal of Cancer* **134**, 2373-2382 (2014).

316. Legrand, D., *et al.* Surface nucleolin participates in both the binding and endocytosis of lactoferrin in target cells. *European Journal of Biochemistry* **271**, 303-317 (2004).

317. Zhang, Y., Lima, C.F. & Rodrigues, L.R. Anticancer effects of lactoferrin: underlying mechanisms and future trends in cancer therapy. *Nutrition reviews* **72**, 763-773 (2014).

318. Shi, H., *et al.* Nucleolin is a receptor that mediates antiangiogenic and antitumor activity of endostatin. *Blood* **110**, 2899-2906 (2007).

319. Dubail, J., *et al.* ADAMTS-2 functions as anti-angiogenic and anti-tumoral molecule independently of its catalytic activity. *Cellular and molecular life sciences* **67**, 4213-4232 (2010).

320. Callebaut, C., *et al.* Identification of V3 loop-binding proteins as potential receptors implicated in the binding of HIV particles to CD4+ cells. *Journal of Biological Chemistry* **273**, 21988-21997 (1998).

321. El Khoury, D., *et al.* Targeting surface nucleolin with a multivalent pseudopeptide delays development of spontaneous melanoma in RET transgenic mice. *BMC Cancer* **10**, 325 (2010).

322. Destouches, D., *et al.* A simple approach to cancer therapy afforded by multivalent pseudopeptides that target cell-surface nucleoproteins. *Cancer research* **71**, 3296-3305 (2011).

323. Krust, B., El Khoury, D., Soundaramourty, C., Nondier, I. & Hovanessian, A.G. Suppression of tumorigenicity of rhabdoid tumor derived G401 cells by the multivalent HB-19 pseudopeptide that targets surface nucleolin. *Biochimie* **93**, 426-433 (2011).

324. Destouches, D., *et al.* Multivalent pseudopeptides targeting cell surface nucleoproteins inhibit cancer cell invasion through tissue inhibitor of metalloproteinases 3 (TIMP-3) release. *J Biol Chem* **287**, 43685-43693 (2012).

325. Birmpas, C., Briand, J.P., Courty, J. & Katsoris, P. The pseudopeptide HB-19 binds to cell surface nucleolin and inhibits angiogenesis. *Vascular cell* **4**, 1 (2012).

326. Latorre, A., Couleaud, P., Aires, A., Cortajarena, A.L. & Somoza, Á. Multifunctionalization of magnetic nanoparticles for controlled drug release: A general approach. *European journal of medicinal chemistry* **82**, 355-362 (2014).

327. Kossatz, S., *et al.* Efficient treatment of breast cancer xenografts with multifunctionalized iron oxide nanoparticles combining magnetic hyperthermia and anti-cancer drug delivery. *Breast Cancer Research* **17**, 1-17 (2015).

328. Bates, P.J., Laber, D.A., Miller, D.M., Thomas, S.D. & Trent, J.O. Discovery and development of the G-rich oligonucleotide AS1411 as a novel treatment for cancer. *Experimental and molecular pathology* **86**, 151-164 (2009).

329. Soundararajan, S., Chen, W., Spicer, E.K., Courtenay-Luck, N. & Fernandes, D.J. The nucleolin targeting aptamer AS1411 destabilizes Bcl-2 messenger RNA in human breast cancer cells. *Cancer research* **68**, 2358-2365 (2008).

330. Soundararajan, S., *et al.* Plasma membrane nucleolin is a receptor for the anticancer aptamer AS1411 in MV4-11 leukemia cells. *Molecular pharmacology* **76**, 984-991 (2009).

331. Girvan, A.C., *et al.* AGRO100 inhibits activation of nuclear factor-κB (NF-κB) by forming a complex with NF-κB essential modulator (NEMO) and nucleolin. *Molecular cancer therapeutics* **5**, 1790-1799 (2006).

332. Teng, Y., *et al.* AS1411 alters the localization of a complex containing protein arginine methyltransferase 5 and nucleolin. *Cancer research* **67**, 10491-10500 (2007).

333. Reyes-Reyes, E.M., Teng, Y. & Bates, P.J. A new paradigm for aptamer therapeutic AS1411 action: uptake by macropinocytosis and its stimulation by a nucleolin-dependent mechanism. *Cancer research* **70**, 8617-8629 (2010).

334. Reyes-Reyes, E.M., Šalipur, F.R., Shams, M., Forsthoefel, M.K. & Bates, P.J. Mechanistic studies of anticancer aptamer AS1411 reveal a novel role for nucleolin in regulating Rac1 activation. *Molecular oncology* **9**, 1392-1405 (2015).

335. Rosenberg, J.E.*, et al.* A phase II trial of AS1411 (a novel nucleolin-targeted DNA aptamer) in metastatic renal cell carcinoma. *Investigational new drugs* **32**, 178-187 (2014).

336. Xing, H.*, et al.* Selective delivery of an anticancer drug with aptamer-functionalized liposomes to breast cancer cells in vitro and in vivo. *Journal of Materials Chemistry B* **1**, 5288-5297 (2013).

337. Wang, C.*, et al.* Toward targeted therapy in chemotherapy-resistant pancreatic cancer with a smart triptolide nanomedicine. *Oncotarget* (2016).

338. Malik, M.T.*, et al.* AS1411-conjugated gold nanospheres and their potential for breast cancer therapy. *Oncotarget* **6**, 22270 (2015).

339. Sader, M., Courty, J. & Destouches, D. Nanoparticles Functionalized with Ligands of Cell Surface Nucleolin for Cancer Therapy and Diagnosis. *J Nanomed Nanotechnol* **6**, 2 (2015).

340. Wu, J.*, et al.* Nucleolin targeting AS1411 modified protein nanoparticle for antitumor drugs delivery. *Molecular pharmaceutics* **10**, 3555-3563 (2013).

341. Dam, D.H.M., Culver, K.S.B. & Odom, T.W. Grafting aptamers onto gold nanostars increases in vitro efficacy in a wide range of cancer cell types. *Molecular pharmaceutics* **11**, 580-587 (2014).

342. Li, L.*, et al.* Nucleolin-targeting liposomes guided by aptamer AS1411 for the delivery of siRNA for the treatment of malignant melanomas. *Biomaterials* **35**, 3840-3850 (2014).

343. Guo, J.*, et al.* Aptamer-functionalized PEG–PLGA nanoparticles for enhanced anti-glioma drug delivery. *Biomaterials* **32**, 8010-8020 (2011).

344. Zhou, W.*, et al.* Aptamer-nanoparticle bioconjugates enhance intracellular delivery of vinorelbine to breast cancer cells. *Journal of drug targeting* **22**, 57-66 (2014).

345. Qin, M., Zong, H. & Kopelman, R. Click conjugation of peptide to hydrogel nanoparticles for tumor-targeted drug delivery. *Biomacromolecules* **15**, 3728-3734 (2014).

346. Winer, I.*, et al.* F3-targeted cisplatin-hydrogel nanoparticles as an effective therapeutic that targets both murine and human ovarian tumor endothelial cells in vivo. *Cancer research* **70**, 8674-8683 (2010).

347. Hah, H.J.*, et al.* Methylene blue-conjugated hydrogel nanoparticles and tumor-cell targeted photodynamic therapy. *Macromolecular bioscience* **11**, 90-99 (2011).

348. Hu, Q.*, et al.* F3 peptide-functionalized PEG-PLA nanoparticles co-administrated with tLyp-1 peptide for anti-glioma drug delivery. *Biomaterials* **34**, 1135-1145 (2013).

349. Drecoll, E.*, et al.* Treatment of peritoneal carcinomatosis by targeted delivery of the radio-labeled tumor homing peptide 213 Bi-DTPA-[F3] 2 into the nucleus of tumor cells. *PLoS One* **4**, e5715 (2009).

350. Gomes-da-Silva, L.C.*, et al.* Toward a siRNA-containing nanoparticle targeted to breast cancer cells and the tumor microenvironment. *International journal of pharmaceutics* **434**, 9-19 (2012).

351. Gomes, C.P.*, et al.* Impact of PLK-1 silencing on endothelial cells and cancer cells of diverse histological origin. *Current gene therapy* **13**, 189-201 (2013).

352. Gomes-da-Silva, L.C.*, et al.* Efficient intracellular delivery of siRNA with a safe multitargeted lipid-based nanoplatform. *Nanomedicine* **8**, 1397-1413 (2013).

353. Gomes-da-Silva, L.C., Ramalho, J.S., de Lima, M.C.P., Simões, S. & Moreira, J.N. Impact of anti-PLK1 siRNA-containing F3-targeted liposomes on the viability of both cancer and endothelial cells. *European Journal of Pharmaceutics and Biopharmaceutics* **85**, 356-364 (2013).

354. Fonseca, N.A., Gomes-da-Silva, L.C., Moura, V., Simões, S. & Moreira, J.N. Simultaneous active intracellular delivery of doxorubicin and C6-ceramide shifts the additive/antagonistic drug interaction of non-encapsulated combination. **196**, 122-131 (2014).

355. Prickett, W.M., Van Rite, B.D., Resasco, D.E. & Harrison, R.G. Vascular targeted single-walled carbon nanotubes for near-infrared light therapy of cancer. *Nanotechnology* **22**, 455101 (2011).

356. Sader, M.*, et al.* Functionalization of Iron Oxide Magnetic Nanoparticles with the Multivalent Pseudopeptide N6l for Breast Tumor Targeting. *Journal of Nanomedicine & Nanotechnology* **2015**(2015).

357. Chen, X., Shank, S., Davis, P.B. & Ziady, A.G. Nucleolin-mediated cellular trafficking of DNA nanoparticle is lipid raft and microtubule dependent and can be modulated by glucocorticoid. *Molecular Therapy* **19**, 93-102 (2011).

358. Chen, X., Kube, D.M., Cooper, M.J. & Davis, P.B. Cell surface nucleolin serves as receptor for DNA nanoparticles composed of pegylated polylysine and DNA. *Molecular Therapy* **16**, 333-342 (2008).

359. Karamchand, L.*, et al.* Modulation of hydrogel nanoparticle intracellular trafficking by multivalent surface engineering with tumor targeting peptide. *Nanoscale* **5**, 10327-10344 (2013).

360. Carballido, E.M. & Rosenberg, J.E. Optimal Treatment for Metastatic Bladder Cancer. *Current Oncology Reports C7 - 404* **16**, 1-9 (2014).

361. McKeown, E.*, et al.* Current Approaches and Challenges for Monitoring Treatment Response in Colon and Rectal Cancer. *Journal of Cancer* **5**, 31-43 (2014).

362. Wallace, T.J.*, et al.* Current Approaches, Challenges and Future Directions for Monitoring Treatment Response in Prostate Cancer. *Journal of Cancer* **5**, 3-24 (2014).

363. Tevaarwerk, A.J.*, et al.* Survival in patients with metastatic recurrent breast cancer after adjuvant chemotherapy. *Cancer* **119**, 1140--1148 (2013).

364. Haddad, T.C. & Yee, D. Of Mice and (Wo)Men: Is This Any Way to Test a New Drug? (2008).

365. Francia, G., Cruz-Munoz, W., Man, S., Xu, P. & Kerbel, R.S. Mouse models of advanced spontaneous metastasis for experimental therapeutics. *Nat Rev Cancer* **11**, 135-141 (2011).

366. Bos, P.D., Nguyen, D.X. & Massagué, J. Modeling metastasis in the mouse. *Curr Opin Pharmacol* **10**, 571-577 (2010).

367. Gould, S.E., Junttila, M.R. & de Sauvage, F.J. Translational value of mouse models in oncology drug development. *Nature Medicine* **21**, 431-439 (2015).

368. Fidler, I.J. The pathogenesis of cancer metastasis: the 'seed and soil' hypothesis revisited. *Nat Rev Cancer* **3**, 453-458 (2003).

369. Weber, G.F. Why does cancer therapy lack effective anti-metastasis drugs? *Cancer Letters* **328**, 207-211 (2013).

370. Miller, F.R., Miller, B.E. & Heppner, G.H. Characterization of metastatic heterogeneity among subpopulations of a single mouse mammary tumor: heterogeneity in phenotypic stability. *Invasion Metastasis* **3**, 22-31 (1983).

371. Abu, N.*, et al.* In vivo antitumor and antimetastatic effects of flavokawain B in 4T1 breast cancer cell-challenged mice. *Drug Des Devel Ther* **9**, 1401-1417 (2015).

372. Gao, Z.G., Tian, L., Hu, J., Park, I.S. & Bae, Y.H. Prevention of metastasis in a 4T1 murine breast cancer model by doxorubicin carried by folate conjugated pH sensitive polymeric micelles. *J Control Release* (2011).

373. HIRANO, T.*, et al.* Inhibition of Tumor Growth by Antibody to ADAMTS1 in Mouse Xenografts of Breast Cancer. (2011).

374. Wenzel, J., Zeisig, R. & Fichtner, I. Inhibition of metastasis in a murine 4T1 breast cancer model by liposomes preventing tumor cell-platelet interactions. *Clin Exp Metastasis* **27**, 25-34 (2010).

375. Ferrari-Amorotti, G.*, et al.* Suppression of invasion and metastasis of triple-negative breast cancer lines by pharmacological or genetic inhibition of slug activity. *Neoplasia* **16**, 1047-1058 (2014).

376. Sato, M.*, et al.* Differential Proteome Analysis Identifies TGF-beta-Related Pro-Metastatic Proteins in a 4T1 Murine Breast Cancer Model. *PLoS One* **10**, e0126483 (2015).

377. Peiris, P.M.*, et al.* Vascular Targeting of a Gold Nanoparticle to Breast Cancer Metastasis. *Journal of Pharmaceutical Sciences*, n/a--n/a (2015).

378. Aslakson, C.J. & Miller, F.R. Selective events in the metastatic process defined by analysis of the sequential dissemination of subpopulations of a mouse mammary tumor. *Cancer Res* **52**, 1399-1405 (1992).

379. Kim, E.J.*, et al.* Dietary fat increases solid tumor growth and metastasis of 4T1 murine mammary carcinoma cells and mortality in obesity-resistant BALB/c mice. *Breast Cancer Research : BCR* **13**, R78-R78 (2011).

380. Heimburg, J.*, et al.* Inhibition of Spontaneous Breast Cancer Metastasis by Anti—Thomsen-Friedenreich Antigen Monoclonal Antibody JAA-F11. **8**, 939-948 (2006).

381. Lirdprapamongkol, K.*, et al.* Vanillin suppresses in vitro invasion and in vivo metastasis of mouse breast cancer cells. *Eur J Pharm Sci* **25**, 57-65 (2005).

382. Nasti, T.H., Bullard, D.C. & Yusuf, N. P-selectin enhances growth and metastasis of mouse mammary tumors by promoting regulatory T cell infiltration into the tumors. **131**, 11-18 (2015).

383. Samant, R.S.*, et al.* Suppression of murine mammary carcinoma metastasis by the murine ortholog of breast cancer metastasis suppressor 1 (Brms1). **235**, 260-265 (2006).

384. Tao, K., Fang, M., Alroy, J. & Sahagian, G.G. Imagable 4T1 model for the study of late stage breast cancer. *BMC Cancer* **8**, 228 (2008).

385. Benzekry, S.*, et al.* Classical mathematical models for description and prediction of experimental tumor growth. *PLoS Comput Biol* **10**, e1003800 (2014).

386. Norton, L. A Gompertzian model of human breast cancer growth. *Cancer research* **48**, 7067-7071 (1988).

387. Comen, E., Norton, L. & Massague, J. Clinical implications of cancer self-seeding. *Nat Rev Clin Oncol* **8**, 369-377 (2011).

388. Parham, F. & Portier, C. Benchmark Dose Approach. in *Recent Advances in Quantitative Methods in Cancer and Human Health Risk Assessment* 239-254 (John Wiley & Sons, Ltd, 2005).

389. Ludden, T.M., Beal, S.L. & Sheiner, L.B. Comparison of the Akaike Information Criterion, the Schwarz criterion and the F test as guides to model selection. *Journal of Pharmacokinetics and Biopharmaceutics* **22**, 431-445 (1994).

390. Proskuryakov, S.Y. & Gabai, V.L. Mechanisms of tumor cell necrosis. *Current pharmaceutical design* **16**, 56-68 (2010).

391. Leek, R.D., Landers, R.J., Harris, A.L. & Lewis, C.E. Necrosis correlates with high vascular density and focal macrophage infiltration in invasive carcinoma of the breast. *British journal of cancer* **79**, 991 (1999).

392. Vakkila, J. & Lotze, M.T. Inflammation and necrosis promote tumour growth. *Nature Reviews Immunology* **4**, 641-648 (2004).

393. Polyak, K. Breast cancer: origins and evolution. *The Journal of clinical investigation* **117**, 3155-3163 (2007).

394. Singh, M. & Ferrara, N. Modeling and predicting clinical efficacy for drugs targeting the tumor milieu. *Nature biotechnology* **30**, 648-657 (2012).

395. Bailey-Downs, L.C.*, et al.* Development and characterization of a preclinical model of breast cancer lung micrometastatic to macrometastatic progression. *PLoS One* **9**, e98624 (2014).

396. Weng, D.*, et al.* Metastasis is an early event in mouse mammary carcinomas and is associated with cells bearing stem cell markers. *Breast Cancer Research C7 - R18* **14**, 1-13 (2012).

397. Psaila, B. & Lyden, D. The Metastatic Niche: Adapting the Foreign Soil. *Nature reviews. Cancer* **9**, 285-293 (2009).

398. Burton, A.C. Rate of growth of solid tumours as a problem of diffusion. *Growth* **30**, 157-176 (1966).

399. Folkman, J. What Is the Evidence That Tumors Are Angiogenesis Dependent? *Journal of the National Cancer Institute* **82**, 4-7 (1990).

400. Kim, M.-Y.*, et al.* Tumor Self-Seeding by Circulating Cancer Cells. **139**, 1315-1326 (2009).

401. DuPré, S.A., Redelman, D. & Hunter, K.W. The mouse mammary carcinoma 4T1: characterization of the cellular landscape of primary tumours and metastatic tumour foci. *Int J Exp Pathol* **88**, 351-360 (2007).

402. Huang, Y.*, et al.* CD4+ and CD8+ T cells have opposing roles in breast cancer progression and outcome. *Oncotarget* (2015).

403. Liao, D., Luo, Y., Markowitz, D., Xiang, R. & Reisfeld, R.A. Cancer Associated Fibroblasts Promote Tumor Growth and Metastasis by Modulating the Tumor Immune Microenvironment in a 4T1 Murine Breast Cancer Model. *PLoS ONE* **4**, e7965 (2009).

404. duPre, S.A., Redelman, D. & Hunter Jr, K.W. Microenvironment of the murine mammary carcinoma 4T1: Endogenous IFN-γ affects tumor phenotype, growth, and metastasis. **85**, 174-188 (2008).

405. Hanahan, D. & Coussens, L.M. Accessories to the Crime: Functions of Cells Recruited to the Tumor Microenvironment. **21**, 309-322 (2012).

406. Chen, F.*, et al.* New horizons in tumor microenvironment biology: challenges and opportunities. *BMC Medicine C7 - 45* **13**, 1-14 (2015).

407. Adiseshaiah, P.P.*, et al.* Longitudinal Imaging of Cancer Cell Metastases in Two Preclinical Models: A Correlation of Noninvasive Imaging to Histopathology. *International Journal of Molecular Imaging* **2014**, 13 (2014).

408. Lim, E., Modi, K.D. & Kim, J. In vivo Bioluminescent Imaging of Mammary Tumors Using IVIS Spectrum. e1210 (2009).

409. Euhus, D.M., Hudd, C., Laregina, M.C. & Johnson, F.E. Tumor measurement in the nude mouse. *Journal of surgical oncology* **31**, 229-234 (1986).

410. Mehrara, E.*, et al.* A new method to estimate parameters of the growth model for metastatic tumours. *Theoretical Biology and Medical Modelling C7 - 31* **10**, 1-12 (2013).

411. Cardoso, F.*, et al.* Locally recurrent or metastatic breast cancer: ESMO Clinical Practice Guidelines for diagnosis, treatment and follow-up. *Annals of Oncology* **23**, vii11-vii19 (2012).

412. Howlader, N.*, et al.* SEER Cancer Statistics Review, 1975-2012, National Cancer Institute. Bethesda, MD, http://seer.cancer.gov/csr/1975_2012/, based on November 2014 SEER data submission, posted to the SEER web site, April 2015.

413. Cardoso, F.*, et al.* Second and subsequent lines of chemotherapy for metastatic breast cancer: what did we learn in the last two decades? *Annals of Oncology* **13**, 197-207 (2002).

414. Chia, S.K.*, et al.* The impact of new chemotherapeutic and hormone agents on survival in a population-based cohort of women with metastatic breast cancer. *Cancer* **110**, 973--979 (2007).

415. Gennari, A., Conte, P., Rosso, R., Orlandini, C. & Bruzzi, P. Survival of metastatic breast carcinoma patients over a 20-year period. *Cancer* **104**, 1742--1750 (2005).

416. Cardoso, F.*, et al.* International Guidelines for Management of Metastatic Breast Cancer: Combination vs Sequential Single-Agent Chemotherapy. *Journal of the National Cancer Institute* **101**, 1174-1181 (2009).

417. Dalmau, E., Almengol-Alonso, A., Muñoz, M. & Seguí-Palmer, M. Current status of hormone therapy in patients with hormone receptor positive (HR+) advanced breast cancer. *The Breast* **23**, 710 - 720 (2014).

418. Slamon, D.J.*, et al.* Use of Chemotherapy plus a Monoclonal Antibody against HER2 for Metastatic Breast Cancer That Overexpresses HER2. *New England Journal of Medicine* **344**, 783-792 (2001).

419. Santa-Maria, C.A. & J., G.W. Changing treatment paradigms in metastatic breast cancer: Lessons learned. *JAMA Oncology* **1**, 528-534 (2015).

420. Toy, W.*, et al.* ESR1 ligand-binding domain mutations in hormone-resistant breast cancer. *Nat Genet* **45**, 1439-1445 (2013).

421. Bose, R., *et al.* Activating HER2 Mutations in HER2 Gene Amplification Negative Breast Cancer. *Cancer Discovery* **3**, 224-237 (2013).

422. Esteva, F.J., *et al.* PTEN, PIK3CA, p-AKT, and p-p70S6K Status: Association with Trastuzumab Response and Survival in Patients with HER2-Positive Metastatic Breast Cancer. *The American Journal of Pathology* **177**, 1647 - 1656 (2010).

423. Niikura, N., *et al.* Loss of Human Epidermal Growth Factor Receptor 2 (HER2) Expression in Metastatic Sites of HER2-Overexpressing Primary Breast Tumors. *Journal of Clinical Oncology* **30**, 593-599 (2012).

424. Serra, V., *et al.* RSK3/4 mediate resistance to PI3K pathway inhibitors in breast cancer. *The Journal of Clinical Investigation* **123**, 2551-2563 (2013).

425. von Minckwitz, G., *et al.* Trastuzumab beyond progression: overall survival analysis of the GBG 26/BIG 3-05 phase III study in HER2-positive breast cancer. *European journal of cancer* **47**, 2273-2281 (2011).

426. Cameron, D., *et al.* Lapatinib plus capecitabine in women with HER-2–positive advanced breast cancer: Final survival analysis of a phase III randomized trial. *The oncologist* **15**, 924-934 (2010).

427. André, F. & Zielinski, C.C. Optimal strategies for the treatment of metastatic triple-negative breast cancer with currently approved agents. *Annals of Oncology* **23**, vi46-vi51 (2012).

428. Beslija, S., *et al.* Third consensus on medical treatment of metastatic breast cancer. *Annals of Oncology* **20**, 1771-1785 (2009).

429. O'Brien, M.E.R., *et al.* Reduced cardiotoxicity and comparable efficacy in a phase III trial of pegylated liposomal doxorubicin HCl (CAELYX™/Doxil®) versus conventional doxorubicin for first-line treatment of metastatic breast cancer. *Annals of Oncology* **15**, 440-449 (2004).

430. European Medicines Agency. Summary of product characteristics: Caelyx (doxorubicin hydrochloride in a pegylated liposomal formulation) 2 mg/mL concentrate for infusion, http://www.ema.europa.eu/ema/index.jsp?curl=pages/medicines/human/medicines/000089/human_med_000683.jsp&mid=WC0b01ac058001d124. (2009).

431. Northfelt, D.W., *et al.* Pegylated-liposomal doxorubicin versus doxorubicin, bleomycin, and vincristine in the treatment of AIDS-related Kaposi's sarcoma: results of a randomized phase III clinical trial. *Journal of Clinical Oncology* **16**, 2445-2451 (1998).

432. Jain, R.K. & Stylianopoulos, T. Delivering nanomedicine to solid tumors. *Nature reviews Clinical oncology* **7**, 653-664 (2010).

433. Noble, G.T., Stefanick, J.F., Ashley, J.D., Kiziltepe, T. & Bilgicer, B. Ligand-targeted liposome design: challenges and fundamental considerations. *Trends in biotechnology* **32**, 32-45 (2014).

434. Fogal, V., Sugahara, K.N., Ruoslahti, E. & Christian, S. Cell surface nucleolin antagonist causes endothelial cell apoptosis and normalization of tumor vasculature. *Angiogenesis* **12**, 91-100 (2009).

435. Zhuo, W., *et al.* Endostatin inhibits tumour lymphangiogenesis and lymphatic metastasis via cell surface nucleolin on lymphangiogenic endothelial cells. *J Pathol* **222**, 249-260 (2010).

436. Gilles, M.-E., *et al.* Abstract 15: Nucleolin-targeting NUCANT normalizes tumor vasculature and inhibits tumor growth and metastasis formation in mouse models of cancer. *Cancer Research* **74**, 15-15 (2014).

437. Pulaski, B.A. & Ostrand-Rosenberg, S. Mouse 4T1 breast tumor model. *Curr Protoc Immunol* **Chapter 20**, Unit 20.22 (2001).

438. Carstens, E. & Moberg, G.P. Recognizing Pain and Distress in Laboratory Animals. *ILAR Journal* **41**, 62-71 (2000).

439. Workman, P.*, et al.* Guidelines for the welfare and use of animals in cancer research. *Br J Cancer* **102**, 1555-1577 (2010).

440. Charrois, G.J.R. & Allen, T.M. Multiple Injections of Pegylated Liposomal Doxorubicin: Pharmacokinetics and Therapeutic Activity. *Journal of Pharmacology and Experimental Therapeutics* **306**, 1058-1067 (2003).

441. Song, N.*, et al.* The nuclear translocation of endostatin is mediated by its receptor nucleolin in endothelial cells. *Angiogenesis* **15**, 697-711 (2012).

442. Tse, J.M.*, et al.* Mechanical compression drives cancer cells toward invasive phenotype. *Proceedings of the National Academy of Sciences* **109**, 911-916 (2012).

443. Padera, T.P.*, et al.* Pathology: cancer cells compress intratumour vessels. *Nature* **427**, 695-695 (2004).

444. Demou, Z.N. Gene expression profiles in 3D tumor analogs indicate compressive strain differentially enhances metastatic potential. *Annals of biomedical engineering* **38**, 3509-3520 (2010).

445. Stylianopoulos, T.*, et al.* Causes, consequences, and remedies for growth-induced solid stress in murine and human tumors. *Proceedings of the National Academy of Sciences* **109**, 15101-15108 (2012).

446. duPré, S.A. & Hunter Jr., K.W. Murine mammary carcinoma 4T1 induces a leukemoid reaction with splenomegaly: association with tumor-derived growth factors. *Experimental and molecular pathology* **82**, 12-24 (2007).

447. Yokoi, K.*, et al.* Abstract P1-07-13: Extramedullary hematopoiesis aids initiation of cancer metastasis. *Cancer Research* **75**, P1-07-13-P01-07-13 (2015).

448. Yan, H.H.*, et al.* Gr-1+ CD11b+ myeloid cells tip the balance of immune protection to tumor promotion in the premetastatic lung. *Cancer research* **70**, 6139-6149 (2010).

449. Zhou, R., Mazurchuk, R. & Straubinger, R.M. Antivasculature Effects of Doxorubicin-containing Liposomes in an Intracranial Rat Brain Tumor Model. *Cancer Research* **62**, 2561-2566 (2002).

450. Pastorino, F.*, et al.* Enhanced Antitumor Efficacy of Clinical-Grade Vasculature-Targeted Liposomal Doxorubicin. *Clinical Cancer Research* **14**, 7320-7329 (2008).

451. Nguyen, L.*, et al.* Spatial morphological and molecular differences within solid tumors may contribute to the failure of vascular disruptive agent treatments. *BMC Cancer C7 - 522* **12**, 1-13 (2012).

452. Hori, K., Akita, H., Nonaka, H., Sumiyoshi, A. & Taki, Y. Prevention of cancer recurrence in tumor margins by stopping microcirculation in the tumor and tumor–host interface. *Cancer Science* **105**, 1196--1204 (2014).

453. Júnior, A.D.*, et al.* Tissue distribution evaluation of stealth pH-sensitive liposomal cisplatin versus free cisplatin in Ehrlich tumor-bearing mice. *Life Sciences* **80**, 659 - 664 (2007).

454. Soares, D.C., *et al.* Antitumoral activity and toxicity of PEG-coated and PEG-folate-coated pH-sensitive liposomes containing 159Gd-DTPA-BMA in Ehrlich tumor bearing mice. *European Journal of Pharmaceutical Sciences* **45**, 58 - 64 (2012).

455. Zhang, H., Li, R.-Y., Lu, X., Mou, Z.-Z. & Lin, G.-M. Docetaxel-loaded liposomes: preparation, pH sensitivity, Pharmacokinetics, and tissue distribution. *Journal of Zhejiang University SCIENCE B* **13**, 981-989 (2012).

456. Paliwal, S.R., *et al.* Estrogen-Anchored pH-Sensitive Liposomes as Nanomodule Designed for Site-Specific Delivery of Doxorubicin in Breast Cancer Therapy. *Molecular Pharmaceutics* **9**, 176-186 (2012).

457. Ishida, T., Okada, Y., Kobayashi, T. & Kiwada, H. Development of pH-sensitive liposomes that efficiently retain encapsulated doxorubicin (DXR) in blood. *International Journal of Pharmaceutics* **309**, 94 - 100 (2006).

458. European Medicines Agency. Summary of product characteristics: Herceptin (150 mg powder for concentrate for solution for infusion), http://www.ema.europa.eu/ema/index.jsp?curl=pages/medicines/human/medicines/000278/human_med_000818.jsp&mid=WC0b01ac058001d124. (2010).

459. Wu, D.-M., *et al.* Phosphorylation and changes in the distribution of nucleolin promote tumor metastasis via the PI3K/Akt pathway in colorectal carcinoma. *FEBS letters* **588**, 1921-1929 (2014).

460. Hovanessian, A.G., *et al.* Surface expressed nucleolin is constantly induced in tumor cells to mediate calcium-dependent ligand internalization. *PLoS One* **5**, e15787 (2010).

461. Haran, G., Cohen, R., Bar, L.K. & Barenholz, Y. Transmembrane ammonium sulfate gradients in liposomes produce efficient and stable entrapment of amphipathic weak bases. *Biochimica et Biophysica Acta (BBA)-Biomembranes* **1151**, 201-215 (1993).

462. Moreira, J.N., Ishida, T., Gaspar, R. & Allen, T.M. Use of the post-insertion technique to insert peptide ligands into pre-formed stealth liposomes with retention of binding activity and cytotoxicity. *Pharmaceutical research* **19**, 265-269 (2002).

463. O'Brien, J., Wilson, I., Orton, T. & Pognan, F. Investigation of the Alamar Blue (resazurin) fluorescent dye for the assessment of mammalian cell cytotoxicity. *European Journal of Biochemistry* **267**, 5421-5426 (2000).

464. Welch, D.R. Technical considerations for studying cancer metastasis in vivo. *Clinical & Experimental Metastasis* **15**, 272-306 (1997).

465. Schindelin, J., *et al.* Fiji: an open-source platform for biological-image analysis. *Nature methods* **9**, 676-682 (2012).

466. Otake, Y., *et al.* Overexpression of nucleolin in chronic lymphocytic leukemia cells induces stabilization of bcl2 mRNA. *Blood* **109**, 3069-3075 (2007).

467. Chen, C., Chen, L., Yao, Y., Qin, Z. & Chen, H. Nucleolin overexpression is associated with an unfavorable outcome for ependymoma: a multifactorial analysis of 176 patients. *Journal of neuro-oncology*, 1-10 (2015).

468. Zhao, H., *et al.* Prognostic Significance of the Combined Score of Endothelial Expression of Nucleolin and CD31 in Surgically Resected Non-Small Cell Lung Cancer. *PLoS ONE* **8**, e54674 (2013).

469. Qi, J.*, et al.* The implications and mechanisms of the extra-nuclear nucleolin in the esophageal squamous cell carcinomas. *Medical Oncology* **32**, 1-8 (2015).

470. Mourmouras, V.*, et al.* Nucleolin protein expression in cutaneous melanocytic lesions. *Journal of Cutaneous Pathology* **36**, 637-646 (2009).

471. Reyes-Reyes, E.M., Šalipur, F.R., Shams, M., Forsthoefel, M.K. & Bates, P.J. Mechanistic studies of anticancer aptamer AS1411 reveal a novel role for nucleolin in regulating Rac1 activation. *Molecular Oncology* **9**, 1392-1405 (2015).

472. Curigliano, G.*, et al.* Should liver metastases of breast cancer be biopsied to improve treatment choice? *Annals of Oncology* **22**, 2227-2233 (2011).

473. Losfeld, M.E.*, et al.* N-Glycosylation influences the structure and self-association abilities of recombinant nucleolin. *FEBS J* **278**, 2552-2564 (2011).

474. Schnitt, S.J. Classification and prognosis of invasive breast cancer: from morphology to molecular taxonomy. *Mod Pathol* **23**, S60-S64 (2010).

475. Foulkes, W.D., Smith, I.E. & Reis-Filho, J.S. Triple-Negative Breast Cancer. *New England Journal of Medicine* **363**, 1938-1948 (2010).

476. Allred, D.C., Brown, P. & Medina, D. The origins of estrogen receptor alpha-positive and estrogen receptor alpha-negative human breast cancer. *Breast cancer research* **6**, 240-257 (2004).

477. Hammond, M.E.H.*, et al.* American Society of Clinical Oncology/College of American Pathologists guideline recommendations for immunohistochemical testing of estrogen and progesterone receptors in breast cancer. *Journal of Clinical Oncology* **28**, 2784-2795 (2010).

478. Sutton, L.M.*, et al.* Intratumoral Expression Level of Epidermal Growth Factor Receptor and Cytokeratin 5/6 Is Significantly Associated With Nodal and Distant Metastases in Patients With Basal-like Triple-Negative Breast Carcinoma. *American Journal of Clinical Pathology* **134**, 782-787 (2010).

479. Sood, N. & Nigam, J.S. Correlation of CK5 and EGFR with Clinicopathological Profile of Triple-Negative Breast Cancer. *Pathology Research International* **2014**, 6 (2014).

480. Sasa, M., Bando, Y., Takahashi, M., Hirose, T. & Nagao, T. Screening for basal marker expression is necessary for decision of therapeutic strategy for triple-negative breast cancer. *Journal of Surgical Oncology* **97**, 30-34 (2008).

481. Fritz, A.*, et al. International classification of diseases for oncology*, (World Health Organization, 2000).